Reconstruction of oceanic currents and climate change in the Transkei Basin, South African gateway

Dissertation
zur Erlangung des Doktorgrades der Naturwissenschaften
im Fachbereich Geowissenschaften der
Universität Bremen

von

Philip Schlüter

Bremerhaven, 22. August 2007

Contents

Abstract

The region south of South Africa has been a crucial gateway for large scale Thermohaline Circulations since late Eocene times. Here, three of the most important currents for maintaining the global heat exchange, namely the warm and surface related Agulhas Current (AC), and the cold and denser North Atlantic Deep Water (NADW) as well as the Atlantic Bottom Water (AABW), flow around South Africa. Due to the special tectonic and geologic situation, a huge amount of the deep and bottom water masses that flow around South Africa have to pass the narrow Agulhas Passage, located between the South African continental shelf and the submarine Agulhas Plateau. As a result, the sedimentary infill of the Transkei Basin, which is located east of the Agulhas Plateau, has been predominantly influenced by NADW and AABW activity since ~36 Ma. Via the analysis of this sedimentary infill, a palaeo current reconstruction of (proto-) NADW and (proto-) AABW revealed changing flow paths and flow strengths since then. These variations in current attributes were triggered by large scale effects, such as the opening of the Tasman Gateway and the Drake Passage in the Late Eocene, or the closure of the Isthmus of Panama in the Pliocene. A more detailed analysis of the Transkei Basin's depocentre locations and interface outlines resulted in a palaeo flow path reconstruction for this region.

Moreover, palaeo climate conditions from the Late Cretaceous were partially reconstructed via the analysis of high amplitude seismic reflections, so called bright spots, from the central Transkei Basin. The evaluation of these bright spots provided indications for anoxic conditions for a period between ~90 Ma and ~80 Ma for the region south of South Africa, which could be related to worldwide Oceanic Anoxic Event 3.

Zusammenfassung

Die Region südlich Südafrikas stellt seit dem Oberen Eozän eine Schlüsselstelle für großmaßstäbliche Thermohaline Zirkulationen dar. Drei der für den globalen Wärmeaustausch wichtigsten Strömungen treffen hier aufeinander. Dabei handelt es sich um den warmen und oberflächennahen Agulhas Strom und das kalte und dichtere Nordatlantische Tiefenwasser (NADW) und das Antarktische Bodenwasser (AABW), welche um die Südspitze Südafrikas fließen. Aufgrund der speziellen tektonischen und geologischen Situation, muss ein Großteil der Tiefen- und Bodenwassermassen durch die enge Agulhas Passage, zwischen dem südafrikanischen Schelf und dem submarinen Transkei Becken, fließen. Daraus resultiert, dass die sedimentäre Füllung des Transkei Beckens, welches sich im Osten an das Agulhas Plateau anschließt, während der vergangenen ~36 Millionen Jahre sehr stark von (proto-) NADW und (proto-) AABW beeinflusst wurde. Durch die Analyse der sedimentären Füllung wurde ein Paläoströmungsmodell erstellt, welches für diesen Zeitraum wechselnde Fließpfade und Fließstärken aufzeigt. Diese Variationen der Strömungseigenschaften wurden von großräumigen Effekten, wie der Öffnung des Tasmanischen Gateways und der Drake Passage im Oberen Eozän, oder der Schließung des Isthmus von Panama im Pliozän, gesteuert. Eine detailliertere Analyse der Depozentren des Transkei Beckens, sowie der Grenzflächen der verschiedenen seismostratigrafischen Einheiten, ergaben eine präzise Rekonstruktion der Paläofließpfade für diese Region.

Zusätzlich wurde anhand von seismischen Reflektoren mit starker Amplitude, sogenannten bright spots, paläoklimatische Bedingungen des Transkei Beckens für die Obere Kreide rekonstruiert. Die Auswertung dieser bright spots geben Anzeichen für anoxische Bedingungen in der Region südlich Südafrikas für einen Zeitraum zwischen ~90 und ~80 Millionen Jahren, was in Verbindung mit dem weltweiten Oceanic Anoxic Event 3 gebracht werden kann.

1 Introduction

The Earth's climate repeatedly has gone through significant variations. Recurrently strong worldwide climate changes have been reported since the Mesozoic (e.g. Corfield, 1994; Diester-Haass et al. 1996; Li and Keller, 1999; Zachos et al., 2001). Especially the period between ~100 Ma and ~50 Ma is characterised by a significant global cooling, commonly referred to as the greenhouse to icehouse transition (Sellwood and Valdes, 2006). The factors that trigger these global climate variations have not been fully understood yet. Certainly it is a difficult venture to reconstruct palaeo climate conditions, because they normally leave none or only inconspicuous traces. Understanding the factors that control the global climate could help us to reconstruct palaeo climate conditions and provide the opportunity for more reliable future climate models.

The different global climate controlling factors are very numerous and it is hard to quantify their particular impact. The main motor for the global heat transfer and, thus, the strongest regulator of the global climate are Thermohaline Circulations. They are basically triggered by density gradients and are responsible for the worldwide dispersal of warm and cold water masses (see Chapter 2.2). A reconstruction of Thermohaline Circulations could shed light not only on palaeo flow paths of water masses and global heat transfer, but also on location and timing of palaeo ocean gateways. This would help us to improve our knowledge about the connections between tectonics/morphology (ocean path- and gateways), flow paths/-strengths of water masses and their impact on global climate change.

A unique location for the study of the development of Thermohaline Circulations is the region south of South Africa. This area represents a crucial gateway within the global conveyor belt, which stands for the worldwide movement of thermohaline driven water masses. Here, since at least Eocene times (Scher and Martin, 2004), cold and dense proto-North Atlantic Deep Water (proto-NADW) from the Northern Hemisphere and proto-Antarctic Bottom Water (proto-AABW), triggered by the Antarctic Circumpolar Current (ACC; Orsi, et al., 1999), flow in an eastward direction from the South Atlantic into the Indian Ocean (see Chapter 2.2). The warm surface Agulhas Current (AC) flows westward from the Southwest Indian Ocean around the southern tip of South Africa into the Southeast Atlantic Ocean. Due to the very geological and tectonic situation south of South Africa (see Chapter 2.1), the deep and bottom waters have to pass the submarine Transkei Basin, where they influence or even shape the basin's sedimentary filling. Additionally, the central Transkei Basin is characterised by the sedimentary Agulhas Drift (see Chapter 2.3), which must have been influenced by bottom current activity (Niemi et al., 2000; Schlüter and Uenzelmann-Neben, 2007).

For a detailed analysis of the basin's sediments, which could reveal more details of the bottom current attributes off South Africa, AWI gathered a high resolution seismic reflection survey (see Chapter 2.4) across the submarine Transkei Basin and the Agulhas Drift in 2005.

The major questions the survey should provide answers to have been:

1) When and how did the large scale heat transfer, triggered by water mass exchange, between the Southeast Atlantic Ocean and Southwest Indian Ocean begin?
2) Is it possible to reconstruct variations in flow paths and flow strengths of (proto-) NADW and (proto-) AABW in detail and what does it look like?
3) What can a detailed deep and bottom current reconstruction reveal about transport and deposition of sediments within the Transkei Basin?
4) Which climatic conditions can be reconstructed for the initial period of sedimentation within the Transkei Basin before the onset of deep and bottom current activity in the Late Cretaceous?

The major aim of the analysis of the seismic reflection data from the central Transkei Basin has been a detailed reconstruction of the deep and bottom current activity south of South Africa for the past ~90 Ma. The results should reveal variations in palaeo climate conditions off South Africa and possibly worldwide. Moreover, the current attributes could lead to a more precise description of (palaeo-) ocean gateways since the late Mesozoic.
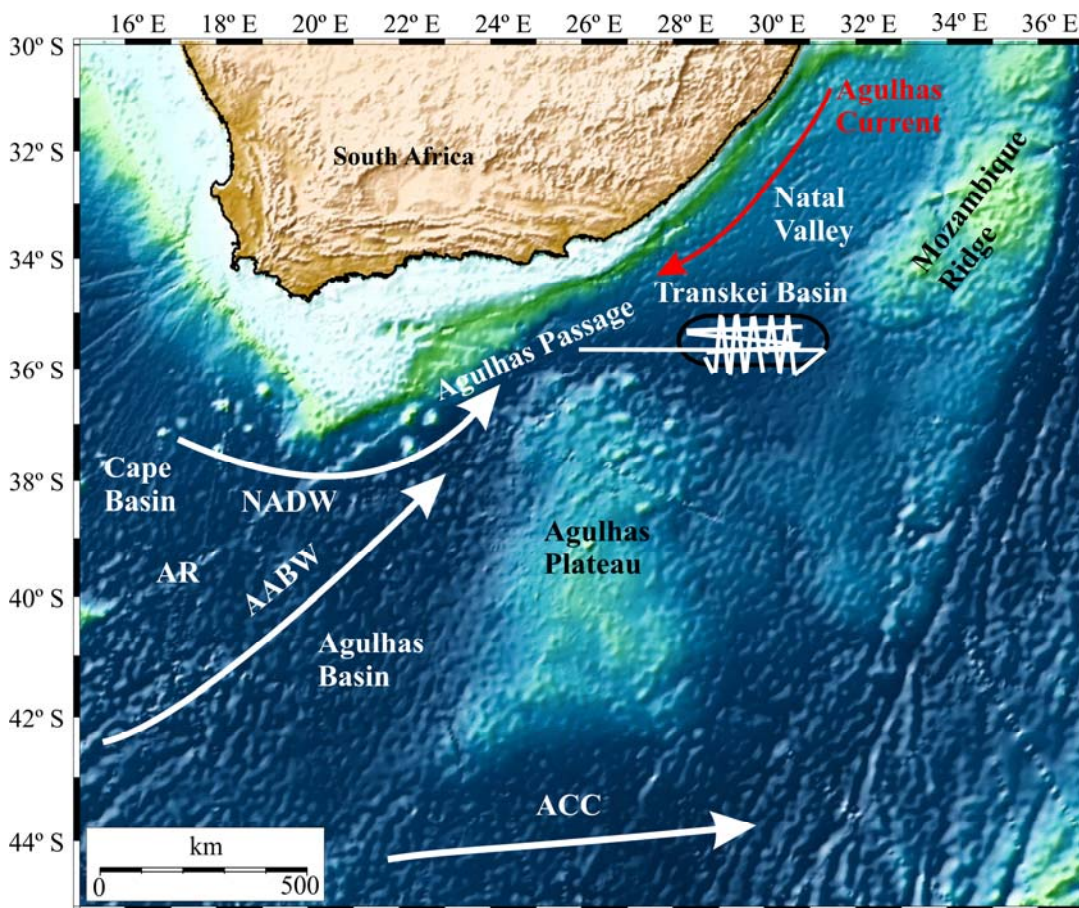
Figure 1: Bathymetric map of the region south of South Africa (after Smith and Sandwell, 1997), including the Transkei Basin as main research area of this thesis. AABW: Antarctic Bottom Water; ACC: Antarctic Circumpolar Current; AR: Agulhas Ridge; NADW: North Atlantic Deep Water. White lines in the Transkei Basin represent locations of the seismic reflection profiles. Black circle indicates schematically the location of the Agulhas Drift.

Agenda

The objective of this thesis is the detailed analysis of seismic reflection data from the submarine Transkei Basin south of South Africa considering its unique location within the global conveyor belt.

The thesis is structured as followed:

Chapter

1) The basic idea about climate variations and the problem of reconstructing palaeo currents and palaeo climate in combination with the main questions of this thesis.

2) Description of the geological and oceanographic background of the Transkei Basin and adjacent regions. Explanation of "Contourite Drifts" and "Thermohaline Circulations". Short description of the seismic reflection data gathering and the seismic processing.

3) *Schlüter, P. and Uenzelmann-Neben, G., 2007. Seismostratigraphic analysis of the Transkei Basin: A history of deep sea current controlled sedimentation. Marine Geology, 240 (1-4), 99-111.*

   In this research paper the seismostratigraphy of the Transkei Basin infill is described in detail. Furthermore, it presents a first model of (proto-) AABW and (proto-) NADW reconstruction for the area south of South Africa since Eocene times.

4) *Schlüter, P. and Uenzelmann-Neben, G., 2007. Indications for bottom current activity since Eocene times: The climate and ocean gateway archive of the Transkei basin, South Africa. In press in Global and Planetary Change.*

   This paper deals with the detailed reconstruction of depocentres, outline interfaces and sedimentation rates of the central Transkei Basin for the past ~36 Ma. The result is a precise reconstruction of palaeo current flow paths and depocentre locations of the research area.

5) *Schlüter, P. and Uenzelmann-Neben, G.,in review. Conspicuous seismic reflections in Upper Cretaceous sediments as evidence for black shales off South Africa. Submitted to Marine and Petroleum Geology.*

   The oldest sediments of the Transkei Basin infill contain recurrently appearing bright spots, whose appearance and attributes are analysed. The result is probably the first description of black shales in this area, which led to the idea of an Oceanic Anoxic Event south of South Africa in the Late Cretaceous.

6) This chapter presents a short summary of the results and presents answers on the main questions of this thesis.

7) Further problems and questions that remain are shortly discussed.

2   Background and Methods

2.1 Geological and oceanographic overview:

The region south of South Africa is characterised by several deep sea basins that are separated from each other by shallower ridges or plateaus (Fig. 1). The up to 5000 m deep Agulhas Basin is located southwest of South Africa and southeast of the Agulhas Ridge. East of the Agulhas Basin, the Agulhas Plateau forms a prominent obstacle for deep water mass movement that rises up to 1800 m below the ocean surface. The adjacent Transkei Basin, east of the Agulhas Plateau, reaches water depths of up to 4500 m and is limited to the east by the Mozambique Ridge, which rises up to 1000 m water depth. The Transkei Basin contains sedimentary sequences of up to 1800 m thickness (Schlüter and Uenzelmann-Neben, 2007). Between the South African continental shelf and the Agulhas Plateau in the south, the very narrow (<50 km width) Agulhas Passage is located, which forms a constriction for deep and bottom waters that have to flow in a west to east direction from the Southeast Atlantic into the Transkei Basin (Fig. 1). Southeast of South Africa the up to 4000 m deep Natal Valley forms, associated with the adjacent Transkei Basin and the Agulhas Passage in the west, the only deep water connection between the Southwest Indian Ocean and the Southeast Atlantic Ocean in this region (Fig. 1).

The evolution of this area started with the beginning break-up of Gondwana at ~160 ±10 Ma (e.g. Tikku et al., 2002; König and Jokat, 2006). The separation was initiated by a rifting of the Somali and Mozambique Basin, associated with ocean floor forming in the Weddell Sea at about 147 Ma (König and Jokat, 2006).

The development of the Transkei Basin is difficult to determine, because it was formed during Cretaceous times, where no magnetic anomalies are recognized (Fullerton et al., 1989). Tectonic reconstructions and the calculation of plate movement velocities and directions led to a presumed age for the development of the Transkei Basin between ~124 Ma and ~90 Ma (e.g. Dingle and Camden-Smith, 1979; Goodlad et al., 1982; Martin and Hartnady, 1986; Ben-Avraham et al., 1993). A determination of an exact age for the Transkei Basin by its sedimentary infill is not possible, either, because no drill core data from this region are available, so far.

The situation of oceanic currents off South Africa today is unique within the world's oceans, due to the large scale thermohaline currents that meet and interact within this rather small environment.

The warm and surface related Agulhas Current (AC) flows from the Indian Ocean through the Natal Valley, Transkei Basin and the Agulhas Passage westward into the Southeast Atlantic. In the Cape Basin, southwest of South Africa, it retroflects as the Agulhas Return Current partially back to the Transkei Basin and Natal Valley (Fig. 1) (Lutjeharms and Ansorge, 2001; Boebel et al., 2003).

North Atlantic Deep Water (NADW) from the polar regions of the Northern Hemisphere flows in an eastward direction through the Agulhas Passage into the Transkei Basin (Arhan et al., 2003; Mantyla and Reid, 1995). There it splits into a southward flowing branch, which becomes part of the Antarctic Circumpolar Current (ACC), and a north eastward flowing branch, which flows through the Natal Valley, the Mozambique and the Somali Basin into the Indian Ocean (Van Aken et al., 2004) A small amount of NADW mixes with other water masses, transforms to Lower Circumpolar Deep Water and flows back into the South Atlantic (Gordon, 1986; Park et al., 1993). Due to its constant inflow strength and direction through the Agulhas Passage, the NADW is, together with

Antarctic Bottom Water (AABW), responsible for the development of the Agulhas Drift in the central Transkei Basin (Fig. 1).

AABW from the polar regions of the Southern Hemisphere flows, as NADW, in an eastward direction through the Agulhas Passage and into the Transkei Basin (Arhan et al., 2003; Mantyla and Reid, 1995) and further into the adjacent Natal Valley and the Mozambique Basin (Tucholke and Embley, 1984). This bottom water is described as a water mass from Antarctic regions that is not part of a circumpolar current, although it gets triggered by the ACC (Orsi, et al., 1999).

2.2 Thermohaline Circulations:

Thermohaline Circulations are currents in the world's oceans that are driven by density gradients within the water column due to differences in water temperature and salt content (e.g. Dietrich et al., 1975; Southard and Stanley, 1976). As part of the global conveyor belt they are the main motor for heat transfer.

The global conveyor belt is a combination of different Thermohaline Circulations like the cold and dense North Atlantic Deep Water (NADW) or the warm and light Gulfstream. The mixture of warm and cold water masses that flow through the world's oceans is an independently but very slowly working motor with flow velocities of not more than some centimetres per second (Stow, et al. 2002). With a time of up to 1600 years per cycle (Primeau, 2005), it is a very slowly but stable operating system.

Warm surface waters flow pole wards (e.g. Gulfstream on the Northern Hemisphere), cool down and partially freeze. The remaining water masses become denser, due to the lower temperatures and the increasing salt content. The result is a downwelling of the denser water masses (NADW), which pulls warm surface water masses to the pole (e.g. Stommel, 1962; Winton, 1995; Marotzke and Scott, 1999). The dense deep and bottom water (NADW) flows southward through the Atlantic and eastward around South Africa into the Indian Ocean (Arhan et al., 2003; Mantyla and Reid, 1995; Van Aken et al., 2004). From the Indian Ocean a branch of NADW flows further into the Pacific, where it becomes mixed with warmer water masses and rises. It then turns back as a surface current and flows through the Indian and Atlantic Ocean back.

The most important thermohaline currents for this thesis are thermohaline driven currents like the NADW and Antarctic Bottom Water (AABW). As NADW, AABW transports cool water masses to the South African coast and partially further into the Indian Ocean. The combination of sedimentary structures, such as contourite drifts (see Chapter 2.3), that are shaped by Thermohaline Circulations (NADW, AABW), can reveal palaeo climate conditions.

2.3 Contourite Drifts:

Contourite drifts are sediment deposits in the world's oceans. The name contourite originates from former observations that those sediment bodies are exclusively located along depth-contourlines (Hollister, 1967). Recent studies (e.g. Faugères et al. 1999; Rebesco and Stow, 2001) revealed that contourite drifts are principally (though not necessarily exclusively) formed by sediment deposition of bottom currents. Bottom currents are driven by thermohaline currents (see also Chapter 2.2), wind-driven surface currents and tidal forces and they flow slope-parallel. Bottom currents move very slowly, normally between 1-2 cm/s (Stow, et al. 2002) and persist over long periods of time (more than several thousand years), so they can develop equilibrium conditions. Due to the Coriolis Force, which is triggered by the Earth's rotation, currents (also winds) are deflected to the left (right) side of their flow direction on the Southern (Northern) Hemisphere (e.g. Faugères et al., 1999; Rebesco et al., 2002; Shanmugam, 2006; see Chapter 2.2). As a result, the sedimentary content of the bottom currents become deflected to the left (right) side of the flow direction on the Southern (Northern) Hemisphere, too. Figure 2 shows a sketch of a mounded elongated drift (such as the Agulhas Drift) on the Southern Hemisphere, which must have been build-up by a current that flowed into the indicated direction (out of the plain of the Figure).

The resulting contourite drifts consist to a large amount of well sorted sand with high porosity, due to the winnowing away of mud by the bottom currents (Rebesco and Stow, 2001; Stow et al., 2002).
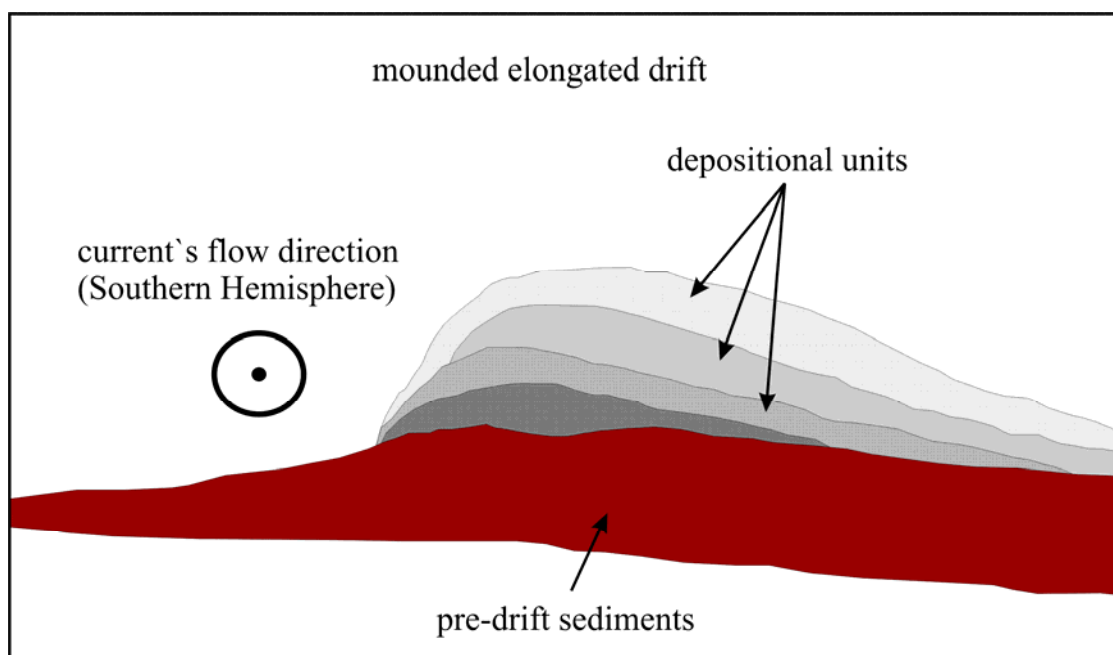

Figure 2: Simplified sketch of a mounded elongated drift with the corresponding bottom current flow direction according to the Coriolis Force on the Southern Hemisphere. (Modified after Stow et al., 2002)

Contourite drifts principally can be found in every depth location below 300 m water depth and nearly all over the world's oceans (Stow et al., 2002). They are observed on shelf breaks (e.g. Norwegian Sea, Laberg, et al., 2002) or close to continental rises (e.g. Nova Scotia Rise, McCave et al., 2002) but also in the deep sea (e.g. central Scotia Sea, Maldonado et al., 2003).

Due to the sand content sediment drifts have a large economic potential and are of high interest for the oil industry. They contain a record of palaeo environmental conditions, such as palaeo climate and palaeo oceanographic variations. Deposition and erosion of contourite drifts give evidence for changing oceanographic conditions and, thus, for climate change or large-scale tectonic events. Contourite drifts are an important tool for reconstructing palaeo environmental conditions in not only south of South Africa.

The shape and size of a contourite drift is dependent on its surrounding environment and the attributes of the corresponding bottom currents. It provides information about palaeo flow paths and palaeo flow strengths of the bottom currents and, consequentially, of palaeo climate conditions. The problem is to identify contourite drifts on seismic sections, because they are partially interbedded into the surrounding sediments, making their identification difficult. According to the different depth ranges, shapes and sizes, contourite drifts can be subdivided into seven different types (Figure 3; Rebesco and Stow, 2001; Stow et al., 2002):

1) *Sheeted drifts* are characterised by a low relief, as part of the fill of basin plains or plastered against the continental margin. They comprise a layer of constant thickness (up to some hundred meters) that covers a large area, with a slight decrease in thickness towards its margins. The internal seismofacies is of low amplitude and discontinuous reflectors or partially transparent. They are located in abyssal regions and at the continental slope. (e.g. Argentine Basin, Gloria Drift)

2) *Mounded elongated drifts* are characterised by a moderate to high relief and a variable lateral extend between tens of km to more than 1000 km in length. They can occur everywhere in the world's oceans, from the shelf/slope to the abyssal plains, depending on the depth at which the bottom current flows. The margins are generally flanked by distinct moats along the flow axis. The internal seismofacies shows progradation with lenticular, convex-upward deposition. Partially sediment waves can occur. (e.g. Agulhas Drift, Feni Drift)

3) *Channel-related drifts* are sheeted drifts with a mounded or cone-shaped geometry. They occur within channels, moats, passageways or gateways through which the bottom circulation is constrained so that flow velocities increase. The areal extend varies between a few tens of square kilometres up to ten thousand square kilometres. The internal seismofacies can show chaotic structures or even be reflector free. (e.g. Vema Channel, Faroe-Shetland Channel)

4) *Confined drifts* are rarely observed within subsiding basins or troughs that are tectonically active. The areal extend varies between thousand and some ten thousand square kilometres. Their seismic characters are comparable to mounded elongated drifts. (e.g. Chatham Rise, Aleutian Trench)

5) *Infill drifts* are characterised by a moderate relief with a variable shape that are formed as the local infill of topographic depressions. They can be found at the head of slump scars or at the margins of slumps. The seismofacies shows downwards prograding reflectors. (e.g. Hebridian slope, Gulf of Cadiz)

6) *Mixed drift systems* are mixtures of downslope and alongslope structures like turbidite-contourites, debris-contourites or glacigenic-contourites. They are observed at ocean margins, as well as in the deep sea. Their size can vary between moderate to extreme values. (e.g. Weddell Sea, Nova Scotian margin)

7) *Fault-controlled drifts* can be found at a fault-generated basement relief or at reactivated syn-depositional faults.
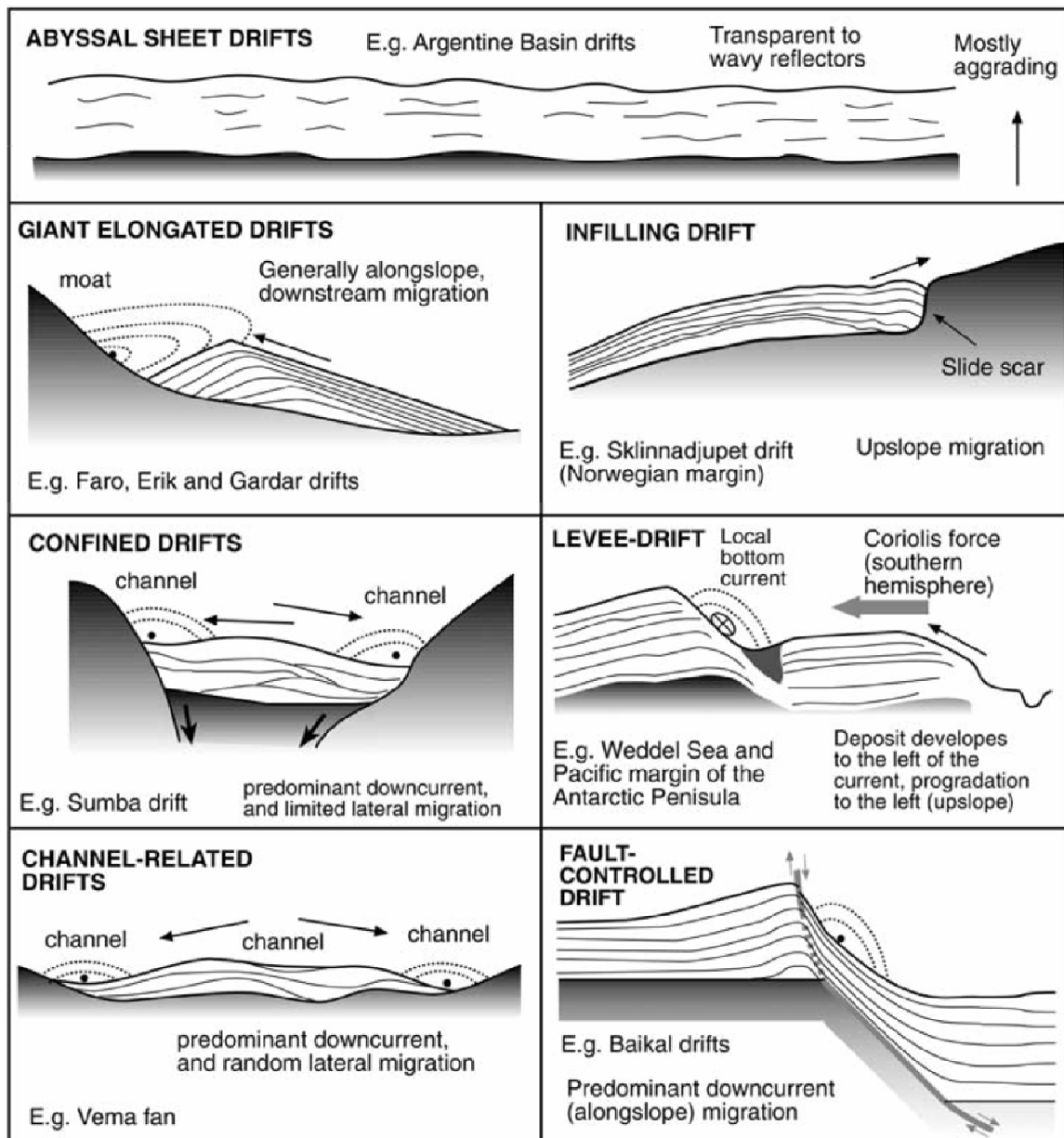

Figure 3: Summary of different types of contourite drifts showing large-scale geometry, migration trend (black arrows) and inferred axis of bottom-currents flow (dashed arches). After Rebesco and Stow, 2001.

2.4 Seismic Reflection data:

2.4.1 General seismic arrangement and equipment:

The multichannel seismic reflection data this thesis deals with, were collected by *RV SONNE* in April and May 2005 south of South Africa under direction of the Alfred Wegener Institute for Polar and Marine Research (AWI) and consisted of 16 profiles with a total length of more than 2800 km. As source three GI-Guns ™ with a total gun chamber volume of 7.2 l were used. Each GI-Gun ™ consisted of a generator chamber (0.7 l) and an injector chamber (1.7 l), which produced the seismic signal and suppressed the bubble. The guns were fired every 10 s, which corresponds to an average shot spacing of ~25 m. The record length of the incoming reflected seismic signals was 9 s at a time and comprised frequencies of up to 300 Hz. The guns were towed approximately 20 m behind the ships stern and ~2 m below the water surface. The reflected waves from the subsurface were detected with a 2400 m long (2250 m active length) Sercel SEAL ™ streamer that consisted of 180 channels (Fig. 4).

The first profile AWI 20050001 was shot from the very west to the east of the Transkei Basin (Fig. 1) to determine the exact location of the Agulhas Drift, which has not been exactly known until then (Niemi et al., 2000). After locating the drift in the central Transkei Basin, we shot the following 15 seismic profiles grid-like in a zigzag style to cover as much as possible of the Agulhas Drift (Fig. 1).
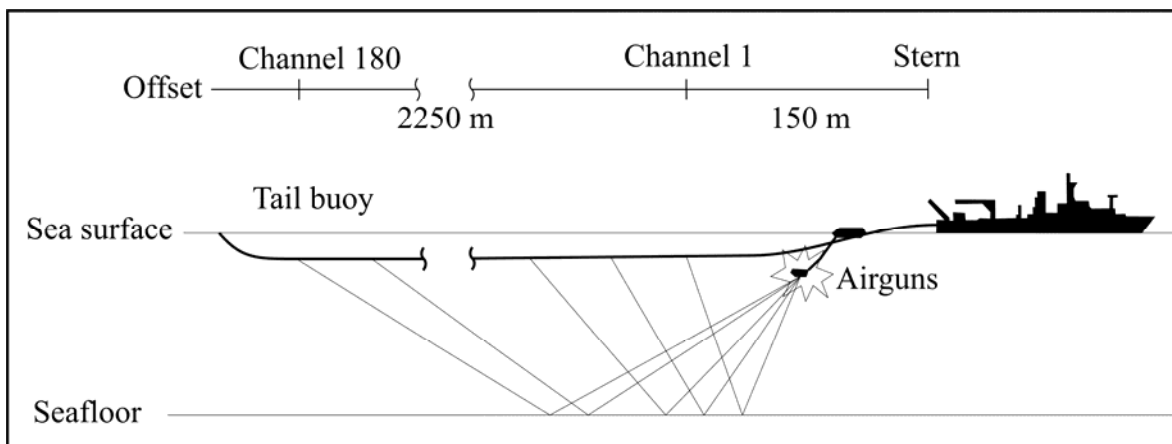

Figure 4: Reflection seismic data acquisition geometry on RV SONNE cruise SO 182. Active streamer with 180 digital channels (hydrophones) and a lead in cable of 150 m. Modified after Ehrhardt, 2004)

2.4.2 Multichannel seismic data processing:

The following processing steps were applied to the seismic data:

- Inverting the navigational data
- CDP Sorting
- Trace Editing
- Velocity Analysis
- Normal Moveout Correction
- Filtering
- Stacking
- Depth Migration

At first the incoming digital data were stored on magnetic tapes, followed by the sorting within 25 m subsurface intervals to form common depth point gathers (CDP Sorting). The trace editing comprised the detection and deleting of conspicuous signals with extreme frequencies and amplitudes. A velocity analysis was carried out for every 50th CDP. The normal moveout correction (NMO) reduced the differences in traveltime from a reflecting surface to the source-to-geophone distance. A bandpass filter cut all frequencies less than 10 Hz and more than 180 Hz and partially cut frequencies between 10 and 20 Hz and 150 and 180 Hz. Finally, the CDPs were stacked, according to the velocity analysis and the NMO-correction (Yilmaz, 2001).

After stacking, a velocity depth model was applied to the data to create depth migrated sections (Yilmaz, 2001).

All seismic processing steps were carried out with Focus/Disco software from Paradigm ™.

2.4.3 Seismic data interpretation:

The processed seismic reflection data were uploaded and interpreted on a Landmark Seisworks 2D ™ system. The stratigraphy for the Transkei Basin was correlated from Niemi et al`s. (2000) seismic stratigraphy from the adjacent Natal Valley, except for reflector E. This reflector was added to the stratigraphy, because, in contrast to the seismic reflection data from the Natal Valley, a significant change in reflection characteristics within the Transkei Basin was observed.

The interface outlines for 5 different time slices between the Late Cretaceous and the Pliocene were created by exporting the depth information of each stratigraphic horizon from the Landmark system into an external database. The depth information for each horizon was then gridded and displayed with the Generic Mapping Tool (GMT ™) software (Wessel and Smith, 1991).

The depocentres for each stratigraphic unit were defined by the root mean square (rms) value of the according unit thickness. Values with more than 50% of the rms were defined as depocentre. Both the interface outlines, as well as the depocentre locations were used to analyse sediment deposition. Furthermore, sedimentation processes, in accordance to palaeo current activities were reconstructed.

3 References

Arhan, M., Mercier, H. and Park, Y.-H., 2003. On the deep water circulation of the eastern South Atlantic Ocean. Deep Sea Research Part I: Oceanographic Research Papers, 50, 7, 889 – 916.

Ben-Avraham, Z., Hartnady, C. J. H. and Malan, J. A., 1993. Early tectonic extension between the Agulhas Bank and the Falkland Plateau due to the rotation of the Lafonia microplate. Earth and Planetary Science Letters, 117, 43 – 58.

Boebel, O., Lutjeharms, J., Schmid, C., Zenk, W., Rossby, T., Barron, C., 2003. The Cape Cauldron: a regime of turbulent inter-ocean exchange. Deep Sea Research II, 57 – 86.

Corfield, M., 1994. Palaeocene oceans and climate: An isotopic perspective. Earth Science Reviews, 37, 3-4, 225 – 252.

Diester-Haass, L., Robert, C., Chamley, H., 1996. The Eocene-Oligocene preglacial-glacial transition in the Atlantic sector of the Southern Ocean (ODP Site 690). Marine Geology, 131, 123 – 149.

Dietrich, G., Kalle, K., Krauss, W., Siedler, G., 1975. Allgemeine Meereskunde. Eine Einführung in die Ozeanographie. Gebr. Borntraeger, Berlin, 328 pp.

Dingle, R. V. and Camden-Smith, F., 1979. Acoustic stratigraphy and current-generated bedforms in deep ocean basins off southeastern Africa. Marine Geology, 33, 3-4, 239 – 260.

Erhardt, L. A., 2004. Seismic and Hydroacoustic Studies of Surficial Sediment Tectonics along the Northern Red Sea Rift and the Dead Sea Transform Fault. Dissertation Universität Hamburg.

Faugères, J.-C., Stow, D. A. V., Imbert, P. and Viana, A., 1999. Seismic features diagnostics of contourite drifts. Marine Geology, 162, 1 – 38.

Fullerton, L. G., Frey, H. V., Roark, J, H. and Thomas, H. H., 1989. Evidenec for a remanent contribution in Magsat data from the Cretaceous Quiet Zone in the South Atlantic. Geophysical Research Letters, 16, 1085 – 1088.

Goodlad, S. W., Martin, A. K. and Hartnady, C. J. H., 1982. Mesozoic magnetic anomalies in the southern Natal Valley. Nature, 295, 686 – 688.

Gordon, A. L., 1986. Interocean exchange of thermocline water. Journal of Geophysical Research, 91, 5037 – 5046.

Hollister, C. D., 1967. Sediment distribution and deep circulation in the western North Atlantic. In: Gordon, A. L. (Ed.), Studies in Physical Oceanography, vol. 2, Gordon and Breach Science Publishers, New York, 37 – 66.

König, M., and Jokat, W., 2006. The Mesozoic breakup of the Weddell Sea. Journal of Geophysical Research, 111, doi:10.1029/2005JB004035.

Laberg, J. S., Vorren, T. O., Knutsen, S. M., 2002. The Lofoten Drift, Norwegian Sea. Geological Society, London, Memoirs, 22, 57 – 64.

Li, L., Keller, G., 1999. Variability in Late Cretaceous climate and deep waters: evidence from stable isotopes. Marine Geology, 161, 3-4, 171 – 190.

Lutjeharms, J. R. E. and Ansorge, I. J., 2001. The Agulhas Return Current. Journal of Marine Systems, 30, 1-2, 115 – 138.

Maldonado, A., Barnolas, A., Bohoyo, F., Galindo-Zaldivar, J., Hernandez-Molina, J., Lobo, F., Rodriguez-Fernandez, J., Somoza, L., Vazquez, J. T., 2003. Contourite deposits in the central Scotia Sea: The importance of the Antarctic Circumpolar Current and the Weddell Gyre flows. Palaeogeography, Palaeoclimatology, Palaeoecology, 198, 1-2, 187 – 221.

Mantyla, A. W. and Reid, J. L., 1995. On the origins of deep and bottom waters of the Indian Ocean. Journal of Geophysical Research, 100 (c2), 2417 – 2439.

Marotzke, J., Scott, J., 1999. Convective mixing and the thermohaline circulation. Journal of Physical Oceanography, 29, 2962 – 2970.

Martin, A. K. and Hartnady, C. J. H., 1986. Plate tectonic development of the Southwest Indian Ocean: a revised reconstruction of East Antarctica and Africa. Journal of Geophysical Research, 91, 4767 – 4786.

McCave , I. N., Chandler, R. C., Swift, S. A., Tucholke, B. E., 2002. Contourites of the Novia Scotian continental rise and the HEBBLE area. Geological Society, London, Memoirs, 22, 21 – 38.

Niemi, T. M., Ben-Avraham, Z., Hartnady, C. J. H. and Reznikov, M., 2000. Post-Eocene seismic stratigraphy of the deep ocean basin adjacent to the Southeast African continental margin: a record of geostrophic bottom current systems. Marine Geology, 162, 2-4, 237 – 258.

Orsi, A. H., Johnson, G. C. and Bullister, J. L., 1999. Circulation, mixing, and production of Antarctic Bottom Water. Progress in Oceanography, 43, 55 – 109.

Park, Y.-H., Gamberoni, L., Charriaud, E., 1993. Frontal structure, water masses, and circulation in the Crozet Basin. Journal of Geophysical Research, 98, 12361 – 12385.

Primeau, F., 2005. Characterizing transport between the surface mixed layer and the ocean interior with a forward and adjoint global ocean transport. Journal of Physical Oceanography, 35, 545 – 564.

Rebesco, M. and Stow, D. A. V., 2001. Seismic expression of contourites and related deposits: a preface. Marine Geophysical Researches, 22, 303 – 308.

Rebesco, M., Pudsey, C. J., Canals, M., Camerlenghi, A., Barker, P. F., Estrada, F., Giorgetti, A., 2002. Sediment drifts and deep-sea channel systems, Antarctic Peninsula Pacific Margin. Geological Society Memoirs, 22, 353 – 372.

Scher, H. D. and Martin, E. E., 2004. Circulation in the Southern Ocean during the Paleogene inferred from neodymium isotopes. Earth and Planetary Science Letters, 228, 3-4, 391 – 405.

Schlüter, P. and Uenzelmann-Neben, G., 2007. Seismostratigraphic analysis of the Transkei Basin: A history of deep sea current controlled sedimentation. Marine Geology, 240 (1-4), 99-111.

Sellwood, B. W., Valdes, P. J., 2006. Mesozoic climates: General circulation models and the rock record. Sedimentary Geology, 190, 1-4, 269 – 287.

Shanmugam, G., 2006. Deep-water processes and facies Models. Handbook of Petroleum Exploration and Production, vol. 5, Elsevier.

Smith, W., H., F., and Sandwell, D., T., 1997. Global seafloor topography from satellite altimetry and ship depth soundings, Science, 277, 1957 - 1962.

Southard, J. B., Stanley, D. J., 1976. Shelf-break processes and sedimentation. In: Stanley, D. J., Swift, D. J. P. (Eds.), Marine Sediment Transport and Environmental Management. John Wiley & Sons, New York, 351 – 377.

Stommel, H., 1962. On the smallness of sinking regions in the ocean. Proceedings of the National Academy of Sciences, Washington, 48, 766 – 772.

Stow, D. A. V., Faugères, J.-C., Howe, J. A., Pudsey, C. J., Viana, A. R., 2002. Bottom currents, contourites and deep-sea sediment drifts: current state-of-the-art. Geological Society, London, Memoirs, 22, 7 – 20.

Tikku, A. A., Marks, K. M., Kovacs, L. C., 2002. An Early Cretaceous extinct spreading center in the northern Natal Valley, Tectonophysics, 347, 1-3, 87 – 108.

Tucholke, B. E., Embley, R. W., 1984. Cenozoic regional erosion of the abyssal sea floor off South Africa. Interregional Unconformities and Hydrocarbon Accumulation. AAPG Memoir, 36, 145 – 164.

Van Aken, H. M., Ridderinkhof, H., de Ruijter, W. P. M., 2004. North Atlantic Deep Water in the south-western Indian Ocean. Deep Sea Research Part I: Oceanic Research Papers, 51, 6, 755 – 776.

Wessel, P., and Smith, W. H. F., 1991. Free software helps map and display data, Eos Trans., AGU, 72, 441.

Winton, M., 1995. Why is the deep sinking narrow? Journal of Physical Oceanography, 25, 997 – 1005.

Yilmaz, Ö., 2001. Seismic data analysis. Processing, Inversion and Interpretation of seismic data. Society of Exploration Geophysicists.

Zachos, J., Pagani, M., Sloan, L., Thomas, E., Billups, K., 2001. Trends, rhythms and aberrations in global climate 65 Ma to present. Science, 292, 686 – 693.

4 Seismostratigraphic analysis of the Transkei Basin: A history of deep sea current controlled sedimentation

Philip Schlüter, Gabriele Uenzelmann-Neben

4.1 Abstract:

The Earth`s climate is controlled by various factors, with large scale ocean currents playing a significant role. In particular, the global thermohaline circulation of water masses like the Antarctic Bottom Water (AABW), or the North Atlantic Deep Water (NADW), is a global motor for maintaining the exchange of water masses. The AABW and NADW have met and interacted off South Africa since Oligocene times. Here, the narrow deep Agulhas Passage gateway, located between South Africa and the submarine Agulhas Plateau, constrains bottom water exchange between the southeast Atlantic and the southwest Indian Ocean. A seismostratigraphic analysis of sedimentary structures in the Transkei Basin, which opens up at the eastern end of the Agulhas Passage, was carried out, to reconstruct the palaeocurrents off South Africa. The analysis of newly collected high resolution seismic reflection data showed the effect of large scale current deposition. There are at least 5 major sedimentary phases to observe, some of which seem to be influenced by NADW and AABW. The first stage represents ongoing deep sea sedimentation from middle Cretaceous to middle Tertiary times. Later stages are separated by discordances, which represent the onset of AABW and NADW, among others, triggered by the opening of the Drake Passage gateway (~35 Ma) and the closure of the Isthmus of Panama (~3 Ma). We found two large drift bodies located one above the other. Corresponding to their shape and position, the older drift is inferred to have been deposited by currents flowing in a north-southerly direction, whereas the younger drift lies perpendicular to it and seems to be built up by west-east flowing currents.

Keywords: Contourite Drifts; Transkei Basin; deep sea currents; seismostratigraphy; palaeoceanography, Agulhas Drift

Published in: Schlüter, P. and Uenzelmann-Neben, G., 2007. Seismostratigraphic analysis of the Transkei Basin: A history of deep sea current controlled sedimentation. Marine Geology, 240 (1-4), 99-111.

4.2 Introduction:

The area off South Africa is a crucial gateway for thermohaline water masses circulating between the Indian and the Atlantic Ocean. Warm and saline surface water masses of the Agulhas Current (AC), which originate in the Indian Ocean, meet cold and dense deep water masses like the North Atlantic Deep Water (NADW) and the Weddell Sea originating Antarctic Bottom Water (AABW) (Fig. 1). The AC flows westward and separates from South Africa at the Agulhas Bank, close to Cape Agulhas and retroflects as the Agulhas Return Current backwards into the Transkei Basin and Natal Valley (Boebel et al., 2003). Contrary to the AC, the AABW and the NADW flow eastward around the southern tip of Africa. AABW is mainly produced in the Weddell Sea and partially flows north eastwards into the Cape Basin and through the Agulhas Passage into the Transkei Basin and adjacent Natal Valley and Mozambique Basin (Tucholke and Embley, 1984). NADW is formed in Arctic regions and flows southward into the Cape Basin and, like parts of the AABW, through the Agulhas Passage into the Mozambique and Somali Basin (Van Aken et al., 2004). Due to mixing and upwelling, parts of NADW become transformed to Lower Circumpolar Deep Water, which flows back into the South Atlantic (Gordon, 1986; Park et al., 1993).

The submarine Transkei Basin is a small deep sea basin, located south of the continental margin off South Africa and southwest of the Natal Valley (Fig. 1). The western flank of the basin is limited by the submarine Agulhas Plateau and its eastern flank is limited by the Mozambique Ridge. The Transkei Basin is characterised by a sedimentary infill with a thickness of up to 2 s Two-Way-Traveltime (TWT) (~1800 m) of unknown origin, whereas its average water depth lies around 4500 m. In fact, these sediments are shaped by strong deep sea and bottom currents (Niemi et al., 2000).

The Agulhas Plateau forms a 2000 m high obstacle to deep currents, leaving only the very narrow Agulhas Passage gateway between it and the African coast as a deep water path. NADW and a western branch of AABW have to flow through the Agulhas Passage to enter the Transkei Basin and the adjacent Natal Valley (Fig. 1). A second branch of AABW flows northward along the eastern flank of the Agulhas Plateau into the southern Transkei Basin (Garabato et al., 2002).

Thus, the influence of NADW and AABW on deposition and re-deposition of sediments in the Transkei Basin is strong. Due to the deep water constriction the flow velocity increases and with it the ability to transport higher amounts of sediment within the water column. Sediments, which are transported within the water column of the deep sea currents, rush through the Agulhas Passage and are deposited in the Transkei Basin. As a consequence, the Transkei Basin sediments represent a record of NADW and AABW variability.

A tectonic reconstruction of the Transkei Basin's development is difficult. The exact age of the basement cannot be determined precisely, because it was developed during the magnetic quiet zone in Cretaceous times (Fullerton et al., 1989). The initial rifting between South America and Africa began at about 124 Ma (Goodlad et al., 1982; Tikku et al., 2002) first forming the Natal Valley and later the Transkei Basin. Early studies by Dingle and Camden-Smith (1979) revealed a maximum age of Lower Cretaceous for the Transkei Basin. Finally, it is presumed that spreading in the Transkei Basin was complete by around 90 Ma (Martin and Hartnady, 1986; Ben-Avraham et al., 1993).

Here, we present the analysis of a tight grid of newly collected seismic reflection data, which lead to a better understanding of the depositional processes and hence the evolution of the ocean currents in the Transkei Basin area.

4.3 Data acquisition:

In 2005, the Alfred Wegener Institute for Polar- and Marine Research gathered more than 2800 km of high resolution seismic reflection data in the Transkei Basin off South Africa with the German research vessel SONNE (Fig. 1). Three GI-guns©, with a total chamber volume of about 7.2 l, were used as seismic source. Each of the Gi-guns© consisted of a generator chamber (0.7 l volume) producing the seismic signal and an injector chamber (1.7 l volume), which was triggered with a 33 ms delay to suppress the bubble. The guns were fired every 10 seconds (corresponding to a shot-spacing of approximately 25 m), producing signals with frequencies of up to 300 Hz. The guns were towed about 20 m behind the ship, 2 m below the surface. Data were received using a high resolution seismic data acquisition system (SERCEL SEAL©), consisting of both onboard and in-sea equipment. The total active streamer length was 2250 m, consisting of 180 channels, and additionally a lead-in cable length of 150 - 170 m (depending on the seismic profile). Navigation data were specified by GPS (Global Positioning System). Processing of the seismic reflection data comprised demultiplexing, geometry definition using the ship`s navigation data, and CDP-sorting with a CDP spacing of 25 m. No deconvolution was carried out, since the very high signal to noise ratio and absence of multiples did not require this. A precise velocity analysis (every 50 CDP) was carried out and used for spherical divergence and normal moveout correction. After stacking, a time-migration was carried out. Filtering or gain modules were applied to the data only for on-screen analysis.
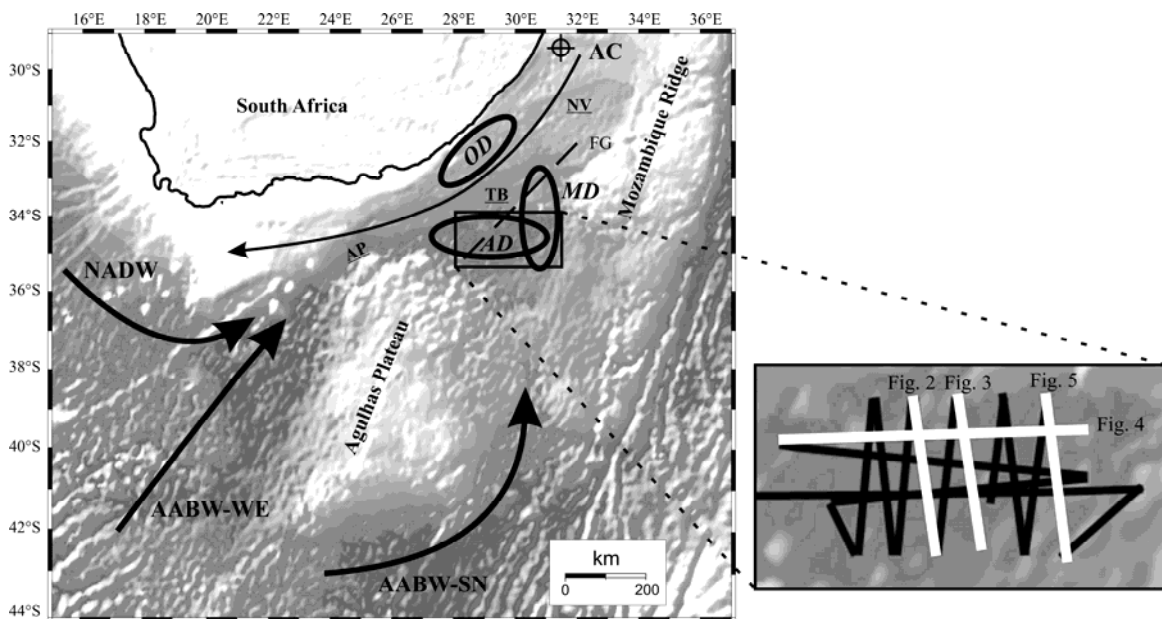

Figure 1: Bathymetric map of the reasearch area off South Africa. AABW-SN: Antarctic Bottom Water flowing in south-north direction, east of the Agulhas Plateau; AABW-WE: Antarctic Bottom Water flowing in west-east direction through the Agulhas Passage; AC: Agulhas Current; AD: Agulhas Drift; AP: Agulhas Passage; FG: Seismic reflection line F-G of Niemi et al. (2000); MD: M-Drift; NV: Natal Valley; NADW: North Atlantic Deep Water; OD: Oribi-Drift; Crossed circle: Borehole on the continental shelf; TB: Transkei Basin. Arrows indicate approximate flow paths of the AABW, the AC and NADW. Black lines indicate high resolution seismic reflection survey profiles. The grey lines show the location of the seismic lines displayed in Figs. 2-5.

4.4 Seismostratigraphic concept:

Numerous seismostratigraphic models have been created for the Transkei-Basin, Natal-Valley and adjacent regions. In 2000, Niemi et al. reviewed all existing models and created a revised stratigraphy (Table 1). We define our seismostratigraphy based on this model. Furthermore, our seismic reflection data cross the locations of Niemi et al.´s (2000) data (line F-G in Fig. 1) and, thus, the stratigraphy should correlate well. However, the seismic reflection data used by Niemi et al. (2000) were collected with a gun-chamber volume of 3 l and a 6 channel streamer, while we used 7.2 l gun-chamber volume and a 180 channel digital streamer. The different survey equipment generated qualitatively different results, which made a correlation more difficult than anticipated. Because of the lack or inaccessibility of any DSDP, ODP, IODP or other drill core data in abyssal regions off southern Africa, the dating of units or prominent horizons remains uncertain. Only one borehole, located on the continental shelf near Stanger, South Africa, is useful for this purpose (Fig. 1) (Du Toit and Leith, 1974). Unfortunately, the drill site is located about 1000 km away from our survey and contains only data from the continental shelf, which makes correlation a difficult venture. Seismic line R-74-10 of Niemi et al. (2000; their Fig. 6) shows the problem in correlating any stratigraphic information from the shallow continental shelf region above the shelf break into the deep sea. We are aware of the fact that the well is a long way from our set of seismic lines and influenced by its proximal depositional environment. Thus, a direct tie was not possible. Still, drilling results provided information on the nature of several discontinuities observed in the sedimentary column and the processes that shaped the southeast African margin in general. This information was used to date the prominent unconformities in our lines. In the following section, the sedimentary units are described seismostratigraphically from bottom to top, beginning with the seismic basement.

seismostratigraphic units of the Transkei Basin	thickness TWT (ms)	estimated age (Ma)	material	characteristics	defined stratigraphy
Unit 1 (Paleocene/Eocene)	800 - 1000	>90 - ~36	homogenous, pelagic sediments (?)	slow deep sea sedimentation	Mid-Cretaceous (1), Cenomanian (4), McDuff (5)
Unit 2 (E) (Late Eocene)	20 - 30	~36 - ~34	heterogeneous, mid grained clastics, pelagic sediments (?)	transition unit during onset of AABW	E (7), LE (4)
Unit 3 (O) (Eocene/Oligocene)	0 - 80	~34 - ~15	heterogeneous, mid grained clastics, pelagic sediments (?)	W-E flowing AABW transported sediments into Transkei Basin and Natal Valley; development of Oribi Drift	O (1), LO (4), Angus (5), A (6)
Unit 4 (M) (Middle Miocene)	50 - 130	~15 - ~3	heterogeneous, mid grained clastics, pelagic sediments (?)	Miocene cooling shifted major flow path of AABW to east of the Agulhas Plateau; development of M-Drift	M (1), D (2), P.E. (3), UM (4), A1 (6)
Unit 5 (P) (Early Pliocene)	100 - 500	~3	heterogeneous, mid grained clastics, pelagic sediments (?)	Onset of NADW by closure of Isthmus of Panama; development of Agulhas-Drift	P (1), C (3), J (5), A3 (6)

Table 1: Compilation of defined seismic stratigraphy and seismic reflector nomenclature according to author: (1) Niemi et al. (2000); (2) Emery et al. (1975); (3) Westall et al. (1984), Dingle, Robson (1985); (4) Tucholke, Embley (1984); Martin et al. (1982); Raillard (1990); (7) this paper. After Niemi et al. (2000).

4.4.1 Seismic Basement:

The seismic basement represents the top of the oceanic crust, which appears on all seismic sections as a very high amplitude reflection in depths of between 7100 and 7800 ms TWT (Figs. 2 – 5). On the more eastern profiles, the boundary of sedimentary layers and oceanic crust appears as a linear reflector with some small scale uplifts, which do not affect the overlying sediment pile intensively. In contrast, the western profiles show, especially in their southerly parts, a rugged and indented structure (Fig. 2, CDPs 0 - 2000). The sediments directly overlying these regions are homogeneous and possess nearly no internal structure, which is an indication for continuous sedimentation of similar material over a longer period of time. Oceanic crust of the Transkei Basin was accreted over a 30 m.y. period during Early Cretaceous times at a spreading ridge south of the Falkland-Agulhas Fracture Zone. By Middle Cretaceous times, about 90 Ma (Martin and Hartnady, 1986; Ben-Avraham et al., 1993), the ridge segment had passed the Agulhas Plateau into the South Atlantic. The occurrence of partly rugged oceanic crust (Fig. 2, CDPs 0 – 2000) can be described as the result of interaction between oceanic crustal accretion processes and the cooling effect of the adjacent continental lithosphere (Reznikov et al., 2005).

Profile AWI-20050009 (Fig. 2, CDPs 4100 – 4300) shows a basement high in the north, where the basement reflector rises from 7700 ms TWT to 6900 ms TWT. The adjacent sediments are only slightly disturbed by this feature. The basement rises up to ~ 800 ms TWT above the surrounding level, but the adjacent sediments are pushed up by only 50 ms TWT (Fig. 2, CDPs 4100 – 4300; 6400 – 7600 ms TWT). A syn-sedimentary basement deformation, occurring roughly between 90 and 20 Ma, would explain the only slightly disturbed sediments around this feature. We cannot say whether the basement deformation is still continuing because of the ambiguous reflection characteristics of the overlying sediments (Fig. 2, CDPs 4100 – 4300). Additionally, not the whole sedimentary column is deformed. Ben-Avraham et al. (1994) described a similar basement high observed in the Natal Valley and interpreted it as an intrusive body related to active volcanism. We can add little to this theory of ongoing volcanism, since this is the only basement high resolved within our data.

4.4.2 Unit 1:

On all seismic sections, unit 1 is characterized by mostly very weak internal reflections. Unit 1 is by far the thickest reflection unit in the investigated area. The thickness varies between 800 and 1000 ms TWT (~700 – 900 m). Internal reflections are mostly weak and partially transparent (Fig. 3, e.g. CDPs 100 – 800; 6800 – 7400 ms TWT). Occasional high amplitude reflectors can be observed (Fig. 3, CDPs 2500 – 3200; 7000 – 7200 ms TWT). Reflector spacing slightly increases with increasing depth. The whole of unit 1 seems to have been built up by slow deep sea sedimentation. Within unit 1, there are bunches of small vertical to sub-vertical faults. These faults (small scale, vertical to sub-vertical, swarm-like appearance) may be caused by fluids moving within the sediment, possibly initiated by changing sedimentation rates, or varying current strengths or directions. We do not have any borehole information from within the Transkei Basin sediments. The nearest drill site is located on the continental shelf off southeast Africa (Du Toit and Leith, 1974).
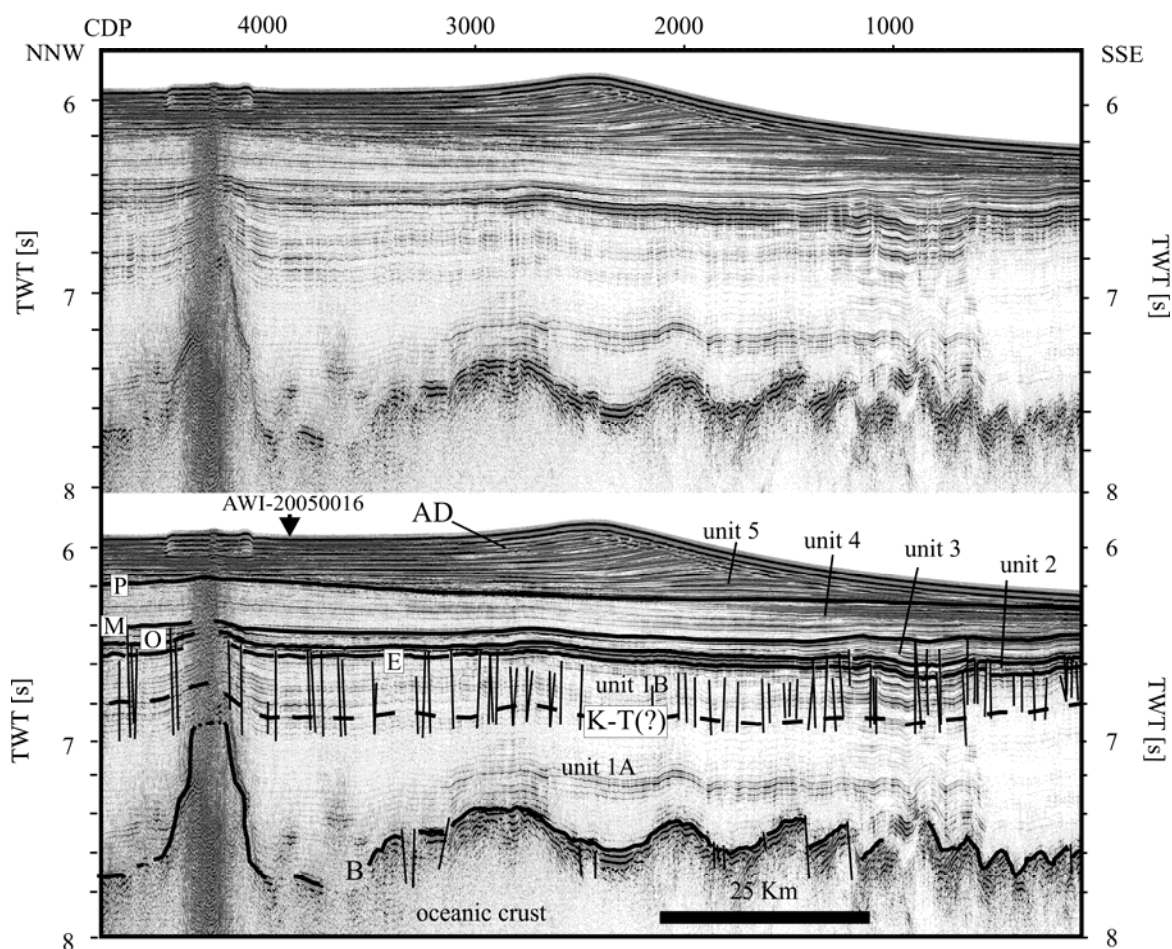
Figure 2: Seismic reflection profile AWI-20050009 showing acoustic basement and seismostratigraphic units 1-5. AD: Agulhas Drift; B: Basement; E: Late Eocene; M: middle Miocene; O: Eocene/Oligocene boundary; P: early Pliocene; dashed line: K-T boundary; the arrow indicates the intersection with seismic reflection profile AWI-20050016 (Fig. 4).

Niemi et al. (2000) used the downhole stratigraphy to correlate with their seismic reflection data from the adjacent Natal Valley. The well data revealed two major unconformities, which were related to events at the Cretaceous-Tertiary

boundary (K-T boundary) and the Eocene-Oligocene boundary (Du Toit and Leith, 1974).

The Eocene-Oligocene boundary can be identified on our profiles as the reflector "O" (Niemi et al., 2000), which will be discussed later. According to Niemi et al. (2000), the transition zone from undisturbed, homogeneous sediments of lower unit 1 to the overlying heavily faulted part correlates with the K-T boundary (Figs. 2 – 5). Hence, we can subdivide unit 1 into subunits 1A (Late Cretaceous) and 1B (early Tertiary).

A reflection band with higher amplitude reflections is observed on nearly all profiles, between 7100 and 7400 ms TWT. This band appears as a cluster of 2 to 4 reflectors,

which represent higher amounts of energy than in the adjacent regions (Fig. 3, CDPs 2500 – 3200; Fig. 4, CDPs 1100 – 1900). Apart from the increased amplitude, there is no fault-cut or other kind of discontinuity with respect to the surrounding reflectors. The observations are more easily interpreted as the result of diagenetic processes within the sediment, perhaps as a result of dewatering and superimposed load. Another possible explanation for these high amplitude features could be the existence of black shales. Huge amounts of black shales were found, by drilling on ODP leg 207 off Guyana, close to the Demerara Rise (Erbacher et al. 2004), in an environment similar to the Transkei Basin.

We assume a crustal age of approximately 90 Ma for the Transkei Basin (Martin and Hartnady, 1986; Ben-Avraham et al., 1993). A short cooling event occurred about 36 Ma ago, possibly leading to a variation of current attributes and, hence, modifications of the depositional environment in the Transkei Basin (Diester-Haass et al., 1996). In our data this event is documented by reflector "E" (Table 1). Additionally, the K-T boundary could be identified within unit 1. As a consequence we presume the whole unit 1 (subunits 1A and 1B) to have been deposited between Middle Cretaceous and late Eocene times (~90 - ~36 Ma).

4.4.3 Unit 2:

On almost every north-south trending profile, unit 2 appears as a thin but very strong reflection band, consisting of two prominent reflectors (Fig. 3). This band occurs between 6300 and 6700 ms TWT and dips slightly to the south. At the southern end of the profiles, its thickness is constant at 20 to 30 ms TWT (~15 – 25 m). However, from the centres of the profiles, the unit thickens out northwards and reaches up to 60 ms TWT in thickness (~50 m) in the north. This thickening defines a wedge-like sediment pile that occurs in between the two prominent reflectors (Fig. 3, CDPs 2800 – 4400; 6500 ms TWT). The sediment pile is a nearly transparent area with only weak reflection amplitudes, suggesting constant sedimentation. This wedge lies above areas of numerous small scale faults in subunit 1B, separated from them by reflector E. The faults do not offset unit 2 layers, but instead slightly deform them. On Profile AWI-20050016, unit 2 thins out towards the west and finally disappears totally (Fig. 4, CDPs 2700 – 2900; 6500 ms TWT). Unit 2 and subunit 1B are the only units to be partially disturbed by plentiful sedimentary fault-cuts (Fig. 4, CDPs 2500 – 5000 and CDPs 8000 - 8700). The unit 2 faults originate in underlying unit 1. Thus, unit 2 must have been deposited during or shortly after the development of the small-scale faults. Basically, unit 2 seems to represent a regional transition from more or less undisturbed and slowly ongoing deep sea sedimentation, represented by subunits 1A and 1B, to deposition of sediment with altered composition or by altered current strengths and directions. The reflection characteristics imply a composition of mid-grained clastics and pelagic sediments (Table 1) (Sangree and Widmier, 1979). Diester-Haass et al. (1996) and Scher and Martin (2004) reported from a cooling event that took place about 36 Ma ago. This cooling event may have coincided with the onset of Antarctic Intermediate Water and proto-AABW, which would have changed the inflow of water masses into the Transkei Basin (Diester-Haass et al., 1996). The intensified reflection characteristics of unit 2 are consistent with this scenario. The top of unit 2 is marked by reflector "O", which represents a hiatus at the Eocene-Oligocene boundary, about 34 Ma ago (Du Toit and Leith, 1974; Niemi et al., 2000; Coxall et al., 2005; Zachos and Kump, 2005). Hence, unit 2 must have been deposited between 36 and 34 Ma.
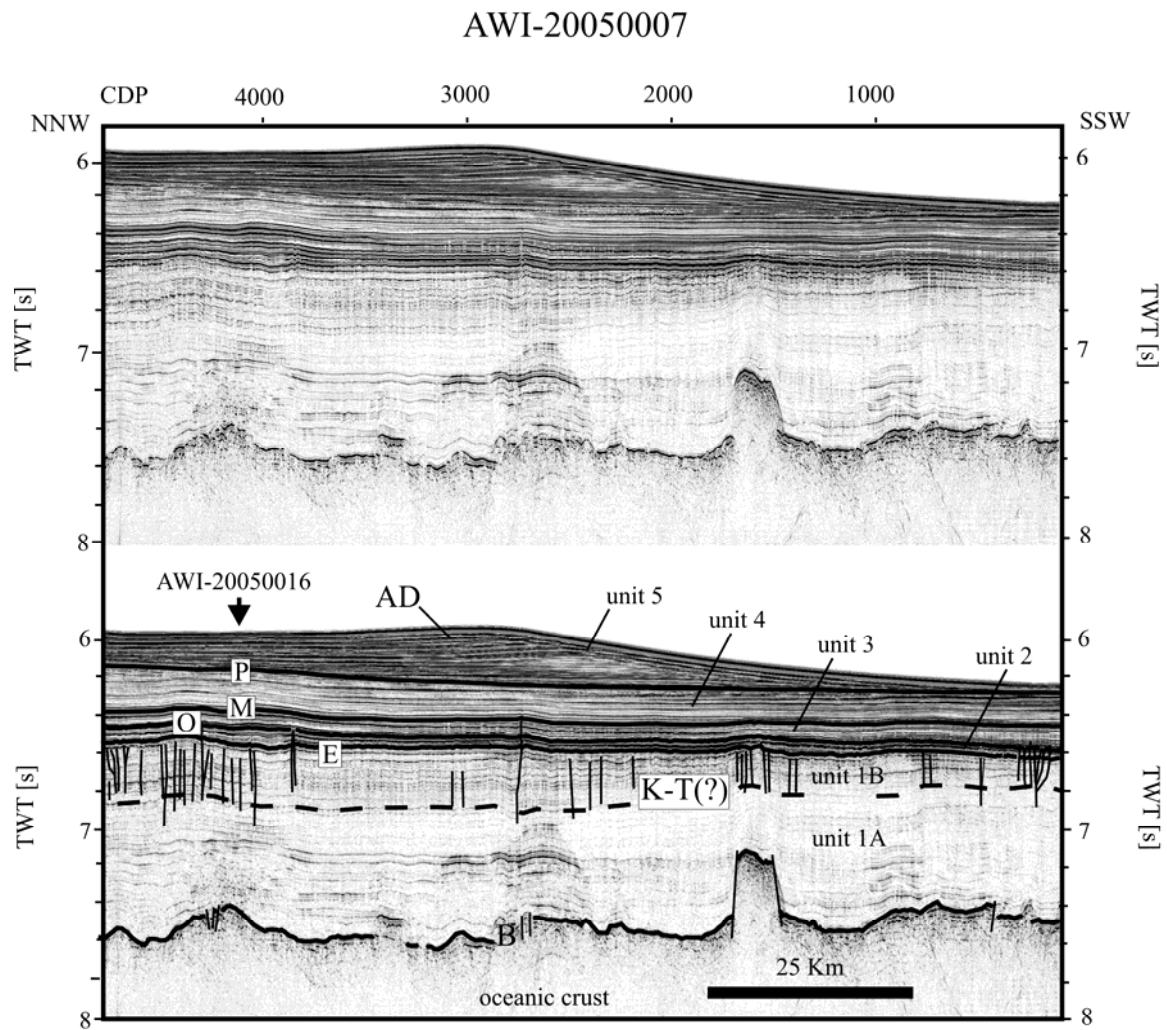
Figure 3: Seismic reflection profile AWI-20050007 showing acoustic basement and seismostratigraphic units 1-5. AD: Agulhas Drift; B: Basement; E: Late Eocene; M: middle Miocene; O: Eocene/Oligocene boundary; P: early Pliocene; dashed line: K-T boundary; the arrow indicates the intersection with seismic reflection profile AWI-20050016 (Fig. 4).
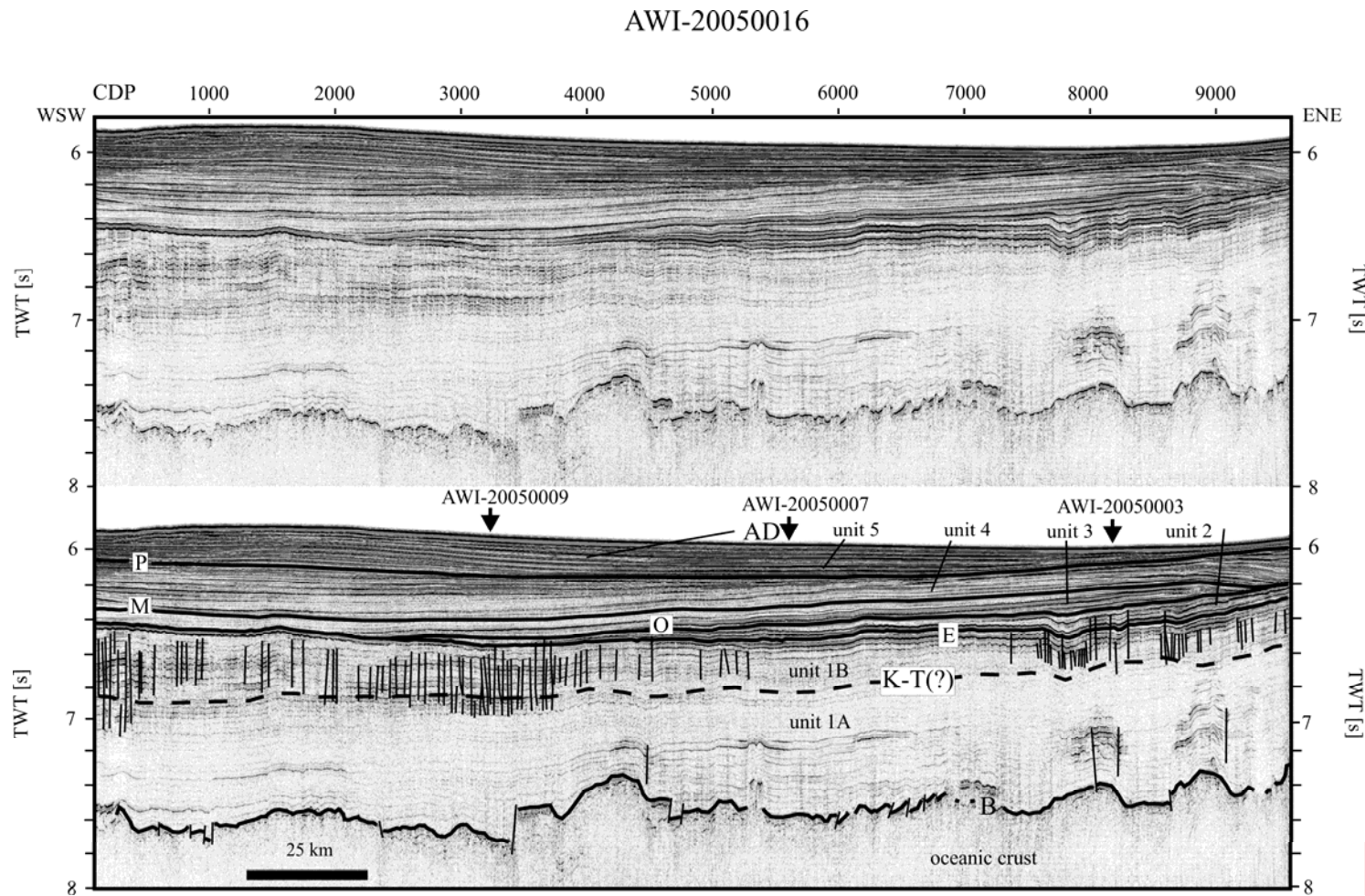
22

Figure 4: Seismic reflection profile AWI-20050016 showing acoustic basement and seismostratigraphic units 1-5. AD: Agulhas Drift; B: Basement; E: Late Eocene; M: middle Miocene; O: Eocene/Oligocene boundary; P: early Pliocene; dashed line: K-T boundary; the arrows indicate the intersections with seismic reflection profiles AWI-20050003, AWI-20050007 and AWI-20050009 (Figs. 5, 3, 2).

4.4.4 Unit 3:

The appearance of unit 3 is somewhat variable. On north-south oriented profiles, its thickness varies from 20 ms TWT (~15 m) on westerly sections to 80 ms TWT (~70 m) in the east. Additionally, unit 3 thickens somewhat from north to south to form a slight wedge (Fig. 5, CDPs 2400 - 4900, 6200 – 6400 ms TWT). Amplitudes are moderate to occassionally strong (Fig. 4, CDPs 2000 – 4000, 6300 – 6500 ms TWT). Reflector spacing decreases slightly to the west, implying slightly higher current velocities and/or less sediment being transported within the water column.

The lower boundary of unit 3 is characterized by an unconformity, which forms a downlap-sequence by very slightly cutting the basal reflector (Fig. 4). According to its depth and reflection characteristics, we interpret this basal reflector (Table 1) as equivalent to Niemi et al.`s (2000) reflector "O", which marks the Eocene-Oligocene boundary roughly 34 Ma ago (Niemi et al., 2000). The Eocene-Oligocene boundary is characterised by the onset of perennial glaciation of Antarctica (Coxall et al. 2005; Zachos and Kump, 2005), which has been related to the final opening of the Drake Passage gateway to abyssal depths and the resulting onset of the Antarctic Circumpolar Current (ACC) (Scher and Martin, 2004; Livermore et al. 2005). As a consequence, a proto-AABW has been suggested to have developed due to the extension of Antarctic shelf ice over the shelf break (Diester-Haass et al., 1996). More cold and dense waters could then directly flow down the continental slope and northward into the global abyss.

Niemi et al. (2000) stated that the margin parallel orientated Oribi-Drift appeared in the Natal Valley and northern parts of the Transkei Basin above reflector O (Fig. 1). The drift is thought to have formed in the Lower Oligocene due to intensified southwest northeast AABW flow off the southeast continental margin off South Africa (Niemi et al., 2000). In fact, unit 3 owns the smallest sedimentation rate of the Transkei Basin infill (Fig. 6). Thus, we suggest that unit 3 may be the result of AABW strengthening, which resulted in an increase in transportation (erosion) of sediments from the Transkei Basin into the adjacent Natal Valley.

As the Oribi-Drift was formed above reflector O it is equivalent to our unit 3 sediments, which also overlie this reflector. Niemi et al. (2000) showed that the Oribi-Drift was buried under later sediments. It seems possible that the slight wedge of unit 3 sediments could represent drift-like deposition, which is much less pronounced in the Transkei Basin than in the adjacent Natal Valley. Certainly, we cannot be sure wether the Oribi-Drift itself reached that far south into the Transkei Basin, because of the nearly total erosion of the drift, which makes a correlation virtually impossible.

4.4.5 Unit 4:

Unit 4 shows slight variations in thickness, especially in the north-south direction (Fig. 2). On southern parts of the profiles the thickness varies between 50 ms TWT (~40 m) and 130 ms (~ 110 m) TWT. On the west-east oriented profiles, the thickness increases up to 200 ms TWT (~180 m) in the west (Fig. 5, CDP 5000). In contrast to the underlying unit 3, reflector spacing becomes wider but the amplitudes also vary about moderate values, while the sedimentation rate increases (Fig. 6). From north to south, an increase in reflection energy and a slight decrease in reflector spacing can be observed (Fig. 3, 6200 – 6400 ms TWT). This effect may be due to increasing current velocities to the south, leading to less sedimentation, and higher reflection energy (overlying unit 5 shows a much more pronounced reflection pattern). The bottom of unit 4 is marked by a strong reflector with high amplitude. This reflector "M" (Table 1) (Niemi et al. 2000) can be clearly observed on all seismic sections. Niemi et al. (2000) stated that reflector M marks

the onset of the burial of the Oribi-Drift by a thick sequence of turbidite sediments in the Natal Valley. For reflector M, Niemi et al. (2000) postulated an age between early and middle Miocene, caused by further intensification of AABW in the abyssal plain.

A drift body appears on east-west oriented seismic profiles, which entirely builds up unit 4 (Fig. 4, CDPs 6000 – 9500, 6000 – 6400 ms TWT). Unit 4 reflectors are subparallel, diverging slightly to the west and, finally, after forming a small crest, dipping strongly to the east (Fig. 4, CDPs 8800 – 9500; ~6100 ms TWT). Niemi et al. (2000) stated that this so called M-Drift was deposited under the influence of an eastward directed current during early to middle Miocene times. On our seismic profiles we could identify the M-Drift, which shows a special orientation, perpendicular to the overlying Agulhas Drift (see chapter Unit 5). Due to the Coriolis Force, in the Southern Hemisphere the sediments are dumped to the left side of the current's flow direction (Faugeres et al., 1999). The M-Drift is oriented north-south, and thus must have been formed by a northwards flowing current.

Increased variability in AABW current attributes is thought to have started in middle Miocene times, at roughly 15 Ma (Pekar and DeConto, 2006). They seem to have been triggered by several interlocked factors, which are linked to a global middle Miocene cooling event (Zachos et al., 2001). The control factors for this cooling remain enigmatic (Holbourn et al., 2005). In fact, the cooling was recurrently interrupted by short interglacial periods, which weakened the AABW (Pekar and DeConto, 2006).

As the M-Drift shows a north to south orientation with the steeper flank facing the east, the AABW must have flown along the eastern flank of the Agulhas Plateau into the Transkei Basin and later along the African coast in a northeastward direction.

A first appearance of the M-Drift can be observed already in the underlying unit 3 (Fig. 4, CDPs 8800 – 9200; ~ 6200 ms TWT). We consider this to represent an indication of a transition period in which the major AABW-branch shifted from west to east of the Agulhas Plateau.

We cannot be sure whether any branch of AABW collapsed at any time, but for late to middle Miocene times we assume that due to the M-Drift build up and its S to N orientation, the main inflow of AABW into the Transkei Basin must have come from south of the Transkei Basin.

4.4.6 Unit 5:

Unit 5 is the youngest unit at the seafloor, and forms the prominent Agulhas Drift body in the central Transkei Basin and parts of the Natal Valley (Figs. 1 to 5) (Niemi et al., 2000). Caused by the asymmetrical geometry of the drift body, its thickness varies greatly. Unit 5 is thinnest in the eastern part of the Transkei Basin (Fig. 5), reaching 100 ms TWT (~85 m), while 150 miles further west, it thickens up to about 500 ms TWT (375 m) (Fig. 2). Additionally, in accordance with its northerly migrating crest (Fig. 2, CDPs 1500 – 2400) the vertical drift dimension varies between 100 ms TWT and 500 ms TWT (~80 – 420 m) in the north-south direction. The sedimentation rate of unit 5 with more than 100 m/my is the highest of all seismostratigraphic units in the Transkei Basin (Fig. 6). The unit shows high continuity and high amplitude reflections (Fig. 2). On the southern flank of the drift, the reflectors are somewhat sigmoidal and form toplaps to the overlying, strongly reflective seafloor (Fig. 2, CDPs 1000 - 2500). North of the crest, reflections become subhorizontally stratified and dip slightly to the north (Fig. 2, CDPs 2400 – 3000). The thickest parts of the drift show undulating reflectors with high amplitudes (Fig. 3, CDPs 2000 – 3500). Further north, the reflection pattern only shows strong reflectors and no weak intersecting reflectors are observed. According to the reflection characteristics of the

unit, the drift deposits are most probably composed of mid grained clastics (Sangree and Widmier, 1979).
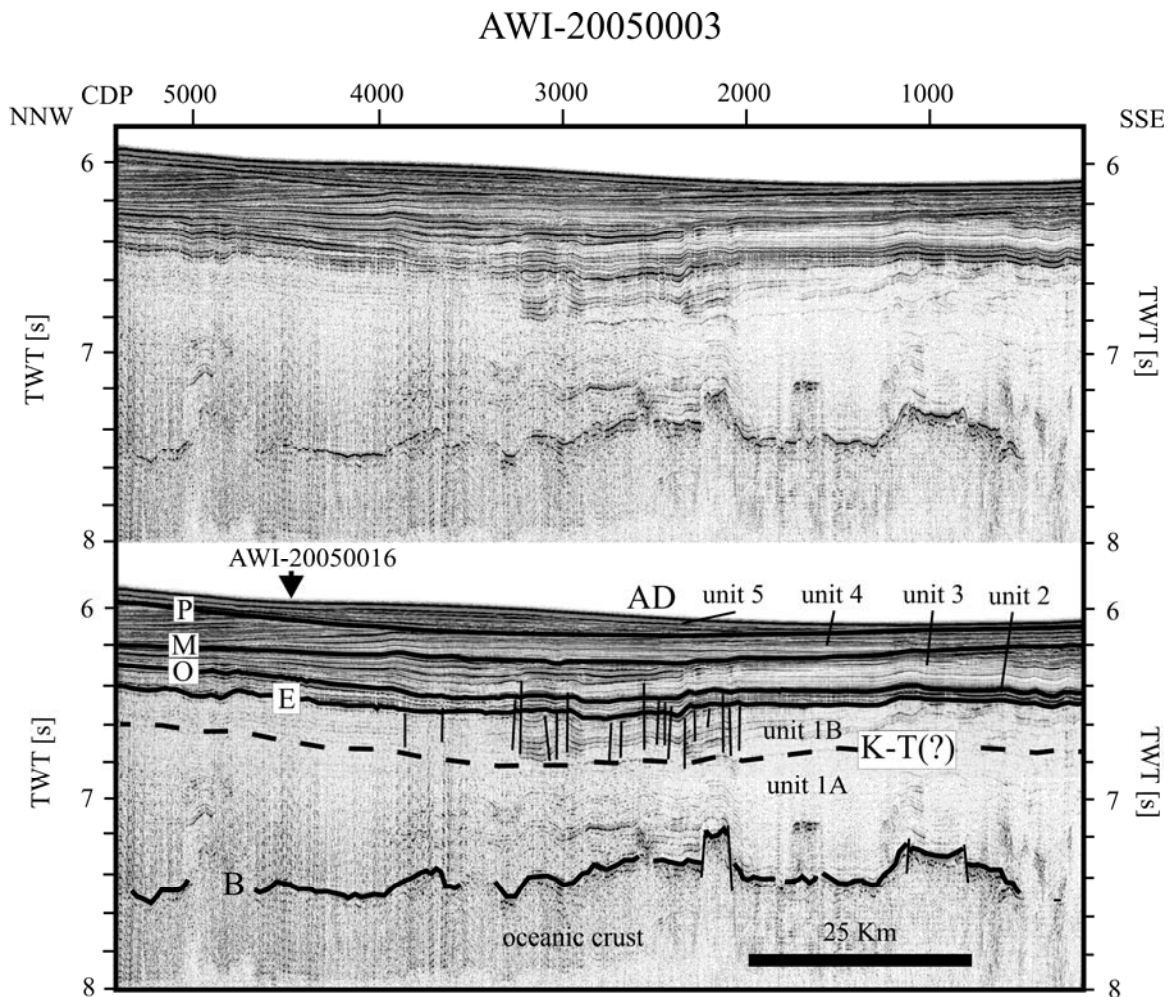
AWI-20050003

Figure 5: Seismic reflection profile AWI-20050003 showing acoustic basement and seismostratigraphic units 1-5. AD: Agulhas Drift; B: Basement; E: Late Eocene; M: middle Miocene; O: Eocene/Oligocene boundary; P: early Pliocene; dashed line: K-T boundary; the arrow indicates the intersection with seismic reflection profile AWI-20050016 (Fig. 4).

The base of unit 5 is characterised by down- and onlapping of the reflectors onto the prominent discordance "P" (Table 1, Fig. 3, CDPs 2800 - 4800) (Niemi et al. 2000), which may represent erosion accompanying changing current direction and/or strength. Niemi et al. (2000) suggested reflector P to represent a basin- and margin wide erosional surface scoured by AABW and NADW water masses at the end of the Miocene, due to a southward shift and deepening of bottom current flow. Furthermore, they stated that the Agulhas Drift was solely built up by AABW, which decelerated in the southern Transkei Basin. However, it seems likely that the depositional Agulhas Drift may also have been initiated by NADW, whose attributes also changed in early Pliocene times due to the closure of the Panama Isthmus (Frank et al. 2002; Lear et al., 2003). Recently, NADW variability in response to this event has been the subject of debate. Burton et al. (1997) presented evidence for a Northern Hemisphere strengthening of NADW after the closure

26

of the Panama Isthmus. In the Southern Hemisphere, Frank et al. (2002) observed a decreasing in NADW activity since early Pliocene times. NADW attributes undoubtedly changed in response to the closure of the gateway between North and South America. The variation of NADW could explain the differences in sedimentation between unit 5 and unit 4. Nevertheless, because of the large sediment thickness of unit 5 (up to 500 ms TWT), it seems safe to conclude that more sediments must have been transported into the Transkei Basin since early Pliocene times. As no turbidites have been reported for the southern Transkei Basin, because it is too far off the continental slope (Niemi et al., 2000), these sediments must have been derived from elsewhere. Most probably, NADW eroded sediments from the continental margins off Namibia and southwestern South Africa (Weigelt and Uenzelmann-Neben, 2004) and transported them through the narrow Agulhas Passage where the current velocity increased. At the western opening of the Transkei Basin, the flow velocity of NADW decreased and the sediment load was deposited.

The northward trending crest of the drift, in particular, is thought to be the result of small scale modifications in current attributes, such as the flow velocity and flow path of both AABW and NADW. These modifications can be related to relocations of the frontal system in response to glacial-interglacial activity.

4.5 Discussion:

The five seismostratigraphic units of the Transkei Basin were caused by changing current attributes and varying sediment input (Table 1). Due to the lack of boreholes in the Transkei Basin area, we cannot exactly determine the sediments` provenance. As a consequence, the reconstruction of the ocean currents, which dumped these sediments into the Transkei Basin, becomes more difficult.

The lower part of the Transkei Basin sedimentary infill (Figs. 2 – 5), draping the acoustic basement (unit 1), shows homogeneous reflection characteristics, which were interpreted as mostly pelagic or hemipelagic clays and ooze (Sangree, Widmier, 1979). The upper part (units 2-5) shows more heterogeneous reflection characteristics, which were interpreted as a mixture of pelagic/hemipelagic and terrigeneous sediments (Sangree and Widmier, 1979). This initial subdivision shows that there seem to have been two different main stages of sedimentation in the Transkei Basin, with the older stage imaging stable deep sea conditions and the younger stage a somewhat varying deep sea environment.

The different characteristics of the seismic units and the thus derived depositional environment led to the development of a model (Fig. 6), comprising direction and strength of the major currents, which where active during the different periods.

Between about 90 Ma and 36 Ma, with a sedimentation rate of 17 m/m.y., the Transkei Basin was characterised by moderate deep sea sedimentation, which Zachos et al. (2004) also observed in Maastrichtian pelagic sediments close to the Walvis Ridge. The homogeneous sedimentary layering suggests that the conditions for deposition must have been stable (Sangree and Widmier, 1979). Due to the absence of any current controlled sedimentary feature, we have no evidence for any prolonged strong deep sea current (Fig. 6a).

For the period between 36 and about 15 Ma, we observe an abrupt change in deep sea sedimentation. At the end of Eocene times, we see high amplitude reflections, which led to several possible interpretations, but due to an increasing proto-AABW inflow into the Transkei Basin and the build up of the Oribi-Drift in the adjacent Natal Valley we suggest more sandy sediment. Due to the lack of ponded geometry within the southern Transkei Basin, we can preclude continental margin related turbidites as the source of these sediments. Diester-Haass et al. (1996) found evidence for a cooling event which

occurred shortly before the isolation of Antarctica at the Eocene–Oligocene boundary. They stated that, along with this cooling, a broader dispersal of Antarctic particles into the Southern Ocean set in. Furthermore, due to the transport of Antarctic derived material into the South Atlantic, they suggested the development of proto-AABW. Similarly, Scher and Martin (2004) also interpreted an onset of proto-AABW coincident with the Drake Passage opening at about 35 Ma, which would have led to a stronger current inflow into the South Atlantic. Although it is in sharp contrast to the first stage of 90 to 36 Ma, the period between 36 and 34 Ma represents only a relatively short period in the sedimentation history of the Transkei Basin and marks the transition from a deep sea to a current controlled environment. In fact, the abrupt change in deep sea deposition seems to have been triggered by the onset of proto-AABW in late Eocene times (Fig. 6b). At approximately 34 Ma, we observe an unconformity within the sedimentary column. Due to the final opening of the Drake Passage gateway roughly 35 Ma ago (Livermore et al., 2005) Antarctica became isolated and glaciated, leading to an intensification of AABW inflow into the South Atlantic (Diester-Haass et al., 1996). In middle Eocene times proto-AABW may have reached the equatorial regions of the Atlantic Ocean (Jones and Okada, 2006). Wildeboer-Schut and Uenzelmann-Neben (2005) reported from proto-AABW activity in the Cape Basin in Early Oligocene. The build up of the Oribi-Drift marks the northward flow of AABW to the South African continental margin, into the Transkei Basin and Natal Valley (Niemi et al., 2000). The southwest to northeast orientation of the Oribi-Drift (Niemi et al., 2000) indicates that AABW must have flown in a southwest-northeast direction close to the South African continental margin (Faugères et al., 1999; Ben-Avraham et al., 1994). Thus, the main inflow of AABW into the Transkei Basin and Natal Valley must have come through the narrow Agulhas Passage (Fig. 6b).

At about 15 Ma, reflection characteristics slightly change. The reflector spacing becomes wider and the amplitudes weaken, indicating a variation in deep sea sedimentation conditions. Additionally, we observe a decrease in reflection energy from south to north. In the southeastern Transkei Basin, we found depositional remains of the M-Drift (Niemi et al., 2000), first appearing in the upper parts of unit 3, leading to the assumption that the drift build up started a short time before 15 Ma. Due to the location and orientation of the M-Drift, the corresponding bottom current must have flown into the southern Transkei Basin along the east of the Agulhas Plateau. A possible shifting of AABW coincides with a global cooling event in middle Miocene times (~15 Ma) (Zachos et al., 2001). Holbourn et al. (2005) stated that the amplitude of Earth`s eccentricity increased, resulting in an intensified ACC flow, followed by a growing ice shield and an increasing isolation of Antarctica. At the same time, glacial-interglacial cycles, related to increased obliquity produced oscillations in the Antarctic ice sheet, which were accompanied by melting pulses. This cyclicity weakened the AABW, especially during interglacials (Pekar and DeConto, 2006), but caused it to extend further northwards and mix with warmer bottom waters during glacials. The middle Miocene cooling thus probably caused the flow paths and/or strengths of the two branches of AABW off South Africa to change. Niemi et al. (2000) observed a shift of AABW to deeper water depths, which could result in a weakening of bottom current flow along the continental slope. In the Natal Valley, close to the continental margin, only turbiditic sediments overly reflector M (Niemi et al., 2000).

Thus, there is evidence from which we conclude that the main inflow of AABW into the Transkei Basin must have shifted from the Agulhas Passage to a path further east that took it directly into the southern Transkei Basin (Fig. 6c). With the shift of AABW to deeper regions, we observe a main flow path around the Agulhas Passage, from the south, into the Transkei Basin (Fig. 6c).

Our data show evidence for the most recent big event in the sedimentation history of the Transkei Basin at about 3 Ma. The reflector spacing becomes smaller, and the amplitude energy higher. The most characteristic feature of the youngest stage is the giant elongated mounded Agulhas Drift (Niemi et al., 2000). The Agulhas Drift is oriented in a west to east direction and its reflection characteristics are to some extend comparable to the reflection characteristics of the M-Drift, except from the drifts` orientation.

With up to 500 ms TWT (375 m), the sediments deposited during the last 3 Ma are much thicker than any underlying unit. In fact, since 3 Ma a larger amount of material must have been transported into the Transkei Basin. Due to a lack of ponded geometry, we preclude continental slope derived turbidites as the source. Ledbetter and Bork (1993) reported several stages of increasing AABW flow strength, also between 3.3 and 3.1 Ma, and therefore a variation in AABW activity. Niemi et al. (2000) dated reflector P to early Pliocene, contemporaneous with the final closure of the Isthmus of Panama at roughly 3 Ma (Table 1). Proto NADW has been observed at least since middle Miocene times (Frank et al., 2002), or possibly even since the opening of Drake Passage gateway, which initiated the onset of a thermohaline circulation around South America. At 3 Ma, the attributes of NADW changed due to the final closure between North and South America. At first, NADW flow strengthened and flowed northwards, forcing a Northern Hemisphere cooling (Burton et al., 1997; Lear et al. 2003; Schneider and Schmittner, 2006). Due to this Northern Hemisphere cooling, the southward flowing NADW branch weakened and changed its attributes (Frank et al. 2002). Consistent with this, Weigelt and Uenzelmann-Neben (2004) observed a westward shift of the Benguela Current upwelling system at the same time, which led to increasing sediment input from the continental shelf of Namibia into the deep sea off southwestern Africa. As a consequence, NADW flowed close to the Namibian and South African continental margin and eroded parts of this terrigeneous material, before transporting it through the Agulhas Passage. At the eastern opening of the Agulhas Passage, the flow velocity of the NADW decreased due to the end of the constriction, which would have resulted in the growth of the Agulhas Drift (Fig. 6d). We interpret this as indicating how the main inflow of AABW must have shifted back to the constriction of the Agulhas Passage.

The top of unit 5 is built up by a small crest with northerly migrating sedimentary "foresets" (Fig. 2, CDPs 1600 - 2400). This migration may be related to ongoing northward movement of bottom currents.

4.6 Conclusions:

Five seismostratigraphic units were defined for the Transkei Basin off South Africa. Their ages range from Middle Cretaceous to Holocene times, and they document the depositional history of the Transkei Basin infill. It has been possible to reconstruct different stages of deep sea environments according to the seismostratigraphic units. The sedimentary features, their location and orientation led to the formulation of a first model for the prevailing oceanic currents.

The oldest stage represents a deep sea environment from Middle Cretaceous to middle Eocene times (Fig. 6a). It is characterised by homogeneous reflection characteristics, without any evidence for a prevailing deep sea current, until about 36 Ma.

At 36 Ma, sedimentation changed significantly. A short transition from the stable early Tertiary deep sea environment to a regime of stronger deep sea currents is recorded in unit 2. The sediments show the onset of proto-AABW in late Eocene times, which was initiated by a short term cooling event, roughly 2 m.y. before the final opening of a deep water gateway in the Drake Passage.

At 34 Ma, the Eocene-Oligocene boundary, we suggest that AABW intensified due to the isolation of Antarctica, flowing through the Agulhas Passage into the Transkei Basin and along the southeastern continental margin of South Africa, where it built up the Oribi-Drift (Fig. 6b).
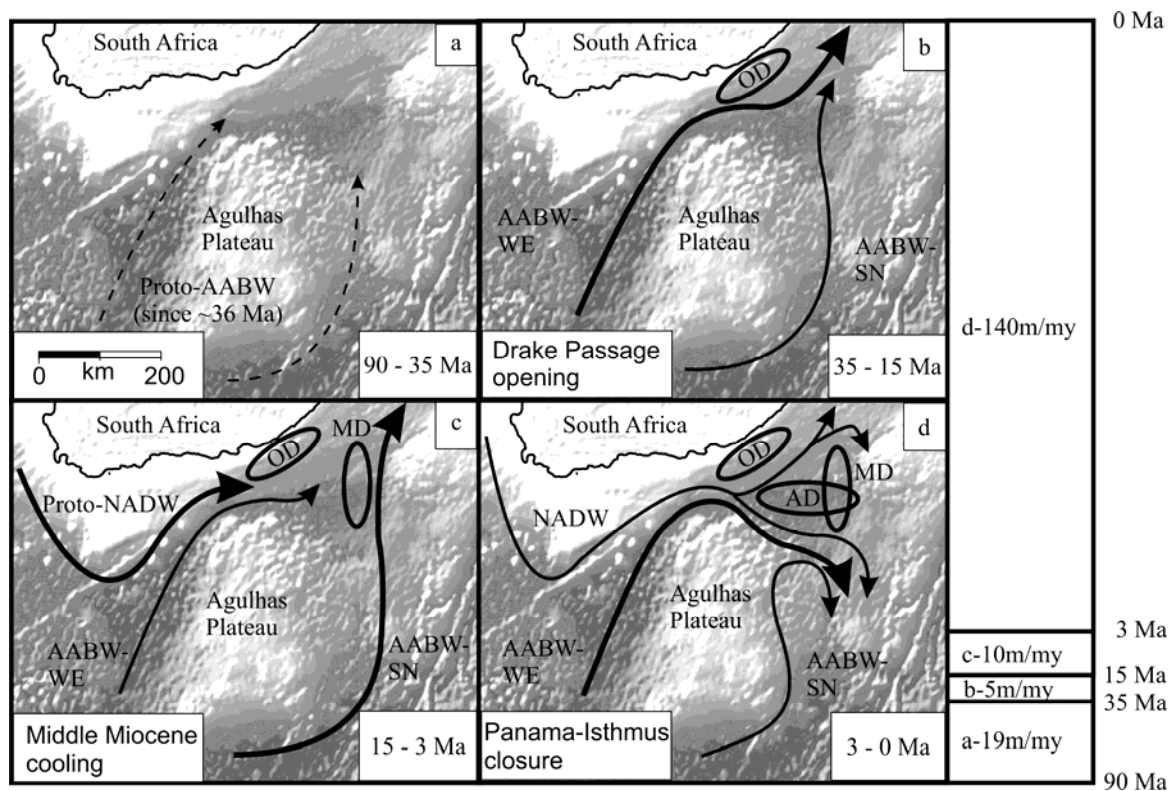

Figure 6a-d: Model of the development of the current system from Middle Cretaceous to Holocene times. AABW-SN: Antarctic Bottom Water flowing in south-north direction; AABW-WE: Antarctic Bottom Water flowing in west-east direction; AD: Agulhas Drift; MD: M-Drift; NADW: North Atlantic Deep Water; OD: Oribi Drift; Proto-AABW: Prototype of AABW; Proto-NADW: Prototype of NADW. The beam on the right side shows the maximum sedimentation rate of each time stage of the four figure's sketches.

At 15 Ma, bottom current activity in the Transkei Basin became more variable in response to a middle Miocene cooling event; the main inflow of AABW shifted from the Agulhas Passage to east of the Agulhas Plateau (Fig. 6c), and the M-Drift was deposited at the southern opening of the Transkei Basin. This system remained stable until the final closure of the Isthmus of Panama in early Pliocene times, at about 3 Ma. The NADW responded to this closure by transporting more terrigeneous sediments from the continental slope off Namibia and western South Africa, through the Agulhas Passage and into the Transkei Basin, where it was deposited to form the east-west oriented Agulhas Drift (Fig. 6d). With this regime change, the main inflow of AABW shifted back to the Agulhas Passage, supporting NADW flow.

Future drilling within the central Transkei Basin would be highly beneficial for a detailed analysis the sedimentary content and its exact age.

4.7 Acknowledgments:

4.8 References:

Ben-Avraham, Z., Hartnady, C.J.H., Malan, J. A., 1993. Early tectonic extension between the Agulhas Bank and the Falkland Plateau due to the rotation of the Lafonia microplate. Earth and Planetary Science Letters, 117, 43 – 58.

Ben-Avraham, Z., Niemi , T., Hartnady, C. J. H., 1994. Mid-Tertiary changes in deep ocean circulation patterns in the Natal Valley and Transkei Basin, Southwest Indian Ocean. Earth and Planetary Science Letters 121, 639 – 646.

Boebel, O., Lutjeharms, J., Schmid, C., Zenk, W., Rossby, T., Barron, C., 2003. The Cape Cauldron: a regime of turbulent inter-ocean exchange. Deep Sea Research II, 57 – 86.

Burton, K., W., Ling, H.-F., O`Nions, R., K., 1997. Closure of the Central American Isthmus and its effect on deep-water formation in the North Atlantic. Nature, 386, 382 – 386.

Coxall, H., K., Wilson, P.,A., Pälike, H., Lear, C., H., Backmann, J., 2005. Rapid stepwise onset of Antarctic glaciation and deeper calcite compensation in the Pacific Ocean. Nature, 433, 53 – 57.

Dingle , R., V., Camden-Smith, F., 1979. Acoustic stratigraphy and current-generated bedforms in deep ocean basins off southeastern Africa. Marine Geology, 33, 3-4, 239 – 260.

Dingle, R., V., Robson, S., 1985. Slumps, canyons and related features on the continental margin off East London, SE Africa (SW Indian Ocean). Marine Geology, 28, 89 – 106.

Diester-Haass, L., Robert, C., Chamley, H., (1996. The Eocene-Oligocene preglacial-glacial transition in the Atlantic sector of the Southern Ocean (ODP Site 690). Marine Geology, 131, 123 – 149.

Du Toit, S. R., Leith, M. J., 1974. The J(c)-1 bore-hole on the continental shelf near Stanger, Natal. Geological Society of South Africa, 77, 247 – 252.

Emery, K. O. Uchupi, E., Bowin, C., O., Phillips, J., Simpson, E., S., W., 1975. Continental margin off western Africa: Cape St. Francis (South Africa) to Walvis Ridge (south-west Africa). AAPG Bulletin, 59, 3 – 59.

Erbacher, J., Mosher, D., C., Malone, M., J., 2004. Proceedings of the Ocean Drilling Programm, Initial Reports, 207.

Faugères, J.-C., Stow, D. A. V., Imbert, P., Viana, A., 1999. Seismic features diagnostics of contourite drifts. Marine Geology, 162, 1 – 38.

Frank, M,. Whiteley, N., Kasten, S., Hein, J., R., O`Nions, K., 2002. North Atlantic Deep Water export over the past 14 Myr: Evidence from Nd and Pb isotopes in ferromanganese crusts. Paleoceanography, 17, 2, 12-1 – 12-9.

Fullerton, L., G., Frey, H., V., Roark, J., H., Thomas, H., H., 1989. Evidenec for a remanent contribution in Magsat data from the Cretaceous Quiet Zone in the South Atlantic. Geophysical Research Letters, 16, 1085 – 1088.

Garabato, A., C., N., McDonagh, E., L., Stevens, D., P., Heywood, K.,J., Sanders, R., J, 2002. On the export of Antarctic Bottom Water from the Weddell Sea. Deep Sea Research Part II: Topical studies in Oceanography, 49, 21, 4715 – 4742.

Goodlad, S., W., Martin, A., K., Hartnady, C., J., H., 1982. Mesozoic magnetic anomalies in the southern Natal Valley. Nature, 295, 686 – 688.

Gordon, A. L., 1986. Interocean exchange of thermocline water. Journal of Geophysical Research, 91, 5037 – 5046.

Holbourn, A., Kuhnt, W., Schulz, M., Erlenkeuser, H., 2005. Impacts of orbital forcing and atmospheric carbon dioxide on Miocene ice-sheet expansion. Nature, 438, 483 – 487.

Jones, E. J. W., Okada, H., 2006. Abyssal circulation change in the equatorial Atlantic : Evidence from Cenozoic sedimentary drifts off West Africa. Marine Geology, 232, 1-2, 49 – 61.

Lear, C. H., Rosenthal, Y., Wright, J. D., 2003. The closing of a seaway: ocean water masses and global climate change. Earth and Planetary Science Let., 210, 425 – 436.

Ledbetter, M., T., Bork, K., R., 1993. Post-Miocene fluctuations of Antarctic Bottom Water paleospeed in the southwest Atlantic Ocean. Deep Sea Research Part II: Topical Studies in Oceanography, 40, 4-5, 1057 – 1071.

Livermore, R., Nankivell, A., Eagles, G., Morris, P., 2005. Paleogene opening of Drake Passage. Earth and Planetary Science Letters, 236, 1-2, 459 – 470.

Martin, A. K., Goodlad, S.W., Salmon, D. A., 1982. Sedimentary basin in-fill in the northernmost Natal Valley, hiatus development and Agulhas Current palaeo-oceanography. Journal of the Geological Society London, 139, 183 – 201.

Martin, A. K., Hartnady, C. J. H., 1986. Plate tectonic development of the southwest Indian Ocean: a revised reconstruction of east Antarctica and Africa. Journal of Geophysical Research, 91, 4767 – 4786.

Niemi, T. M., Ben-Avraham, Z., Hartnady, C. J. H., Reznikov, M., 2000. Post-Eocene seismic stratigraphy of the deep ocean basin adjacent to the southeast African continental margin: a record of geostrophic bottom current systems. Marine Geology, 162, 2-4, 237 – 258.

Park, Y.-H., Gamberoni, L., Charriaud, E., 1993. Frontal structure, water masses, and circulation in the Crozet Basin. Journal of Geophysical Research, 98, 12361 – 12385.

Pekar, S. F., DeConto, R. M., 2006. High-resolution ice-volume estimates for the early Miocene: Evidence for a dynamic ice sheet in Antarctica. Palaeogeography, Palaeoclimatology, Palaeoecology, 231, 1-2, 101 – 109.

Raillard, S., 1990. Les marges de l`Afrique de l`Est et les zones de fracture associees: Chaine Davie et Ridge du Mozambique-Champagne MD-60/MACA MO-11. PhD dissertation, Universite Pierre et Marie Curie, Paris, 272 pp.

Reznikov, M., Ben-Avraham, Z., Hartnady C., Niemi, T., 2005. Structure of the Transkei Basin and Natal Valley, Southwest Indian Ocean, from seismic reflection and potential field data. Tectonophysics, 397, 127 – 141.

Sangree, J. B., Widmier, J. M., 1979. Interpretation of depositional facies from seismic data. Geophysics, 44, 2, 131 – 160.

Scher, H. D., Martin, E. E., 2004. Circulation in the Southern Ocean during the Paleogene inferred from neodymium isotopes. Earth and Planetary Science Letters, 228, 3-4, 391 – 405.

Schneider, B., Schmittner, A., 2006. Simulating the impact of the Panamanian seaway closure on ocean circulation, marine productivity and nutrient cycling. Earth and Planetary Science Letters, 246, 3-4, 367 – 380.

Tikku, A., A., Marks, K., M., Kovacs, L., C., 2002. An Early Cretaceous extinct spreading center in the northern Natal Valley. Tectonophysics, 347, 87 – 108.

Tucholke , B. E., Embley, R. W., 1984. Cenozoic regional erosion of the abyssal sea floor off South Africa. Interregional Unconformities and Hydrocarbon Accumulation. AAPG Memoir, 36, 145 – 164.

Van Aken, H. M., Ridderinkhof, H., de Ruijter, W. P. M., 2004. North Atlantic Deep Water in the south-western Indian Ocean. Deep Sea Research Part I: Oceanic Research Papers, 51, 6, 755 – 776.

Weigelt, E., Uenzelmann-Neben, G., 2004. Sediment deposits in the Cape Basin: Indications for shifting ocean currents? AAPG Bulletin, 88, 6, 765 – 780.

Westall, F., 1984. Current-controlled sedimentation in the Agulhas Passage, SW Indian Ocean. Marine Geoscience Unit Bulletin No. 12, Department of Geology, University of Cape Town, 276 pp.

Wildeboer-Schut, E., Uenzelmann-Neben, G., 2005. Cenozoic bottom current sedimentation in the Cape Basin, South Atlantic. Geophysical Journal International, 161, 325 – 333.

Zachos, J., Pagani, M., Sloan, L., Thomas, E., Billups, K., 2001. Trends, rhythms and aberrations in global climate 65 Ma to present. Science, 292, 686 – 693.

Zachos, J., Kroon, D., Shipboard Scientific Party, 2004. Proceedings of the Ocean Drilling Program, Initial Reports, 208.

Zachos, J., Kump, L., R., 2005. Carbon cycle feedbacks and the initiation of Antarctic glaciation in the earliest Oligocene. Global and Planetary Change, 47, 51 – 66.

5 Indications for bottom current activity since Eocene times: The climate and ocean gateway archive of the Transkei Basin, South Africa

Philip Schlüter, Gabriele Uenzelmann-Neben

5.1 Abstract:

The Transkei Basin deposits document the sediment transport around South Africa and, hence, reveal details of palaeocurrent activity of this region for the past 36 my. Thermohaline driven water masses like the North Atlantic Deep Water (NADW) and the Antarctic Bottom Water (AABW), which are part of the global conveyor belt and the main motor for the heat transfer worldwide, have to pass the southern tip of Africa. A large amount of their sedimentary freight is deposited in the submarine Transkei Basin. By the investigation of high resolution seismic reflection data from central Transkei Basin sediments, we reconstructed depocentres and interface outlines for five different time slices since Cretaceous times. Since at least late Eocene times, we observe an increasing activity of proto-AABW and later proto-NADW in the Transkei Basin. The current's settings were recurrently modified by various large scale global events, like the opening of the Drake Passage Gateway and the Tasman Gateway (~34 Ma), respectively, or the closure of the Panama Isthmus (~3 Ma). The investigations reveal a strong influence of global tectonic and climatic events on NADW and (proto-) AABW and their influence on Transkei Basin deposition.

One of the world's most important motors for water exchange and global heat transfer is represented by the global conveyor belt, which is driven by various thermohaline currents spread all over the world's oceans. The flow paths of these thermohaline currents are determined by factors like Earth's rotation, the ocean floor topography, ocean gateways and prevailing wind directions. Sedimentary sequences that have been deposited and shaped by these long-term currents reveal information about flow paths, strengths and directions, and thus shed light on former current attributes and behaviour. A detailed reconstruction of palaeocurrent flow paths improves the knowledge of oceanic gateways and palaeoclimatic conditions and leads to a better understanding of their development. Off South Africa some of these large scale thermohaline currents, namely the cold North Atlantic Deep Water (NADW) and Antarctic Bottom Water (AABW) and the warm Agulhas Current (AC) meet within a small area. AABW is defined as all bottom waters of non-circumpolar water of Antarctic origin (Orsi, et al., 1999). It is triggered by the Antarctic Circumpolar Current (ACC), which can be observed since the opening of the Drake Passage and the Tasman Gateway for deep water at ~36 Ma, respectively (Stickley et al., 2004; Livermoore et al. 2005). One branch of AABW originates in the Weddell Sea and flows northwards into the South Atlantic, where it splits off into an eastward and a westward flowing branch. NADW originates in Arctic regions and flows through the Atlantic southward into the Cape Basin, southwest of South Africa. At the southwestern tip of Africa it turns to the east and flows, like parts of the AABW, through the Agulhas Passage into the Transkei Basin and the Natal Valley and further into the Mozambique and Somali Basin (Van Aken et al., 2004). Parts of NADW transform to Lower Circumpolar Deep Water by upwelling and mixing and flow back into the South Atlantic (Gordon, 1986; Park et al., 1993).

Today, NADW and AABW enter the Transkei Basin from the west through the Agulhas Passage (Arhan et al., 2003; Mantyla and Reid, 1995), while the AC flows from the Natal Valley (Fig. 1) westward into the Transkei Basin and through the Agulhas Passage further into the South Atlantic.

The region south of South Africa is characterised by two features, namely the submarine Agulhas Plateau and the Transkei Basin (Fig. 1). The Agulhas Plateau is a deep-sea plateau that rises up to 2000 m above the surrounding seafloor and lies in water depths around 4500 m. Between the Agulhas Plateau and the South African continental shelf we find the only 50 km wide Agulhas Passage, which represents the only deepwater gateway between the Indian and Atlantic Oceans in this region (Fig. 1).

The Transkei Basin is a small deep-sea basin (~ 4500 m water depth), located east of the Agulhas Plateau (~ 2000 m water depth) and southwest of the Natal Valley (up to 4000 m water depth) (Fig. 1). To the east the basin is limited by the submarine Mozambique Ridge. The basin is filled by sediments with a thickness of up to 1800 m (Schlüter and Uenzelmann-Neben, 2007). There are three deepwater paths into the Transkei Basin, namely the Agulhas Passage in the northwest, the Natal Valley in the northeast and a broad opening to the south of the basin.

Determining the age of the Transkei Basin's basement is tricky, as it was formed during Cretaceous magnetic quiet times (Fullerton et al., 1989). By tectonic reconstruction, the initial rifting between South America and Africa was determined to have taken place around 124 Ma (Goodlad et al., 1982; Tikku et al., 2002). Due to plate movement velocities and directions it is presumed that spreading within the Transkei Basin stopped around 90 Ma (Dingle and Camden-Smith, 1979; Martin and Hartnady, 1986; Ben-Avraham et al., 1993). The exact age of the Transkei Basin sediments unfortunately cannot be determined, because of the lack of any drill core information from the abyssal regions off South Africa. The only accessible bore hole data provides information about the South African continental shelf close to the city of Stanger, approximately 700 km

northeast of the central Transkei Basin (Du Toit and Leith, 1974). It is presumed that deep-sea sedimentation set in with the end of crustal development in this region, i.e. around 90 Ma. The following 90 my of bottom current activity and sedimentation history within the Transkei Basin are mostly unknown.

At present the cold and dense NADW and AABW, as well as the warm Agulhas Current AC have to pass the southern tip of Africa. Off southwest Africa, NADW and AABW-A turn eastward and flow in an eastward direction through the Agulhas Passage into the Transkei Basin. Another branch of AABW (AABW-B) flows northwestward around the southern part of the Agulhas Plateau and enters the Transkei Basin from the south (Fig. 1).
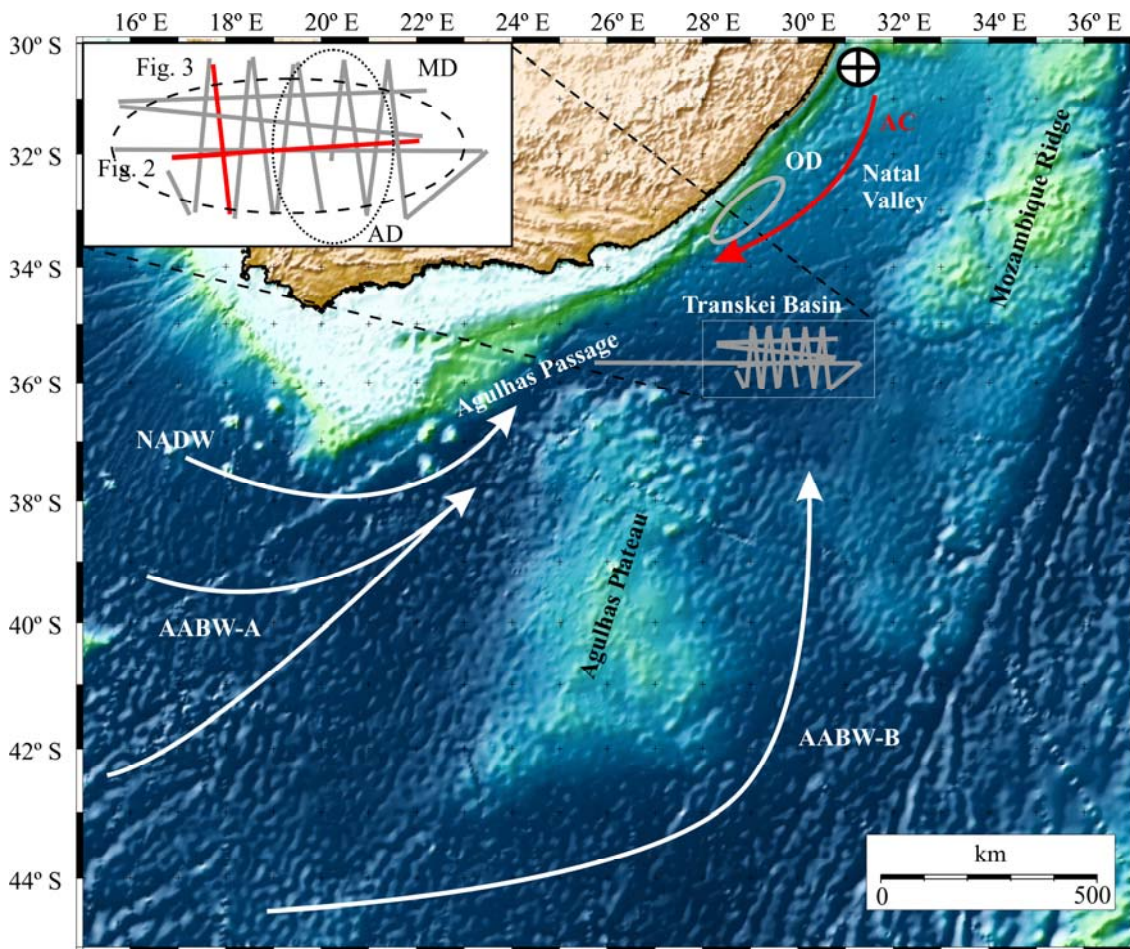
Figure 1: Bathymetric map of the research area off South Africa (Smith and Sandwell, 1997) showing the location of seismic lines and ocean current flow paths (schematically). AABW-A: Antarctic Bottom Water flowing in WE direction; AABW-B: Antarctic Bottom Water flowing in SN direction; AC: Agulhas Current; AD: Agulhas Drift; MD: M-Drift; NADW: North Atlantic Deep Water; OD: Oribi Drift. Circle with cross: Bore hole near Stanger. Grey lines indicate location of seismic reflection profiles. Red indicated lines in blow-up show reflection seismic profiles shown in Figures 2 and 3.

The AC enters the Transkei Basin from the Natal Valley and flows southwestward around South Africa into the Atlantic Ocean.

Numerous investigations have been carried out around South Africa with the purpose of analysing the recent current attributes (e.g. Winter and Martin, 1990; Orsi et al., 1999; Frank et al., 2002; Lutjeharms et al., 2003,). Thus, the recent movement of water masses is well understood. However, the palaeocurrent flow paths off South Africa, which could shed light on palaeoceanographic and palaeoclimatic conditions, remain poorly understood.

For a better understanding of the development of the abyssal regions off South Africa, we analysed the only accessible high resolution seismic reflection data of the central Transkei Basin sediments, gathered in 2005. In this paper, we focus on a detailed reconstruction of interface outlines, depocentre geometries and palaeocurrents in the Transkei Basin and off South Africa in general.

5.3 Seismic Stratigraphy:

We here apply the seismostratigraphic concept developed in Schlüter and Uenzelmann-Neben (2007). In order not to repeat the detailed discussion presented there we only briefly describe the characteristics and age of every unit in the following. Five different units were defined, where the interfaces between the units represent significant changes in seismic reflection characteristics and consequentially, variations in sediment deposition (Table 1, Figure 2). With 700 – 900 m, unit 1 is by far the thickest unit in the central Transkei Basin, characterised by a low energy regime and homogeneous reflections. The interface between units 1 and 2 is marked by reflector E (Figs. 2, 3; Table 1), representing the Late Eocene. The overlying unit 2 marks a short transition zone and appears as a small but very high amplitude reflection band with a thickness around 25 m. Interface unit 2/3 is characterised by reflector O and represents the Eocene/Oligocene boundary. Unit 3 indicates an increasing energy level and thickens up to 70 m (Figs. 2, 3). The boundary between units 3 and 4 is represented by reflector M, which was determined as Middle Miocene. In contrast to unit 3, overlying unit 4 thickens up to 130 m, while the amplitudes weaken. The youngest interface between units 4 and 5 is characterised by the Early Pliocene reflector P (Table 1). The youngest unit 5 reflections show high amplitudes.
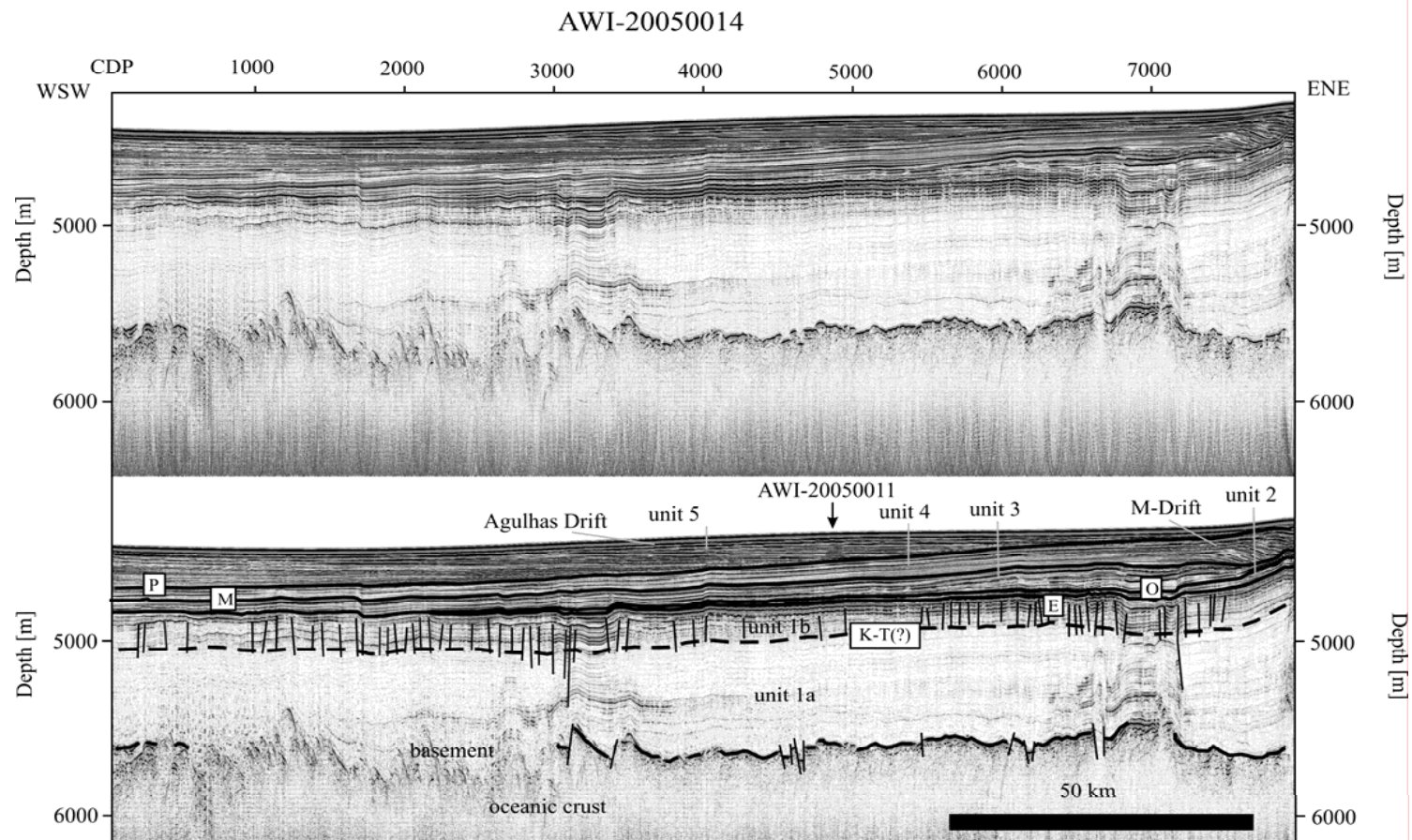
Figure 2: Seismic reflection profile AWI-20050014 showing acoustic basement and seismostratigraphic units 1-5. E: Late Eocene; K-T: Cretaceous-Tertiary boundary; M: middle Miocene; O: Eocene/Oligocene boundary; P: early Pliocene; the arrow indicates the intersection with profile AWI-20050011 (Fig. 3).

5.4 Results:

For a detailed investigation of the different sedimentary environments and the reconstruction of palaeocurrent activity within the Transkei Basin, we tracked the seafloor reflection and interfaces from the acoustic basement to the youngest unit 5, computed the different unit thicknesses and present them in Figures 4a - l. We discuss two terms, the outlines of the interface reflectors and the unit thicknesses. Both interface outlines and depocentres are defined as the root mean square (rms) value of the interface depth and the thickness of a unit, respectively. We use the orientation of the depocentres and their locations relative to the older outlines and depocentres as an indication for a prevailing bottom current flow direction.

The interface between basement and unit 1 shows a kind of wavy structure, with many small basement highs and lows with variations of 100 – 200 m (Fig. 4a). From the centre of the research area towards the northwest and the southeast it deepens from 5300 m down to 5700 m. At 29°E/35.5°S we observe a small basement trough, with a depth of up to ~5800 m (Fig. 4a). Unit 1 shows a varying thickness between 600 and 1000 m, with slightly less sediment coverage at small scale basement highs (Figs. 4a, b). The basement trough is filled with sediments, leading to a small depocentre (Fig. 4b, 29°E/35.5°S). The accumulation rates within unit 1 depocentres amount to ~1.03 $*10^{11}$ m³/my, the sedimentation rate lies at 15.8 m/my (Table 1).

The overlying interface between units 1 and 2 reaches its greatest depth at 4900 m (Fig. 4c, 29.3°E/35.9°S) close to the survey centre and rises continuously up to 4650 m in the east and up to 4700 m in the northwest (Fig. 4c). In fact, its shape appears nearly opposite to the underlying interface between the basement and unit 1 (Fig. 4a). We observe two interface outlines, one in the northwestern area and one in the eastern area. The interface outline in the northwest is northeast to southwest oriented, the interface outline in the east is north-south oriented (Fig. 4c). Within unit 2 we observe a north-south oriented depocentre with 70 – 100 m thickness in the east at 31°E/35.7°S (Fig. 4d), while we find less sediments in the survey centre and nearly no sedimentary coverage towards the south and the west. Additionally, there are some areas, where nearly no sediment can be observed, e.g. at 29°E/35.5°S or 29.2°E/35.3°S (Fig. 4d). Compared to the underlying unit 1, the accumulation rate slightly decreases to 0.88 $*10^{11}$m³/my, while the sedimentation rate increases up to 23.1 m/my (Table 1).
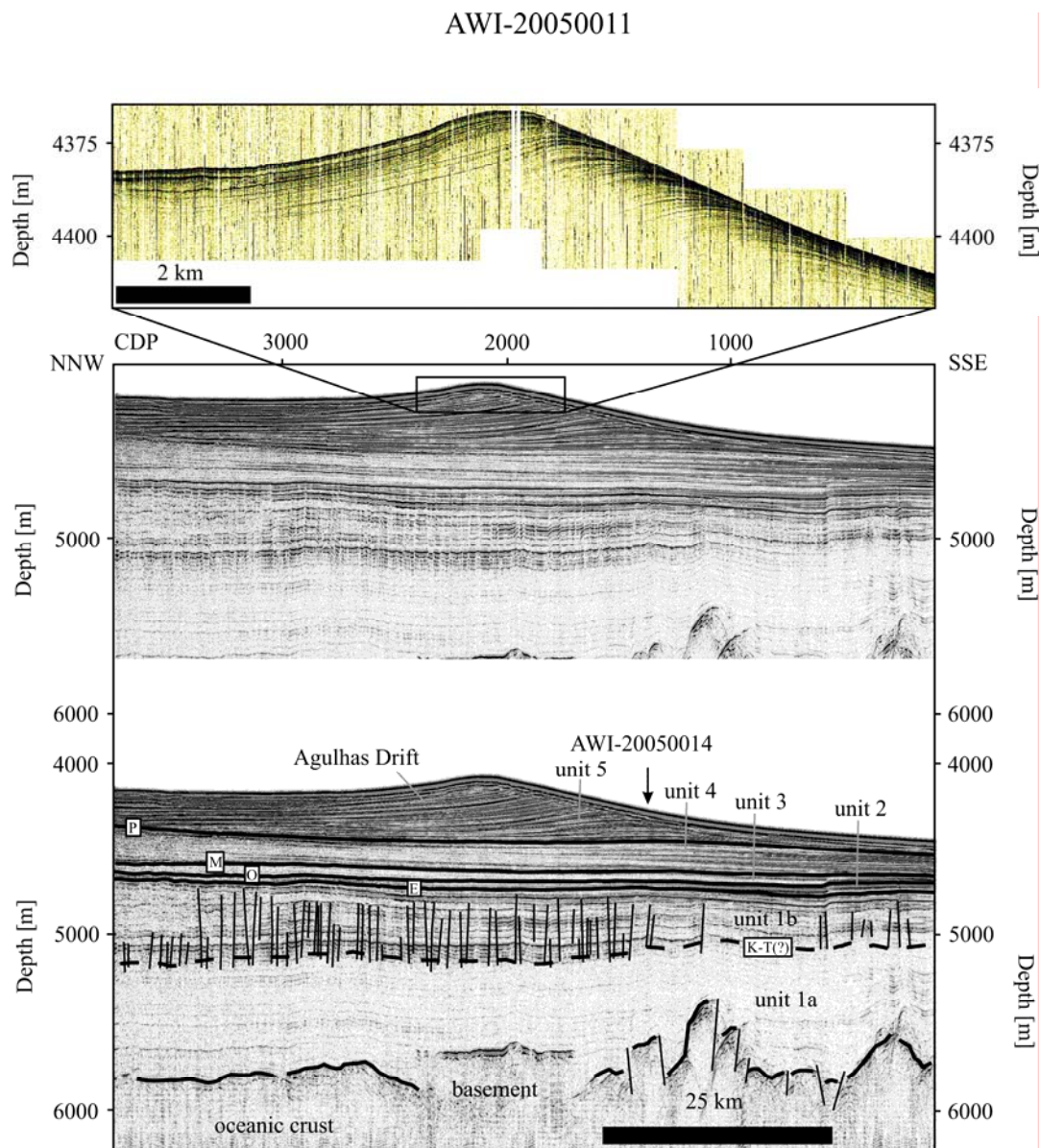
Figure 3: Seismic reflection profile AWI-20050011 showing acoustic basement and seismostratigraphic units 1-5. Blow-up above the seismic reflection profile shows subbottom profiler data from the uppermost 30 m of the drift crest. E: Late Eocene; K-T: Cretaceous-Tertiary boundary; M: middle Miocene; O: Eocene/Oligocene boundary; P: early Pliocene; the arrow indicates the intersection with seismic reflection profile AWI-20050014 (Fig. 2).

The interface of units 2 and 3 shows the same attributes as the underlying interface of units 1 and 2 but more pronounced (Fig. 4e). Again, we observe a trough with about 4900 m in the central to southwestern research area, which now expands partially to the north (Fig. 4e, 29.3°E/35.3°S). The interface depth rises constantly up to 4550 m to the ENE. The interface outline is located in the eastern research area and has a northwest to southeast orientation. The overlying sediments of unit 3 show a pronounced depocentre, which covers the southeastern part of the research area (Fig. 4f, 30.5°E/36.1°S) with an extension to the north (Fig. 4f, 30.4°E/35.4°S). In fact, the depocentre is located slightly west of the underlying interface high and covers a big part of the southeastern area with one sediment arm extending slightly northwards (Fig. 4f, 30.4°E/35.4°S). The rest of unit

3 sediments are NNE to SSW oriented, with a decreasing amount of sediments from east to west. Compared to unit 2, unit 3 accumulation and sedimentation rates decrease drastically to 0.15 *10^{11} m³/my and 4.9 m/my (Table 1).

A predominant east to west orientation was found again at the interface between units 3 and 4. The shallowest area with about 4400 m is found in the east (Fig. 4g). Towards the survey centre, the interface deepens continuously to 4650 m, while the whole southwestern area is characterised by a large trough, reaching a depth of up to 4800 m. There is a small interface trough between units 3 and 4 at 29.3°E/35.2°S (Fig. 4g). The interface outline is north to south oriented and is located in the eastern part of the research area (Fig. 4g). Unit 4 sediments partly fill the deeper areas of the underlying interface of units 3 and 4 (Fig. 4h). We found two small depocentres with thicknesses of up to 200 m. One is located in the west and covers a part of the underlying trough. Another depocentre covers parts of the northern area trough at 29.3°E/35.2°S (Figs. 4g, h). Very few or even no sediments were found at the interface high in the east and partially in the south. The southern part of the interface trough is not completely filled with unit 4 sediments (Fig. 4h). In fact, the depocentres of unit 4 are located contrarily to the depocentres of the underlying unit 3 (Fig. 4f). After the low rates of unit 3, within unit 4 the accumulation and sedimentation rates again increase to 0.58 *10^{11} m³/my and 12.2 m/my (Table 1).

Sedimentary unit	Unit age (Niemi et al., 2000; Schlüter and Uenzelmann-Neben, 2007) [Ma]	Interface reflector nomenclature (Niemi et al., 2000; Schlüter and Uenzelmann-Neben, 2007)	Unit thickness (rms) [m]	Sedimentation rates [m/my]	Accumulation rates [10^{11}m³/my]
Unit 5	0.0 - ~3.0	P	150.4	~50.1	~1.67
Unit 4	~3.0 - ~15.0	M	146.9	~12.2	~0.58
Unit 3	~15.0 - ~34.0	O	92.9	~ 4.9	~0.15
Unit 2	~34.0 - ~36.0	E	46.2	~23.1	~0.88
Unit 1	~36.0 - ~90.0	Basement	854.1	~15.8	~1.03

Table 1: Compilation of sedimentary units, including interface reflector nomenclature, unit ages, unit thicknesses, sedimentation rates and accumulation rates.

The interface of units 4 and 5 shows just slight changes compared to the interface of units 3 and 4 (Fig. 4i). The shallowest areas expand from the east to the northeast reaching 4300 m. south to southwest of the survey centre we find a trough with a depth of 4600 m. Compared to the underlying trough of the interface between units 3 and 4 it shrunk due to the filling by unit 4 sediments in the west. The orientation of the interface outline slightly changed to a northwest to south direction (Fig. 4i). Unit 5 sediments are clearly dominated by the appearance of the Agulhas Drift deposits (Fig. 4j, 30°E/35.4°S-29.8°E/35°S). The biggest amount of sediments (up to 300 m in thickness) is deposited in an elongated depocentre, expanding from the northwest to the centre of the research area, with steep flanks to the south and a more gentle flank to the east and northeast (Fig. 4j). Sediment thickness decreases slowly from the survey centre to the southeast.

Accumulation and sedimentation rates of unit 5 sediments with 1.67 *10^{11} m³/my and 50.1 m/my are the highest within the research area (Table 1).

The seafloor is mainly characterised by the shape of the Agulhas Drift, which extends over the whole research area (Fig. 4k). The shallowest areas of the seafloor with 4200 m are found in the northwest and the survey centre, with a steep flank to the south, due to the Agulhas Drift's crest. Today, the deepest areas of the central Transkei Basin lie in the south and reach a water depth of 4550 m. Subbottom profile data (Fig. 3 top) show undisturbed and continuous reflections at the top of the drift`s crest, indicating that the development of the Agulhas Drift is still active.

In total, during the past ~90 Ma the largest amount of sediment (~1700 m) was deposited in the northeast of the researched area. Except for a small depocentre in the southeast at 30.7°E/36°S and a depocentre in the west at 29°E/35.5°S (Fig. 4l), this amount decreases gently down to a 1000 m thick cover in the south. Additionally, there are some small scale trough-like features spread all over the research area, which are caused by small basement highs (Fig. 4a).
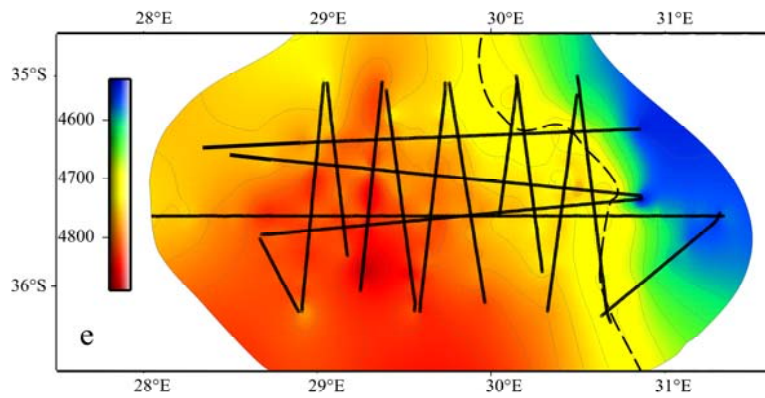
5.5 Discussion:

The five different time periods of the past 90 my as defined by the seismostratigraphic units, are characterised by strong variations in bottom current activity and sediment accumulation within the central Transkei Basin. The definition of the interface outline between two units (rms value) and the unit's depocentres (rms value), leads to an interpretation of the sedimentary structures and a reconstruction of palaeo-currents off South Africa. Furthermore, we created a depositional model for the central Transkei Basin since upper Cretaceous times. This model is presented in Figures 5a-e for five different stages and includes a reconstruction of the different current's flow paths and strengths. The grey to black fading areas indicate regions that are shallower than the interface outline. Hatched areas represent depocentres lying on top of the interfaces. According to their size, arrows indicate current strengths and directions. The different accumulation rates were computed using the size of the unit depocentres and the respective ages (Table 1).

The oldest unit 1, between 90 and 36 Ma shows predominant sedimentation in topographic lows. The seismic reflection sections in Figures 2 (CDPs 1800-2000) and 3 (CDPs 300-600) present unit 1 as a homogeneous sediment sequence. Still, the depocentre is located mainly in the northern area of interest, thus indicating possibly a slight influence of deep-sea currents originating in the west (Fig. 4b; Fig. 5a, dashed arrow). The accumulation rate of more than 1.03 *10^{11} m³/my is in favour of this (Table 1). Although, deep water activity in this region has been observed since the late Paleocene (Pak, 1992), we take the homogeneous reflection characteristics and the depocentre locations as an indication for sediment deposition without strong bottom current activity.

At 36 Ma the shallowest area is located in the eastern survey area with an orientation from north to south and in the northwest with an orientation from northeast to southwest (Fig. 4c). Within the following ~2 my a depocentre is developed above the shallowest region right on top of the outline high of interface units 1/2 in the east of the research area, indicating a predominant bottom current (Fig. 4d, 5b). The depocentre thins to the west and finally disappears (Figures 2, CDPs 6000-2000 and 4d). Since due to the Coriolis Force sediments are deposited to the left of a current's flow direction on the Southern Hemisphere we infer a southsetting bottom current to have shaped this depocentre.

Basement [m]; interface basement/unit 1
>90 Ma

Paleocene-Eocene boundary [m]; interface unit 1/unit 2
~36 Ma

Unit 1 [m]
~90 - ~36 Ma
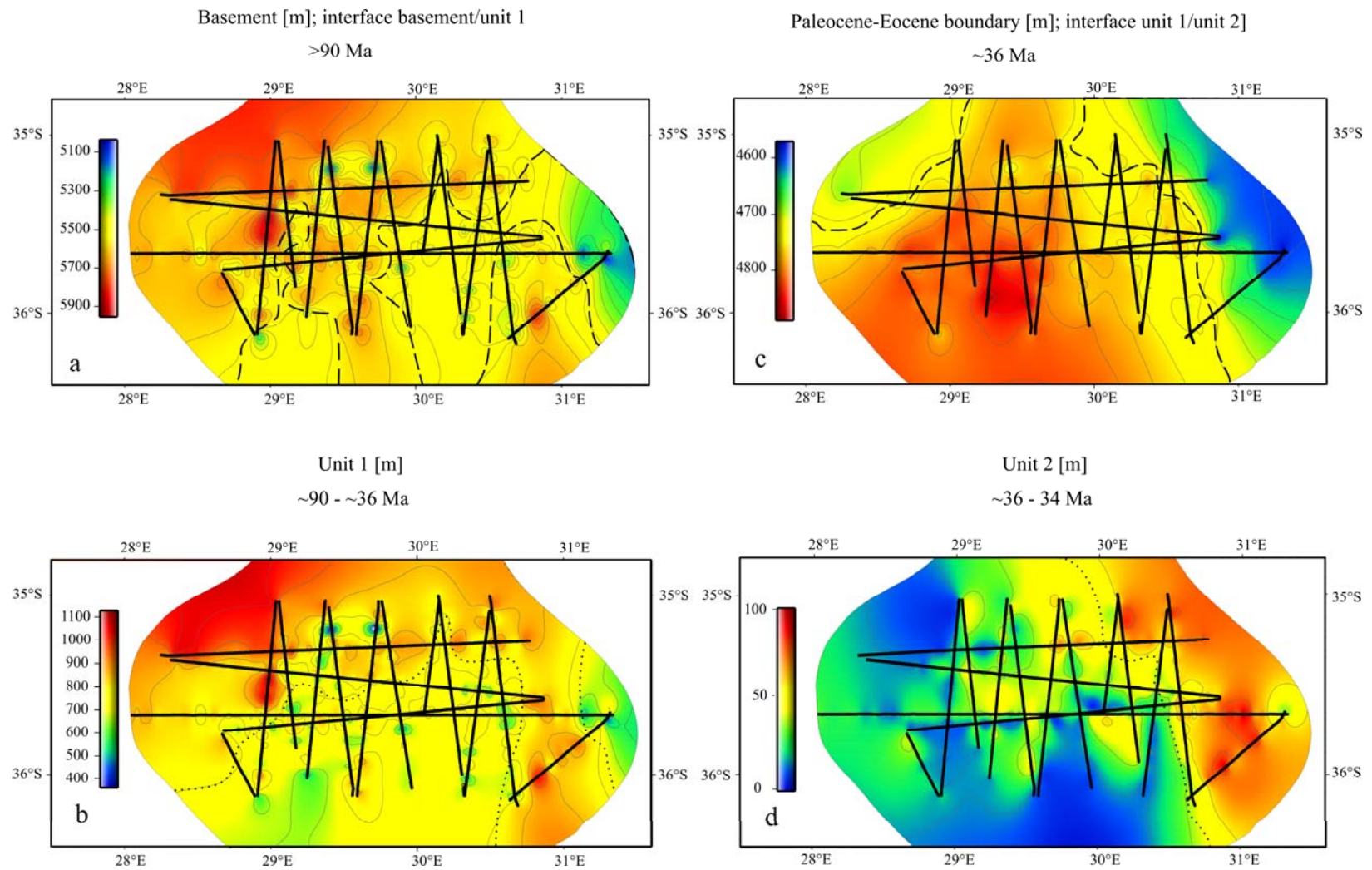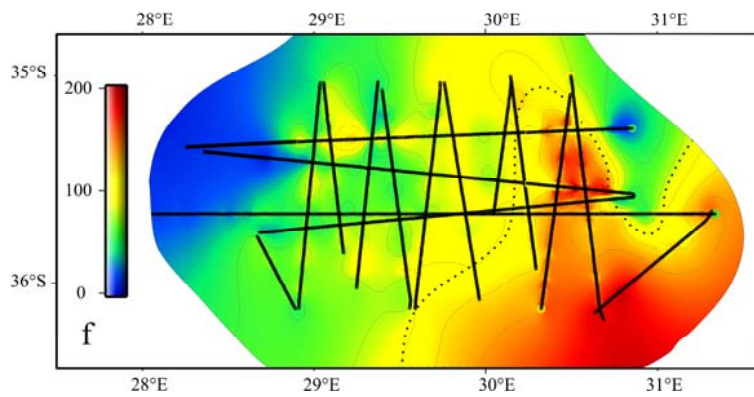
Unit 2 [m]
~36 - 34 Ma

Eocene-Oligocene boundary [m]; interface unit 2/unit3
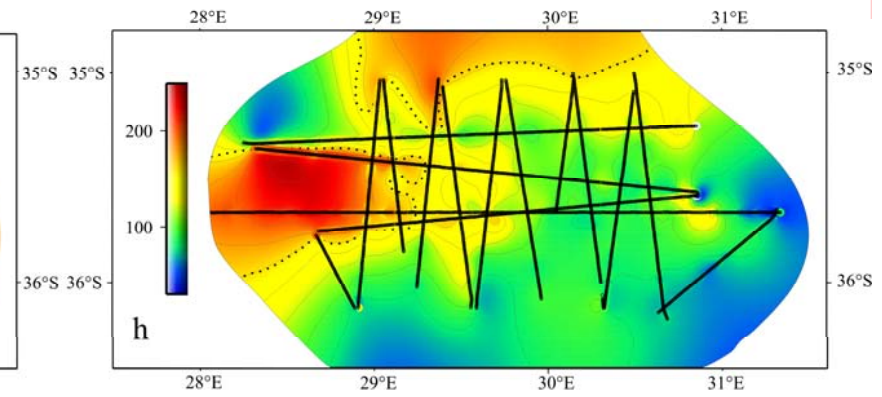~34 Ma

Middle Miocene boundary [m]; interface unit 3/unit 4
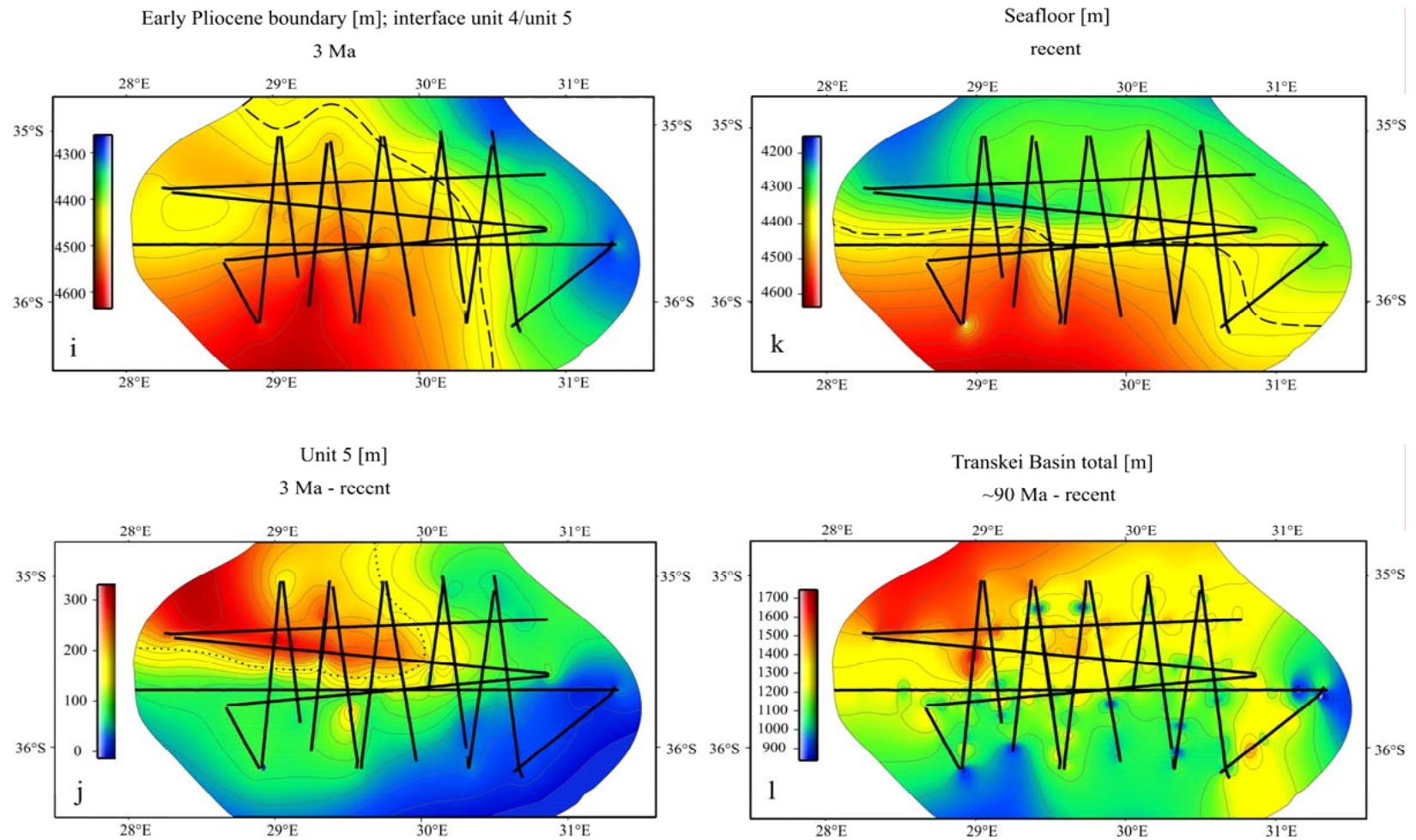~15 Ma
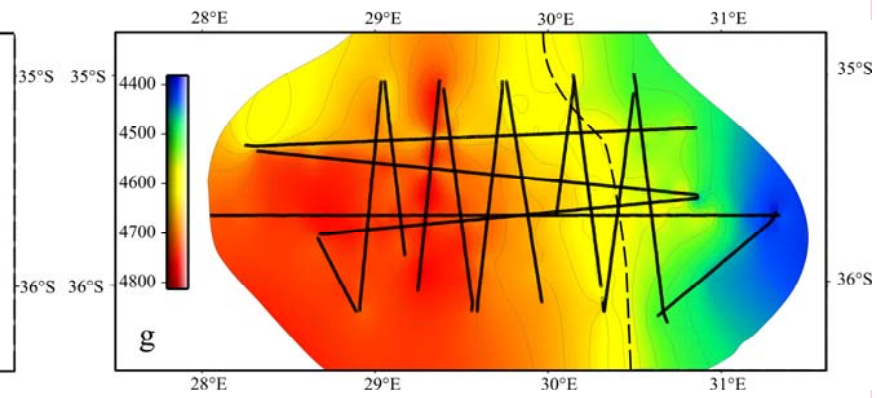
Unit 3 [m]
~34 - 15 Ma

Unit 4 [m]
~15 - 3 Ma

Figure 4a-l: Maps of reflector depth (interface basement/unit 1 to unit 4/unit 5) and unit thicknesses (unit 1 to unit 5 and Transkei Basin total) of the central Transkei Basin. Note the different interface depths and unit thicknesses according to the scale bars on the left hand side. Black lines indicate location of seismic reflection profiles. Hatched lines indicate interface outlines. Dotted lines indicate depocentre out.

Diester-Haass et al. (1996) report a short cooling event at about 36 Ma, which triggered the onset of proto-AABW-A (proto Antarctic Bottom Water) inflow into the Transkei Basin in the Late Eocene (Scher and Martin, 2004). The most likely event for the beginning inflow of bottom water into the Transkei Basin is the final establishment of the Antarctic Circumpolar Current (ACC) by the opening of the Drake Passage Gateway and the Tasman Sea Gateway for deep water at around 36 to 30 Ma (Stickley et al., 2004; Livermoore et al. 2005). It seems possible that the cooling started even before the full establishment of the ACC at around 34 Ma. We assume that at 36 Ma the first intensified proto-AABW-A flowed through the Agulhas Passage into the Natal Valley and continued close to the South African continental slope northward. In the southwestern Natal Valley it recirculated to the southeast and flowed back into the central Transkei Basin, where it developed the depocentre of unit 2 (Fig. 5b).

The shallowest region at 34 Ma is still located in the east to northeast of the research area (Fig. 4e). Additionally, the sediment depocentre until 15 Ma remains located in the eastern to southeastern survey area (Fig. 4f). Compared to the underlying unit 1 (Figs. 4c, d), the orientation of the interface outline at 34 Ma shifted from a south to north direction to a northwest to southeast direction and unit 3's depocentre`s location shifted from the east to the southeast (Figs. 4e, f). As a consequence, we interpret the flow direction of bottom water to have shifted from a southward to a southwestward direction and to have produced a sediment buckle at the southwestern end of the depocentre (Fig. 4f, 30.5°E/36.2°S). The accumulation rate (~0.15*10^{11}m³/my) and sedimentation rate (~4.9 m/my) within this period show the lowest sediment input into the Transkei Basin within the past 90 my (Table 1) and therefore we assume that the bottom water activity in the Transkei Basin within this stage decreased significantly. For the Lower Oligocene, Niemi et al. (2000) report the development of the Oribi Drift in the adjacent Natal Valley, Northeast of the Transkei Basin (Fig. 1), which correlates with the unit 3 sediments of the Transkei Basin (Schlüter and Uenzelmann-Neben, 2007). The approximately 500 km long drift is located close to the South African continental margin in a Southwest to Northeast direction. It is thought to be formed by proto-AABW-A, which flowed through the Agulhas Passage and the Transkei Basin further northeastward into the Natal Valley. The Oribi Drift was buried and partially eroded under younger sediments (Niemi et al., 2000). The main reason for an intensification of proto-AABW-A since 34 or even 36 Ma may be the onset of proto-ACC and consequentially the expansion of proto-AABW-A further North (Diester-Haass et al., 1996). In fact, the proto-AABW-A inflow into the Natal Valley strengthened and built up the Oribi-Drift (Niemi et al., 2000). As a consequence, only a weak southward flowing branch of recirculated proto-AABW-A can be observed in the Transkei Basin for this period. Due to the shift of the depocentre`s location from the east to the southeast (Figs. 5b, c) the flow path of proto-AABW-A must have changed from a southward direction in the Late Eocene (Fig. 5b) to a southwestward direction in Oligocene and early Miocene times (Fig. 5c; Faugères et al., 1999; Ben-Avraham et al., 1994).

Due to the pronounced deposition in the eastern survey area between 34 and 15 Ma (unit 3), at 15 Ma the shallowest region shifted to the southeast (Fig. 4g). Additionally, from unit 3 to unit 4 we observe a significant shift in depocentre location from the east to the west (Figs. 4f, h). Compared to the underlying unit 3, the accumulation and sedimentation rates increase remarkably to 0.58 *10^{11}m³/my and 12.2 m/my (Table 1) in unit 4, which indicates an increase in sediment input into the Transkei Basin. In late Miocene times, the central Transkei Basin is dominated by the development of the M-Drift (Fig. 2, CDPs 5000-7800, Fig. 4h, 29.5°E/35.6°S-28.4°E/35.6°S) with an extension to the north (Fig. 4h, 29.3°E/35.3°S-29.3°E/35°S) (Niemi et al., 2000; Schlüter and Uenzelmann-Neben, 2007). This about 300 km long drift is oriented in a north to south

direction, located between the South African continental margin and the abyssal plain. Niemi et al. (2000) state that it has been formed by bottom currents in early to middle Miocene times, may be due to a variation in bottom current pattern for mainly enigmatic reasons. According to its north-south orientation (Figs. 2 and 3), the M-Drift must have been formed by a northward flowing current. Therefore, we assume that the main inflow of proto-AABW into the Transkei Basin must have taken place from its southern opening (Fig. 1) and further to the adjacent Natal Valley in the northeast. The reason for an increasing proto-AABW-B activity in the Transkei Basin at that time is thought to be a cooling event in Middle Miocene (Zachos et al., 2001). This event produced a changing ACC flow by a stronger glaciation of Antarctica with a northward shift of the polar fronts (Holbourn et al., 2005) and consequently a variation of proto-AABW-B inflow into the Transkei Basin. Additionally, Pekar and DeConto (2006) report recurrent melting pulses on the Southern Hemisphere, triggered by an increasing Earth's eccentricity in middle Miocene times. As a consequence, between 15 and 3 Ma the main flow direction of proto-AABW-B has been northeastward (Fig. 5d). We cannot determine exactly, why the main inflow of proto-AABW shifted from the Agulhas Passage (AABW-A) to the southeast (proto-AABW-B), but according to the depocentre and the M-Drift location at that time, we have evidence for that shift, which coreelates well with the Middle Miocene cooling event.

At 3 Ma the shallowest region shifted from the southeast back to the east of the research area (Figs. 4g, i). The depocentre of unit 5, located in the northwest, is document to the development of the pronounced Agulhas Drift (Fig. 4j, 30°E/35.4°S-29.8°E/35°S), which rises up to 300 m above the surrounding seafloor (Figs. 3, CDP 2100, 5e). Compared to the underlying units, the accumulation rate ($\sim1.67*10^{11}$m³/my) and sedimentation rate ($\sim$50.1 m/my) show a strong increase in sediment input into the basin for this period (Table 1). The biggest depocentre's thickness appears in the west of the research area (Fig. 4j, 28.6°E/35.3°S) slowly thinning to the east, indicating a decreasing flow velocity of bottom water. As a consequence, the Agulhas Drift's orientation from west to east (Figs. 4j, k) mirrors a main bottom current inflow into the Transkei Basin for the latest stage through the Agulhas Passage and further eastward. At about 3 Ma the Isthmus of Panama finally closed and led to an increasing Northern Hemisphere cooling (Burton et al., 1997; Lear et al. 2003; Schneider and Schmittner, 2006). Thus, the attributes of North Atlantic Deep Water (NADW) changed significantly and it transported more sedimentary material through the Agulhas Passage into the Transkei Basin (Schlüter and Uenzelmann-Neben, 2007). Additionally, we do not have any indications for strong sediment input or erosion from the south of the Transkei Basin. Therefore, we think that the main inflow of AABW shifted from southeast (AABW-B) of the Agulhas Plateau (Fig. 5d) back to the Agulhas Passage (AABW-A). Directly behind the eastern opening of the Agulhas Passage's constriction, the flow velocity of NADW and AABW-A slowed down. The sediments were dumped to their left side (Coriolis Force) and produced the large depocentre (Agulhas Drift). At the southeastern tip of the Agulhas Drift body, the NADW split off with one branch further shaping the Agulhas Drift in the northeast (Fig. 5e). The other branch of NADW and AABW-A flowed southward and left the Transkei Basin. Due to the little amount of sediments in the East (Fig. 2, CDPs 7000-7800) and no recognizable erosion around the Agulhas Drift (Figs. 4j, 3), we assume that a possibly weak inflow of AABW-B into the Transkei Basin was blocked by the southeastward and southward flowing branches of NADW and AABW-A (Fig. 5e). Due to the huge depocentre (Agulhas Drift), which was developed within the past 3 Ma, the seafloor topography changed significantly. Figure 4k represents the seafloor topography today, characterised by the appearance of the Agulhas Drift`s crest, oriented in a west to east direction (Fig. 4k, 28.5°E/35.7°S-30.2°E/35.8°S). The shallowest area shifted, mainly

triggered by the appearance of the drift body, from the east to the north to northwestern research area.
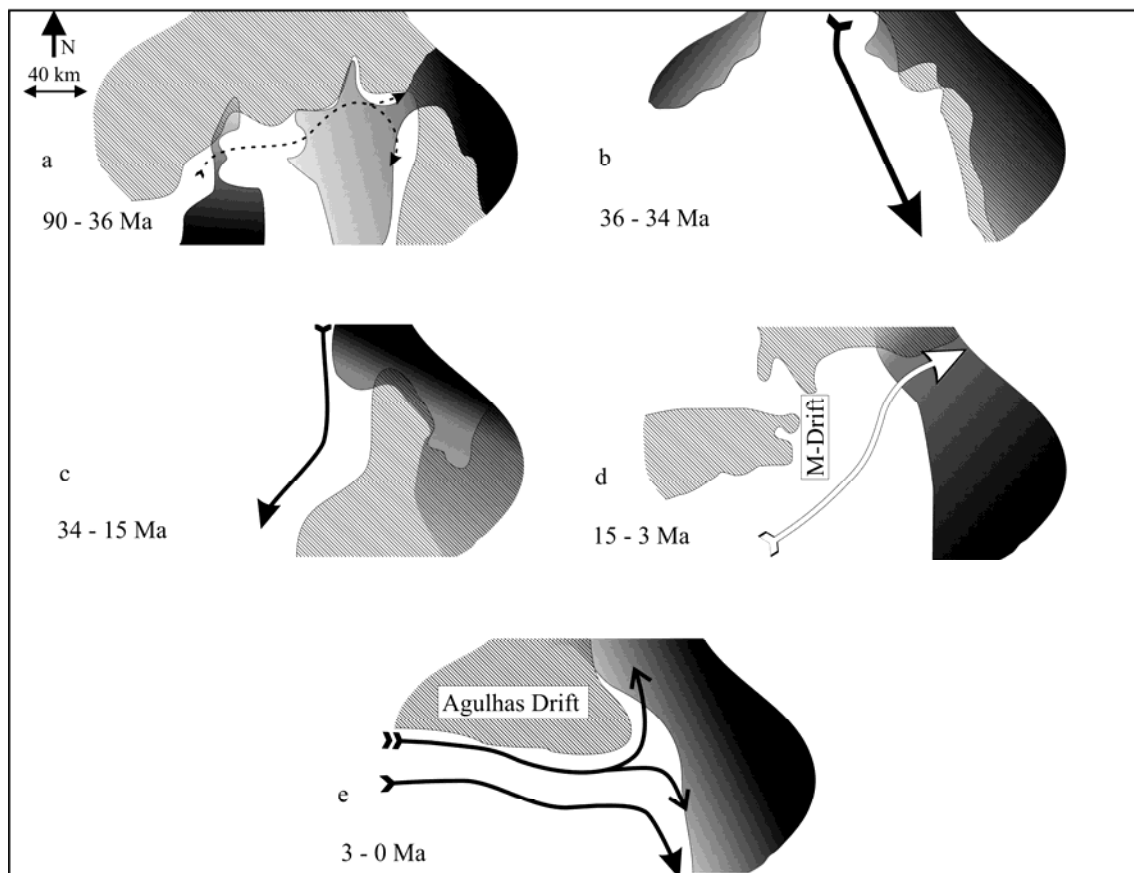

Figure 5a-e: Depositional model for the central Transkei Basin for the past 90 Ma. Each map shows the interface outline between two units, with colours fading from black to grey, where the interface deepens. Depocentres appear hatched. Fully spiked black arrows indicate Antarctic Bottom Water flowing through the Agulhas Passage. Fully spiked white arrows indicate Antarctic Bottom Water flowing from the south into Transkei Basin. Black arrows with open spike indicate North Atlantic Deep Water. Dashed arrows indicate presumed flow path. The thickness of the arrows indicates current strength.

5.6 Conclusions:

The analysis of five time slices within the past 90 Ma of the Transkei Basin depositional history revealed strong variations in sediment input and depocentre development. Especially since the Late Eocene, the geometry of the deposited material has been heavily affected by the flow paths and strengths of deep-sea and bottom currents. For a detailed reconstruction of the different evolutional stages, we developed a depositional model with respect to depocentre locations, interface outline elevations and the according deep-sea currents (Figs. 5a-e).

The Upper Cretaceous to Late Eocene is characterised by trough filling deep-sea sedimentation, with little evidence for a strong influence of bottom current activity (Fig. 5a).

In late Eocene the depocentre location shifts to the east and marks a first onset of proto-AABW-A (Antarctic Bottom Water) inflow into the Transkei Basin as recirculated water masses from the adjacent Natal Valley in the northeast (Fig. 5b). The beginning of proto-AABW-A activity is triggered by the establishment of a deep water gateway between South America and Antarctica and the opening of the Tasman Gateway, respectively.

In early Oligocene the Transkei Basin is characterised by decreasing sedimentation and accumulation rates and a depocentre shifting to the southeast. This is initiated by decreasing inflow of recirculated proto-AABW-A into the Transkei Basin from the north, due to an increasing proto-AABW-A inflow into the Natal Valley (Niemi et al., 2000; Figs. 1, 5c).

An intensified current activity and increasing sediment input since middle Miocene times is triggered by a global cooling event. The location and orientation of the M-Drift in the centre of the survey area reveals a predominant inflow of proto-AABW-B into the Transkei Basin via its southern gateway since 15 Ma (Fig. 5d).

Since 3 Ma the Agulhas Drift has formed a pronounced depocentre in the central to western research area (Fig. 5e), formed by westward flowing North Atlantic Deep Water (NADW) and AABW-A. The final closure of the Panama Isthmus at about 3 Ma is the reason for a shifting of main current activity to the Agulhas Passage and triggered a predominant westward flow direction within the Transkei Basin. Subbottom profiler images (Fig. 3) reveal that the Agulhas Drift development has not ceased yet.

5.7 Acknowledgments:

5.8 References:

Arhan, M., Mercier, H. and Park, Y.-H., 2003. On the deep water circulation of the eastern South Atlantic Ocean. Deep Sea Research Part I: Oceanographic Research Papers, 50, 7, 889 – 916.

Ben-Avraham, Z., Hartnady, C. J. H. and Malan, J. A., 1993. Early tectonic extension between the Agulhas Bank and the Falkland Plateau due to the rotation of the Lafonia microplate. Earth and Planetary Science Letters, 117, 43 – 58.

Ben-Avraham, Z., Niemi , T. and Hartnady, C. J. H., 1994. Mid-Tertiary changes in deep ocean circulation patterns in the Natal Valley and Transkei Basin, Southwest Indian Ocean. Earth and Planetary Science Letters 121, 639 – 646.

Burton, K. W., Ling, H.-F. and O`Nions, R. K., 1997. Closure of the Central American Isthmus and its effect on deep-water formation in the North Atlantic. Nature, 386, 382 – 386.

Diester-Haass, L., Robert, C. and Chamley, H., 1996. The Eocene-Oligocene preglacial-glacial transition in the Atlantic sector of the southern Ocean (ODP Site 690). Marine Geology, 131, 123 – 149.

Dingle, R. V. and Camden-Smith, F., 1979. Acoustic stratigraphy and current-generated bedforms in deep ocean basins off southeastern Africa. Marine Geology, 33, 3-4, 239 – 260.

Du Toit, S. R. and Leith, M. J., 1974. The J(c)-1 bore-hole on the continental shelf near Stanger, Natal. Geological Society of South Africa, 77, 247 – 252.

Faugères, J.-C., Stow, D. A. V., Imbert, P. and Viana, A., 1999. Seismic features diagnostics of contourite drifts. Marine Geology, 162, 1 – 38.

Frank, M., Whiteley, N., Kasten, S., Hein, J., R. and O`Nions, K., 2002. North Atlantic Deep Water export over the past 14 Myr: Evidence from Nd and Pb isotopes in ferromanganese crusts. Paleoceanography, 17, 2, 12-1 – 12-9.

Fullerton, L. G., Frey, H. V., Roark, J, H. and Thomas, H. H., 1989. Evidenec for a remanent contribution in Magsat data from the Cretaceous Quiet Zone in the South Atlantic. Geophysical Research Letters, 16, 1085 – 1088.

Goodlad, S. W., Martin, A. K. and Hartnady, C. J. H., 1982. Mesozoic magnetic anomalies in the southern Natal Valley. Nature, 295, 686 – 688.

Gordon, A. L., 1986. Interocean exchange of thermocline water. Journal of Geophysical Research, 91, 5037 – 5046.

Holbourn, A., Kuhnt, W., Schulz, M., and Erlenkeuser, H., 2005. Impacts of orbital forcing and atmospheric carbon dioxide on Miocene ice-sheet expansion. Nature, 438, 483 – 487.

Lear, C. H., Rosenthal, Y. and Wright, J. D., 2003. The closing of a seaway: ocean water masses and global climate change. Earth and Planetary Science Letters, 210, 3-4, 425 – 436.

Livermore, R., Nankivell, A., Eagles, G. and Morris, P., 2005. Paleogene opening of Drake Passage. Earth and Planetary Science Letters, 236, 1-2, 459 – 470.

Lutjeharms, J. R. E., Boebel, O. and Rossby, H. T., 2003. Agulhas cyclones. Deep-Sea Research II. 50, 13 – 34.

Mantyla, A. W. and Reid, J. L., 1995. On the origins of deep and bottom waters of the Indian Ocean. Journal of Geophysical Research, 100 (c2), 2417 – 2439.

Martin, A. K. and Hartnady, C. J. H., 1986. Plate tectonic development of the Southwest Indian Ocean: a revised reconstruction of East Antarctica and Africa. Journal of Geophysical Research, 91, 4767 – 4786.

Niemi, T. M., Ben-Avraham, Z., Hartnady, C. J. H. and Reznikov, M., 2000. Post-Eocene seismic stratigraphy of the deep ocean basin adjacent to the Southeast African continental margin: a record of geostrophic bottom current systems. Marine Geology, 162, 2-4, 237 – 258.

Orsi, A. H., Johnson, G. C. and Bullister, J. L., 1999. Circulation, mixing, and production of Antarctic Bottom Water. Progress in Oceanography, 43, 55 – 109.

Pak, D. K., 1992. Paleocene to Eocene benthic foraminiferal isotopes and assemblages: Implications for deepwater circulation, Paleoceanography, 7, 4, 405 – 422.

Park, Y.-H., Gamberoni, L., Charriaud, E., 1993. Frontal structure, water masses, and circulation in the Crozet Basin. Journal of Geophysical Research, 98, 12361 – 12385.

Pekar, S. F. and DeConto, R. M., 2006. High-resolution ice-volume estimates for the early Miocene: Evidence for a dynamic ice sheet in Antarctica. Palaeogeography, Palaeoclimatology, Palaeoecology, 231, 1-2, 101 – 109.

Scher, H. D. and Martin, E. E., 2004. Circulation in the Southern Ocean during the Paleogene inferred from neodymium isotopes. Earth and Planetary Science Letters, 228, 3-4, 391 – 405.

Schlüter, P. and Uenzelmann-Neben, G., 2007. Seismostratigraphic analysis of the Transkei Basin: A history of deep sea current controlled sedimentation. Marine Geology, 240 (1-4), 99-111.

Schneider, B. and Schmittner, A., 2006. Simulating the impact of the Panamanian seaway closure on ocean circulation, marine productivity and nutrient cycling. Earth and Planetary Science Letters, 246, 3-4, 367 – 380.

Smith, W. H. F. and Sandwell, D. T., 1997. Global Sea Floor Topography from Satellite Altimetry and Ship Depth Soundings. Science, 277, 1956 – 1962.

Stickley, C. E., Brinkhuis, H., Schellenberg, S. A., Sluijs, A., Röhl, U., Fuller, U., Grauert, M., Huber, M., Warnaar, J., William, G. I., 2004. Timing and nature of the deepening of the Tasman Gateway. Paleoceanography, 19:PA4027,doi:10.1029/2004PA001022.

Tikku, A. A., Marks, K. M. and Kovacs, L. C., 2002. An Early Cretaceous extinct spreading center in the northern Natal Valley. Tectonophysics, 347, 87 – 108.

Van Aken, H. M., Ridderinkhof, H., de Ruijter, W. P. M., 2004. North Atlantic Deep Water in the south-western Indian Ocean. Deep Sea Research Part I: Oceanic Research Papers, 51, 6, 755 – 776.

Winter, A. and Martin, K., 1990. Late quarternary history of the Agulhas Current. Paleoceanography, 5, 4, 479 – 486.

Zachos, J., Pagani, M., Sloan, L., Thomas, E. and Billups, K., 2001. Trends, rhythms and aberrations in global climate 65 Ma to present. Science, 292, 686 – 6.

6 Conspicuous seismic reflections in Upper Cretaceous sediments as evidence for black shales off South Africa

Philip Schlüter, Gabriele Uenzelmann-Neben

6.1 Abstract:

The Upper Cretaceous is commonly associated with greenhouse climate, associated with Oceanic Anoxic Events (OAE), and the ongoing break up of Gondwana. Especially the opening of the Atlantic and the beginning closure of the Tethys resulted in strong variations of the ocean's currents flow paths and in climate change. Only little is known about these changing conditions and OAE appearances, in particular south of South Africa, back then. A high resolution seismic reflection data set from the submarine Transkei Basin off South Africa revealed various depositional stages for this region for the past ~ 90 Ma. In these seismic sections, a recurrently appearing very high amplitude horizon within weak to homogeneous Upper Cretaceous reflections was observed. This reflector could roughly be dated to ~ 80 Ma - ~ 85 Ma and falls within the last big OAE 3 in Upper Cretaceous. According to the appearance and reflection characteristics of the reflector as well as its time/depth information, it could be the first report of black shales, maybe associated with an OAE, for a deep-sea basin in this region.

6.2 Introduction:

The oceanic and climatic conditions off South Africa since the Eocene have been subject to research in several studies (e.g. Tucholke and Embley, 1984; Ben-Avraham et al., 1993; Niemi et al., 2000; Boebel et al., 2003; Schlüter and Uenzelmann-Neben, 2007), but only little is known from earlier stages. The Upper Cretaceous and early Palaeogene are characterised by the ongoing break-up of Gondwana and, hence, the creation of new oceanic basins. Along with this, the oceanic circulation patterns, as well as the global heat exchange altered significantly (Poole et al., 2005). Additionally, the beginning isolation of Antarctica is a key factor for the evolution of the palaeo-climatic conditions at that time (Kennett, 1977). The period between ~100 Ma and ~50 Ma is characterised by a significant cooling of the earth's climate, especially on the Southern Hemisphere (greenhouse to icehouse, Sellwood and Valdes, 2006).

The region south of South Africa is characterised by deep-sea basins and deep-sea plateaus that originate in upper Cretaceous times, caused by the ongoing break-up of Gondwana since the Jurassic (König and Jokat, 2006). Due to the unique location of the submarine Transkei Basin within the varying current system off South Africa, its sedimentary content has been influenced by water masses since then and provides information about possible palaeo-pathways but also palaeo-climate conditions. These data are important for climate reconstructions, because they can shed light on the interdependency between different large scale factors like changing currents systems or ocean gateways and global climate change. Unfortunately, continuous sediment deposits from deep-sea basins since the Upper Cretaceous that are located at crucial gateways are very rare and, consequentially, could not be studied extensively, yet.

In 2005 we gathered a set of high resolution seismic reflection profiles across the Transkei Basin, which shows the whole sedimentary infill at least of the past 90 my. The analysis of these sediments helps us to improve the knowledge about global water exchange, heat transfer and climate change, especially between ~ 90 Ma and ~ 36 Ma.

6.3 Geological Background:

Today, the region south and Southeast of South Africa is mainly characterised by the submarine Agulhas Plateau and the submarine Transkei Basin (Fig. 1). The Agulhas Plateau is a deep-sea plateau rising up to 2700 m above the surrounding seafloor and reaches a water depth of up to 1800 m. It is separated from the African continental shelf by the up to 4500 m deep, east-west oriented Agulhas Passage. The deep-sea Transkei Basin is located east of the Agulhas Plateau and south of the adjacent submarine Natal Valley and reaches a water depth of up to 4500 m (Fig. 1). Within the central Transkei Basin, we observe up to 1800 m thick sedimentary sequences (Schlüter and Uenzelmann-Neben, 2007).

Determining the age of the Transkei Basin and its sedimentary filling is difficult due to the absence of any drill core information within this region. Initial seafloor spreading off Southeast Africa has been observed between the Mozambique Ridge and East Antarctica commencing at 155 Ma (Jokat et al., 2003). The development of an extensional basin south of South Africa before 130 Ma is unlikely, due to the Maurice Ewing Bank (MEB), attached to the Falkland Bank (FB), which only later moved in a westerly direction (König and Jokat, 2006). Figure 2 shows the situation at 80 Ma, where the MEB and the FB have moved along the Agulhas Falkland Fracture Zone further to the southwest. Studies of Goodlad et al. (1982) and Tikku et al. (2002), who used plate movement velocities and directions, revealed an initial rifting and with it the opening of the Transkei Basin at ~124 Ma.
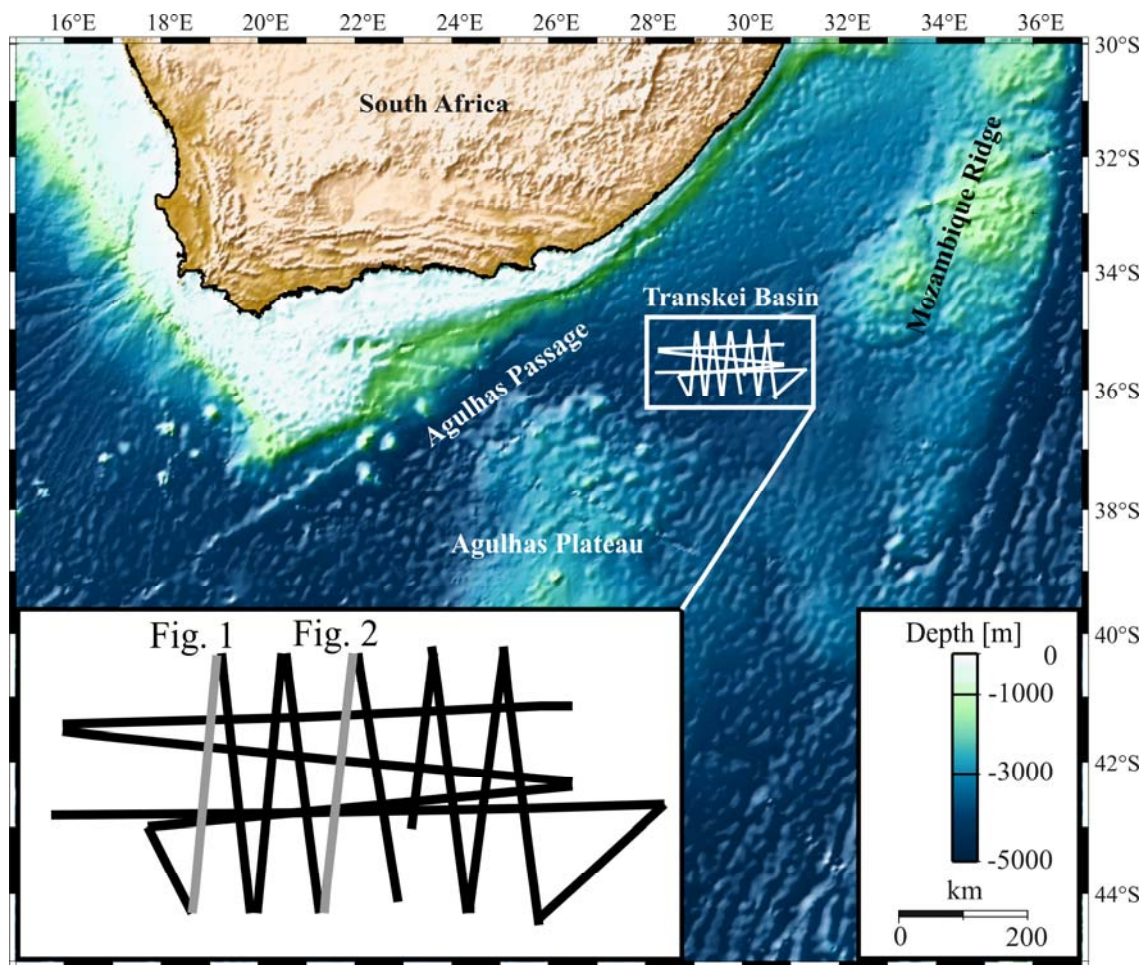
58

Figure 1: Bathymetric map of the research area off South Africa (after Smith and Sandwell, 1997), showing the location of the seismic reflection lines in the central Transkei Basin. Grey indicated lines in the blow-up represent seismic profiles shown in Figures 2 and 3.

Although the rifting happened during the Cretaceous magnetic quiet zone (Fullerton et al., 1989), the development of the Transkei Basin, as well as the Agulhas Plateau, must have been finished at around 90 Ma (Dingle and Camden-Smith, 1979; Labrecque and Hayes, 1979; Martin and Hartnady, 1986; Ben-Avraham et al., 1993). According to the basin's development, the maximum age of its sedimentary content varies around 90 Ma. This sedimentary infill was subdivided into two parts. The topmost ~½ of the basin's sediments (Figs. 3 and 4, units 2 to 5) shows the influence of deep and bottom current activity in this region since late Eocene times (Schlüter and Uenzelmann-Neben, 2007). Since ~36 Ma deep and bottom waters, like the Antarctic Bottom Water (AABW) or the North Atlantic Deep Water (NADW) have flowed in eastward direction through the Agulhas Passage and the Transkei Basin around the South African coast and have influenced the sedimentation in the basins. The warm surface Agulhas Current (AC) flows westward from the Indic into the South Atlantic Ocean.

The lowermost ~½ of the Transkei Basin's sediment contains information about the Upper Cretaceous and the Early Paleogene, on which we focus in this study.

6.4 Seismostratigraphy:

Different seismostratigraphic models of the Natal Valley and parts of the Transkei Basin have led to a revised stratigraphy for the deep-sea off South Africa (Niemi et al., 2000; Schlüter and Uenzelmann-Neben, 2007). In the following, we briefly describe the 5 seismostratigraphic units of the central Transkei Basin

The acoustic basement in the central Transkei Basin is located in depths between 5500 and 6000 m and shows a partially rugged structure with few sub vertical small scale faults (Fig. 4, CDPs 800-1000). Unit 1 is the oldest unit in the Transkei Basin and covers the acoustic basement. With up to 1000 m it is the basin's thickest unit, reaching a maximum depth of ~6000 m (Fig. 4, CDP 2200). It is subdivided into subunits 1a and 1b, separated by the Cretaceous-Tertiary boundary (K-T boundary). Unit 1a appears as a mostly homogeneous area, which partially shows a reflector with strong amplitude variations (reflector "B"), on which we focus in the "Results" chapter (Fig. 3, CDPs 1600-3200; Fig. 4, CDPs 2100, 3800-4600). In contrast to unit 1a, overlying unit 1b shows slightly stronger reflections and is cut by a large amount of sub vertical small scale faults (Fig. 3, CDPs 0-800). Due to the low reflectivity of subunit 1a we cannot determine whether the faults extend further downwards or not.
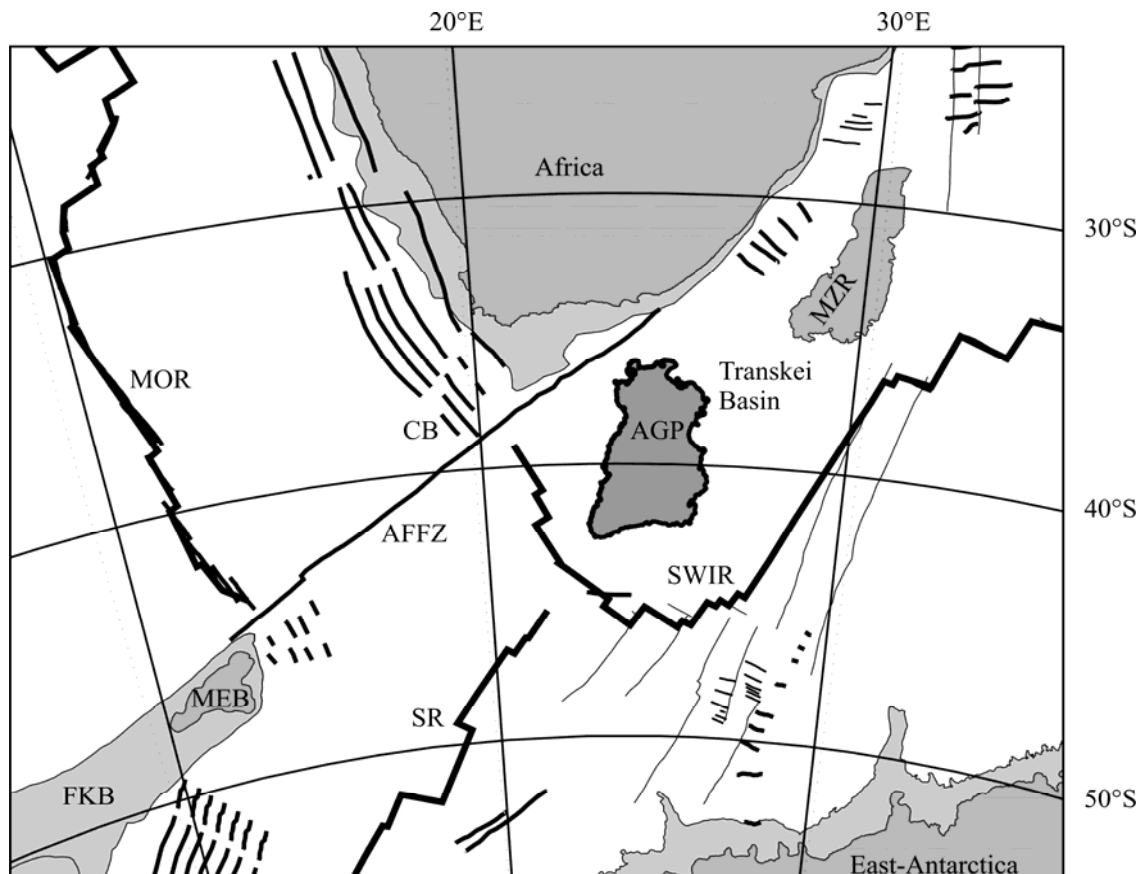

Figure 2: Structural overview of the Southeast Atlantic and the southwest Indic at ~80 Ma. Thick black lines indicate middle oceanic ridges. Thinner black lines indicate spreading anomalies. AFFZ: Agulhas Falkland Fracture Zone; AGP: Agulhas Plateau; CB: Cape Basin; FKB: Falkland Bank; MEB: Maurice Ewing Bank; MZB: Mozambique Ridge; SR: Scotia Ridge; SWIR: South West Indian Ridge.

Reflector E marks the onset of the ~25 m thick unit 2 in late Eocene, indicated by strong reflections (Figs. 3 and 4). The beginning of up to 70 m thick unit 3 is indicated by reflector O, which marks the Eocene-Oligocene boundary. Overlying unit 4 sets in in middle Miocene times and is dominated by weaker reflections than the older units 2 and 3. The youngest unit 5 represents the beginning of the Pliocene with the appearance of high amplitude reflections and a maximum thickness of ~500 m. It is dominated by the appearance of the Agulhas Drift crest in the basin's centre (Fig. 3, CDP 2000; Fig. 4, CDP 1800).

6.5 Results:

As mentioned before, unit 1a is characterised by mostly homogeneous areas and shows only weak internal reflections (Fig. 3, CDP 3800 – 4800). In the lower part of unit 1a (Figs. 3 and 4, between 5200-5700 m) we observe a partially strong, prominent reflection band. This reflector B occurs on nearly all seismic reflection profiles (Figure 5). It shows positive impedance contrasts to the underlying reflections, with moderate amplitude values around 0 - 15000, indicated by the yellow to orange colours on Figure 5. The reflections are partially very weak and therefore difficult to trace on some seismic sections (Fig. 3, CDPs 3800–4800). On most profiles, we observe this reflector with suddenly appearing very strong reflections. The amplitudes of these so called "bright spots" then vary around 20000 – 30000, indicated by the pink colours in Figure 5. The blow-up on Figure 3 (CDPs 1700-3100, unit 1a) shows one of these bright spots of reflector B. East of CDP 3100 and West of CDP 1700 (Fig. 3) the amplitudes decrease, but the reflectors can still be traced. On profile AWI-20050012 we observe reflector B again showing strong amplitude variations (Fig. 4, CDPs 2100-2200 and 3900-4500, unit 1a, blow-up).

Sedimentary unit	Unit age (Niemi et al., 2000; Gradstein et al., 2004; Schlüter and Uenzelmann-Neben, 2007) [Ma]	Duration [my]	Unit thickness (rms) [m]	Sedimentation rates [m/my]
Unit 1	~36.0 - ~90.0	~54.0	854.1	~15.8
Subunit 1b	~36.0 - ~65.5	~29.5	256.5	~ 8.7
Subunit 1a	~65.5 - ~90.0	~24.5	597.6	~24.4
Reflector B/ Basement	~79.4 - ~90.0	~10.6	258.4	~24.4
Subunit 1a*	~65.5 - ~100.0	~34.5	597.6	~17.3
Reflector B/ Basement*	~85.1 - ~100.0	~14.9	258.4	~17.3

Table 1: Compilation of sedimentary unit 1 and subunits 1a and 1b, including unit ages and duration, unit thicknesses and sedimentation rates. Rows without asterisk represent calculated values with a basement age of 90 Ma. Rows with asterisk represent calculated values with a basement age of 100 Ma.
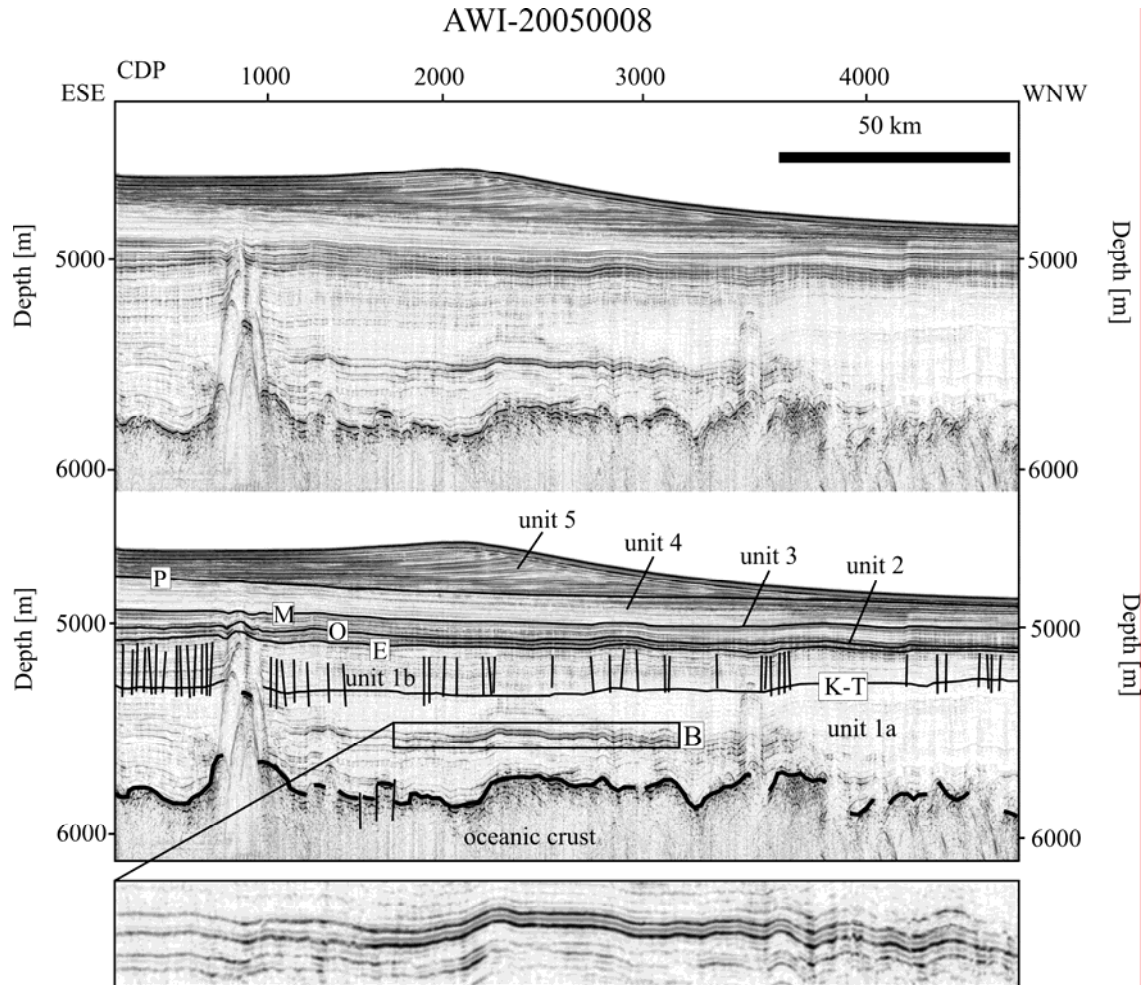
Figure 3: Seismic reflection profile AWI-20050008 showing acoustic basement and seismostratigraphic units 1-5. B: Recurrently appearing high amplitude reflector; E: Late Eocene; K-T: Cretaceous-Tertiary boundary; M: middle Miocene; O: Eocene/Oligocene boundary; P: early Pliocene.

Although reflector B appears on nearly all seismic reflection lines, the bright spots gather predominantly in the basin's centre (Fig. 5, 35.2°S/29.3°E – 36.1°S/29.5°E) and partially towards the West and Southwest (Fig. 5, 35.3°S/28.7°E – 36.2°S/28.9°E).

Determining the age of reflector B is difficult, due to the absence of drill core information from the Transkei Basin. In order to make an attempt in dating reflector B, we first calculated rms values for unit 1 and subunits 1a and 1b thicknesses to estimate the sedimentation rates (Tab. 1). The duration of subunit 1b could be determined by the age of reflector E (top of unit 1) and the Cretaceous-Tertiary Boundary (K-T boundary, Tab. 1). The duration of unit 1 and the subunit 1a could only be estimated with the assumed age of the Transkei Basin's basement as ≥ 90 Ma (Schlüter and Uenzelmann-Neben, 2007). Table 1 shows that the sedimentation must have strongly decreased from upper Cretaceous (~24.4 m/my, subunit 1a) to Paleogene times (~8.7 m/my, subunit 1b). Following, we calculated the rms thickness between the Transkei Basin's basement and reflector B (Tab. 1). By using the approximate sedimentation rate for subunit 1a (~24.4 m/my) we determined the duration for the period from the basement to the sedimentation of reflector B (~10.6 my). Assuming a minimum age of the central Transkei Basins

basement of 90 Ma, we get an estimated age for reflector B of ~79.4 Ma (Tab. 1). Still, we cannot be sure about the exact age of the Transkei Basin's basement, except for its development to have been finished at 90 Ma. If we assume a basement age for the central Transkei Basin of ~100 Ma (Tab. 1, rows with asterisk), we would get slightly different results for the sedimentation rate of subunit 1a (~17.3 m/my) and for the age of reflector B (~85.1 Ma).

According to the different estimated basement ages between ~90 Ma and ~100 Ma, the age of reflector B lies around ~79.4 Ma - ~85.1 Ma.

Oceanic Anoxic Event	Epoch	Time [Ma]
OAE 3	Coniacian-Santonian	87.3-84.6
OAE 2	Late Cenomanian	93.8-93.5
OAE 1d	Late Albian	100.6-100.2
OAE 1c	Early Albian	103.7-103.4
OAE 1b	Early Albian-Late Aptian	110.9-113.2
OAE 1a	Early Aptian	124.2-123.4

Table 2: Compilation of Oceanic Anoxic Events (OAE) 1 to 3 including geological epoch and time in Ma, after Meyers et al. (2006), ages after Ogg et al. (2004) and Wagner et al. (2004).

6.6 Discussion:

The analysis of the oldest Transkei Basin sediments revealed mostly homogeneous areas or weak reflective regions. In the deepest parts of subunit 1a we found the recurrently appearing high amplitude reflector B (Figs. 2 and 3, subunit 1a). This reflector must have been deposited around ~ 80 Ma within upper Cretaceous times. The conditions in the world's oceans during the late Cretaceous and the early Palaeogene changed rapidly, where especially the appearance of the Atlantic Ocean and the Tethys altered significantly. In order to make an attempt at reconstructing palaeo-current flow-paths or palaeo-climatic conditions in the Transkei Basin at that time, we need to determine the origin of reflector B. Its detailed analysis could help to shed light on the deep-sea conditions in this region back then.

There are different possible origins of these bright spots, such as: hydrate related Bottom Simulating Reflectors (BSR), diagenetic related BSRs, horizontal dykes/sills, free gas/oil or black shales. In the following we discuss and evaluate the different features as origin for the development of reflector B.
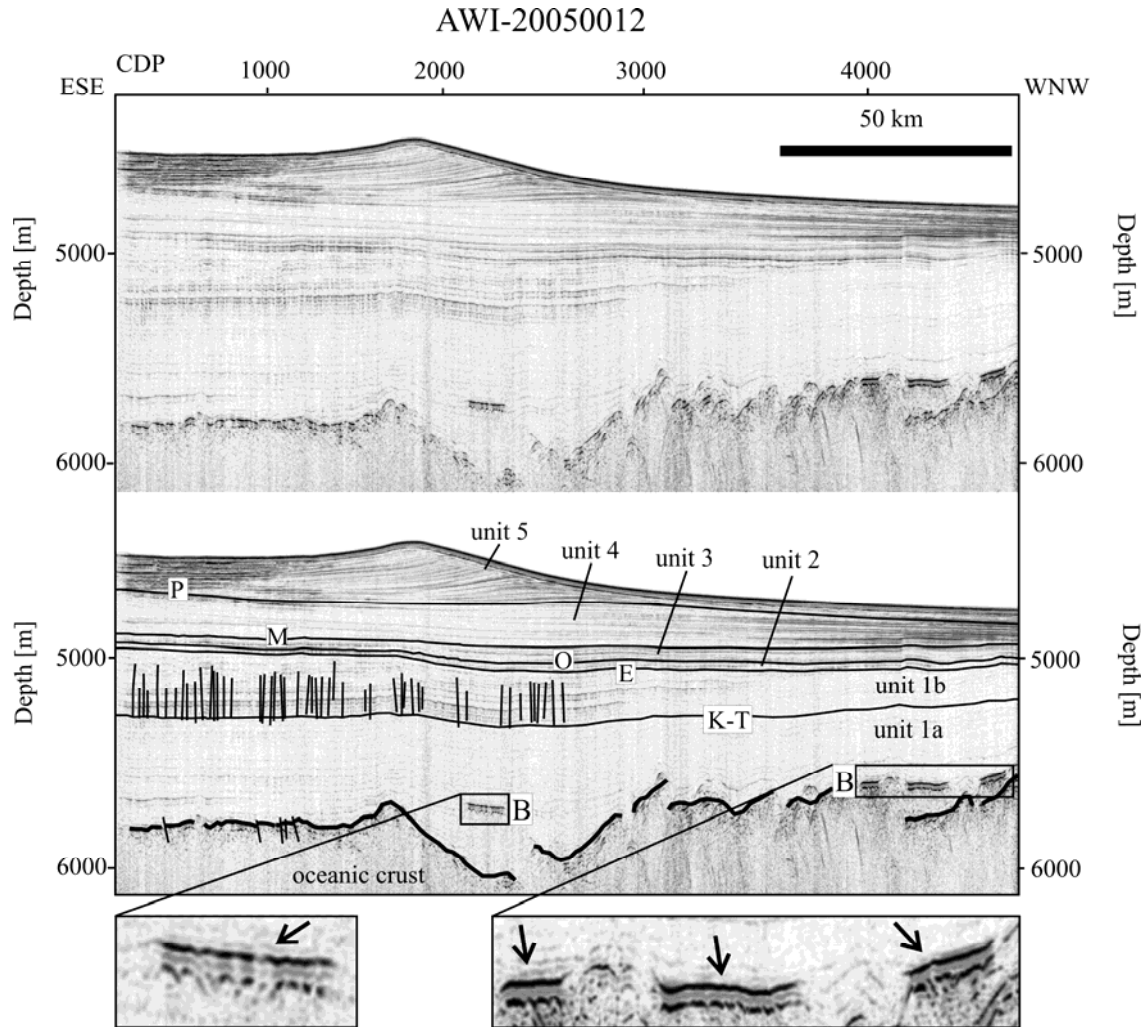
Figure 4: Seismic reflection profile AWI-20050012 showing acoustic basement and seismostratigraphic units 1-5. B: Recurrently appearing high amplitude reflector;E: Late Eocene; K-T: Cretaceous-Tertiary boundary; M: middle Miocene; O: Eocene/Oligocene boundary; P: early Pliocene.

6.6.1 Gas hydrate related Bottom Simulating reflectors:

A gas hydrate related Bottom Simulating Reflector (BSR) is a horizon that is oriented parallel to the seafloor topography, triggered by the appearance of solid methane/ethane. These gas hydrates are stable under a high pressure and temperatures below ~25°C (Sloan, 1998). Stable pressure conditions can be found parallel to the seafloor topography. At this stability zone gas hydrates, which produce BSRs, can be found nearly all over the world's oceans. Beneath the gas hydrate stability zone, free gas can be observed (e.g. Shipley et al., 1979; Petersen et al., 2007). Due to the velocity contrast between the hydrate and the free gas bearing underlying sediment, this causes a highly reflective horizon with reversed polarity (Pecher et al., 1996; Berndt et al., 2004). As shown on Figure 4, reflector B does not follow the seafloor topography at all and also does not show an inverse polarity (Fig. 4, CDPs 2100-2200 and 3900-4500). Consequentially, it does not fit the most important criteria for a gas hydrate related BSR. Additionally, with up to 5000 m water depth plus a sediment cover of ~ 1 km, the

reflector lies much deeper than the gas hydrate stability zone and the surrounding sediment reaches temperatures above 25°C (Sloan, 1998). This excludes a gas hydrate related BSR as source for reflector B.

6.6.2 Diagenetic related Bottom Simulating Reflectors:

Like gas hydrate related BSRs, diagenetic related BSRs are sub-horizontally oriented and often cross-cut the surrounding lithology. Though, in contrast to hydrate related BSRs, diagenetic related BSRs do not have to follow the seafloor topography (Bohrmann et al., 1992; Berndt, et al. 2004). A diagenetic related BSR consists either of opal bearing horizons or porcelanite bearing horizons.

The origin of opal bearing BSRs are biogenic and amorphous opal A, which consists of mostly unicellular siliceous micro-organisms, such as diatoms or radiolarians and principally can be found all over the globe. At specific temperatures around 30°C – 50°C opal A converses to cristobalite containing opal CT (Tribble et al., 1992) and later to quartz (Kastner et al., 1977). Due to diagenesis, caused by the conversion from opal A to opal CT, the seismic velocity increases and creates a positive acoustic impedance (Volpi et al., 2003; Berndt et al., 2004). Because of the resistibility against high pressures, the location of the opal A/CT BSR solely depends on temperature (Grützner and Mienert, 1999). That is why, contrarily to gas hydrate BSRs, opal A/CT BSRs are not explicitly attached parallel to the seafloor. Finally, the sediments beneath the opal A/CT conversion contain opal CT bearing layers, so the regions beneath the opal A/CT BSRs appear higher reflective than the horizons above (Berndt et al., 2004).

Porcellanite is a diagenetic rock also known as chert, resulting from the opal A to opal CT conversion, which consequentially consists of opal CT (Jones and Segnit, 1971; Riech and Von Rad, 1979). Porcellanites have been mostly documented in Tertiary Southern Hemisphere sediments and are restricted only to small areas, where the opal CT to quartz conversion stopped (Bohrmann, et al., 1990).

On all our seismic sections, reflector B shows a positive acoustic impedance and, as mentioned before, it is not attached parallel to the seafloor topography (Fig. 3, CDPs 1700-3100 and Fig. 4, CDPs 2100-2200 and 3900-4500). Contrary to the attributes of opal A/CT BSRs and porcellanites, reflector B is higher reflective than the underlying sediments and it never cross-cuts any other reflections but is part of the surrounding lithology. Furthermore, the whole subunit 1a sediments that contain reflector B originates in upper Cretaceous times (Schlüter and Uenzelmann-Neben, 2007), making porcellanites unlikely. Moreover, as reflector B appears on all seismic sections and is spread all over the central Transkei Basin, this would be a very huge deposit for a rarely appearing material.

6.6.3 Horizontal dykes/sills:

Intrusions of igneous material into sedimentary basin infills are called sills or horizontal dykes. Basically, sills need a submarine volcano or subvertical dykes as source (Lee et al., 2006). Due to the impedance contrast between sedimentary layers and intrusive material, sills are characterised by a strong impedance contrast and, consequentially, produce a highly reflective horizon (Planke et al., 2000). Additionally, sills most commonly show upward trending flanks or at least cross-cut the surrounding strata (Trude et al., 2003; Lee et al., 2006), which is a result of magma chimneys/vents at their flanks (Davies et al., 2002). On one seismic section we observe a feature, penetrating the sediments of units 1 to 3 (Fig. 3, CDP 800). We cannot be sure whether this feature images a vertical intrusive body, but due to its homogeneous appearance nearly without

any internal reflections, this seems very unlikely. Reflector B always follows the surrounding strata and lithology and never shows an upward trend or even further venting at any side (Figs. 3 and 4), which excludes horizontal dykes/sills as a source for reflector B.

6.6.4 Free gas/oil:

The appearance of free gas in deep-sea basins can be explained either by the dissociation of gas hydrates (e.g. Sain et al. 2000) or associated with oil. We already excluded biogenic gas as a source for reflector B, so we focus on the occurrence of thermogenic gas and oil. Oil appears where large amounts of biogenic matter get buried under anoxic conditions at high temperatures and high pressure (oil window). It is lighter than sediment and water and, thus, migrates upwards. The only possibilities to preserve oil within the sediment is a structural trap, a stratigraphic trap, or a combination of both (McQuillin, et al., 1984). In any case, the reservoir or host rock, which contains the oil, has to be enclosed upwards and laterally. If the reservoir rock is not totally sealed, the upward migrating oil (and associated gas) produces chimneys or pockmarks that can be clearly observed on seismic profiles (Tingdahl et al., 2001; Gay et al., 2006). Due to the slight impedance contrast between oil bearing and water bearing sediments (oil-water contact), a phase displacement at the transition from weak to strong reflections occurs.
We do not observe any structural traps within subunit 1a. We are aware that stratigraphical traps are hard to identify, but due to the absence of pockmarks or chimneys at any location above reflector B, their occurrence seems unlikely. Additionally, we do not observe any phase displacement within reflector B as an indication for an oil water contact, which excludes oil as origin of reflector B.
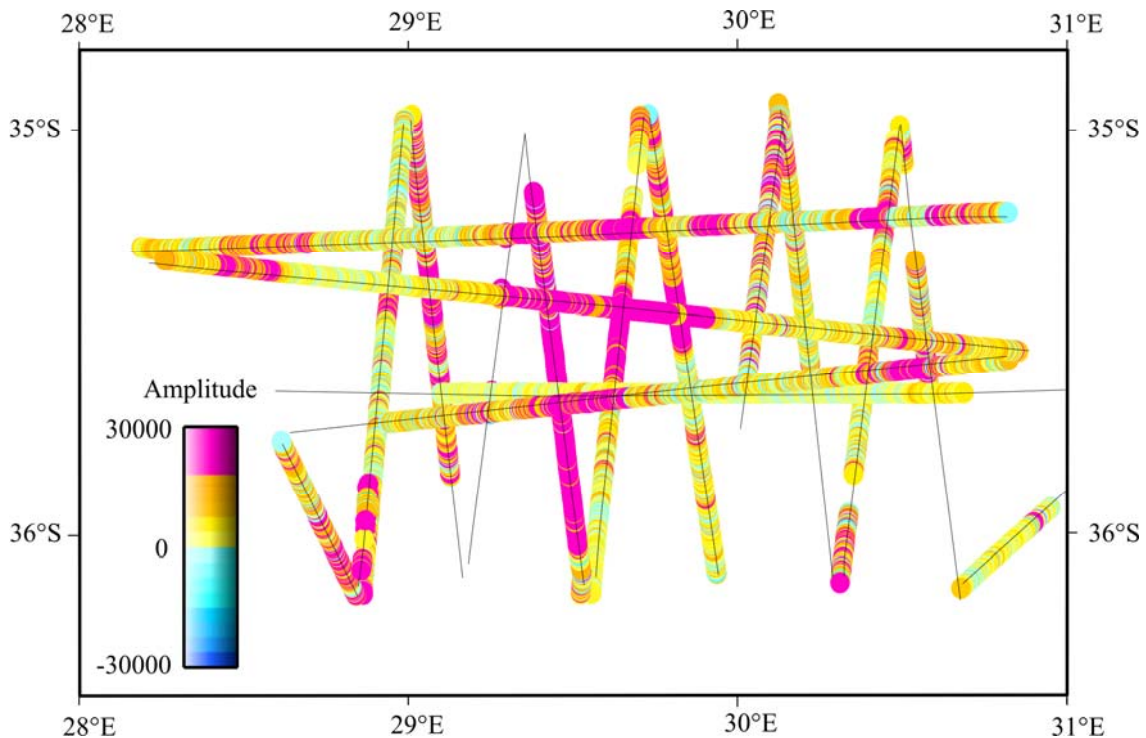

Figure 5: Map showing the reflection amplitude of reflector B within the central Transkei Basin. Thin black lines indicate the locations of the reflection seismic profiles.

6.6.5 Black shales:

Black shales are mudrocks with a large amount of organic-carbon components, mostly between 2% to 30% of Total Organic Carbon components (TOC) (Meyers, 2006). In seismic sections, black shales appear as a highly reflective horizon, due to the impedance contrast to the surrounding sediment. Additionally, the organic material was deposited together with the surrounding sediment and, consequentially, the horizon follows the surrounding lithology or seismic reflectors, respectively (Jones et al., 2007). More important than the seismic characteristics of black shales is their distribution, along with specific events like Oceanic Anoxic Events (OAEs). The principle of the production and preservation of organic matter during OAEs, and thus of black shales, can be explained by an increasing input of biogenic material into the oceans, and anoxic conditions at the ocean's margins (e.g. Bralower and Thierstein, 1984; Meyers, 2006). In total, there are 6 large OAEs that have been identified so far. They have an approximate duration of 0.5 to 1 my (Tab. 2), with OAE 2 being the most pronounced due to its widespread global distribution (e.g. Meyers et al., 2001; Kuroda and Ohkouchi, 2006).

Reflector B is highly reflective, showing an impedance contrast with strong amplitudes (Fig. 5). Besides, it follows the basin's stratigraphy and thus must have been deposited at the same time as the surrounding sediments. The seismic appearance of reflector B fits to black shales, so far.

Locality		Depth of reflector B	Age	Calculated depth after Parsons and McKenzie (1978)	Calculated depth after Crough (1983)
Latitude	Longitude	[m]	[Ma]	[m]	[m]
35.5°S	29.7°E	5600	~80	~3100	~2600
36.0°S	29.0°E	5500	~80	~3000	~2500
35.6°S	30.5°E	5200	~80	~2700	~2200

Table 3: Palaeo depths of reflector B for three locations within the central Transkei Basin, calculated after Parsons and McKenzie (1978) and Crough (1983).

The maximum age of the Transkei Basin's basement was dated to be ~90 Ma to ~100 Ma, setting reflector B to ~79.4 Ma to ~85.1 Ma (Tab. 1). This fits to the dating of OAE 3 (Tab. 2). Black shales have been described for many regions around the South Atlantic, such as from the Cape Basin, southwest of South Africa (DSDP core 361, Stein et al., 1986), but not from the southwestern Indian Ocean. The Transkei Basin is located about 1000 km east of the Cape Basin, so we have to determine whether anoxic conditions in Coniacian to Santonian times (~ 89.3Ma – ~ 83.5 Ma) are likely for this region. The tectonic development of the Transkei Basin and the adjacent regions have been completed around 90 Ma, so we can assume the same morphologic situation as of today (Martin and Hartnady, 1986; Ben-Avraham et al., 1993). The only exception is the depth range of this region. A reconstruction of the palaeo-depth of the research area at ~80 Ma could show whether the Transkei Basin was subject to deep-water circulation or not. If the Transkei Basin was subject to reduced deep and bottom water in/outflow at that time, this would be a strong evidence for anoxic conditions, supporting the thesis of an OAE as origin for reflector B. Therefore, we calculated the palaeo-depth for this region at ~80 Ma (Tab. 3). There are two different formulas to determine the thermal subsidence since then, one for ages up to 80 Ma (Parsons and McKenzie, 1978) and another one for ages more

than 80 Ma (Crough, 1983). Due to the approximated age of reflector B between ~ 80 Ma and ~ 85 Ma, we used both formulas (Tab. 3). For the deepest part of the Transkei Basin at reflector B, we calculated a palaeo-depth between 2200 and 3100 m (Tab. 3), resulting in a subsidence of up to 2500 m since then. Additionally, the surrounding topography, such as the Agulhas Passage or the Agulhas Plateau (Figs. 1 and 2), must also have been much higher than today. Due to the shallower water depth of the Transkei Basin and the surrounding regions, reduced deep-water circulation seems likely at ~80 Ma. Moreover, the Agulhas Falkland Fracture Zone (AFFZ) also may have had a shallower water depth than today (Fig. 2). The AFZ could have acted as an additional barrier for deep water circulation off South Africa. We do not know any palaeo flow-paths from the Upper Cretaceous, but they could have been blocked or at least weakened at any side of the Transkei Basin (Figure 2). Deep and bottom related water masses from the north would have been guided off the basin southwestward by the AFFZ, such as water masses that flowed northwards would have been guided around the basin by the SWIR and the Scotia Ridge.

Due to the shallow water depth along with at least partially blocked deep-water masses, anoxic conditions in the Transkei Basin around ~80 Ma appear very likely. The imprecise dating of reflector B (~79.4 Ma - ~85.1 Ma) leaves the question, whether it originates in OAE 3 (87.3 Ma - ~84.6 Ma, Tab. 2) or may be in a yet unknown OAE for this region slightly later.

6.7 Conclusions:

The analysis of high resolution seismic reflection profiles from the central Transkei Basin revealed the recurrently high amplitude reflector B, which was roughly dated to ~ 79.4 Ma - ~ 85.1 Ma. According to its attributes and appearance, several origins could be excluded, such as Bottom Simulating Reflectors (BSR) due to gas hydrates, diagenetic horizons (e.g. porcellanites), horizontal dykes/sills and free oil/gas. Geological and tectonic settings by recalculation of the thermal subsidence since the Campanian (~ 83.5 Ma – ~ 70.6 Ma) indicate that the Transkei Basin seems to have been subject to reduced water in/outflow (Fig. 2) by a cut off from any global deep water circulation, which resulted in anoxic conditions. The areal extent and partially occurring high amplitudes of reflector B, as well as the dating, which could fit to Oceanic Anoxic Event 3, has led to the conclusion that it is built up of black shales.

6.8 Acknowledgements:

6.9 References:

Ben-Avraham, Z., Hartnady, C. J. H. and Malan, J. A., 1993. Early tectonic extension between the Agulhas Bank and the Falkland Plateau due to the rotation of the Lafonia microplate. Earth and Planetary Science Letters, 117, 43 – 58.

Berndt, C., Bünz, S., Clayton, T., Mienert J., Saunders, M., 2004. Seismic character of bottom-simulating reflections: examples from the mid-Norwegian margin, Marine and Petroleum Geology, 21, 723 – 733.

Boebel, O., Lutjeharms, J., Schmid, C., Zenk, W., Rossby, T., Barron, C., 2003. The Cape Cauldron: a regime of turbulent inter-ocean exchange. Deep Sea Research II, 50, 57 – 86.

Bohrmann, G., Kuhn, G., Abelmann, A., Gersonde, R., Fütterer, D., 1990. A young porcellanite occurence from the southwest Indian Ridge. Marine Geology, 90, 155 – 163.

Bohrmann, G., Spiess, V., Hinze, H., Kuhn, G., 1992. Reflector „Pc" a prominent feature in the Maud Rise sediment sequence (eastern Weddell Sea): Occurrence, regional distribution and implications to silica diagenesis. Marine Geology, 106, 69 – 87.

Bralower, T. J., Thierstein, H. R., 1984. Low productivity and slow deep-water circulation in mid-Cretaceous oceans. Geology, 12, 614 – 618.

Crough, S. T., 1983. The correction for sediment loading on the seafloor. Journal of Geophysical Research, 88, 6449 – 6454.

Davies, R. J., Bell, B. R., Cartwright, J. A., Shoulders, S., 2002. Three-dimensional seismic imaging of Paleogene dike-fed submarine volcanoes from the northeast Atlantic margin. Geological Society of America, 30, 3, 223 – 226.

Dingle, R. V. and Camden-Smith, F., 1979. Acoustic stratigraphy and current-generated bedforms in deep ocean basins off southeastern Africa. Marine Geology, 33, 3-4, 239 – 260.

Fullerton, L. G., Frey, H. V., Roark, J, H. and Thomas, H. H., 1989. Evidenec for a remanent contribution in Magsat data from the Cretaceous Quiet Zone in the South Atlantic. Geophysical Research Letters, 16, 1085 – 1088.

Gay, A., Lopez, M., Cochonat, P., Sermondadaz, G., Seranne, M., 2006. Evidences of early to late fluid migration from an upper Miocene turbiditic channel revealed by 3D seismic coupled to geochemical sampling within seafloor pockmarks, Lower Congo Basin. Marine and Petroleum Geology, 23, 3, 387 – 399.

Goodlad, S. W., Martin, A. K. and Hartnady, C. J. H., 1982. Mesozoic magnetic anomalies in the southern Natal Valley. Nature, 295, 686 – 688.

Gradstein, F. M., Ogg, J. G., Smith, A. G., et al., 2004. A Geologic Time Scale 2004. Cambridge University Press, 589 pp.

Grützner, J., Mienert, J., 1999. Physical property changes as a monitor of pelagic carbonate diagenesis; an empirically derived diagenetic model for Atlantic Ocean basins. American Association of Petroleum Geologists Bulletin, 83, 9, 1485 – 1501.

Jokat, W., Boebel, T., König, M., and Meyer, U., 2003. Timing and geometry of early Gondwana breakup. Journal of Geophysical Research, 108(B9), 2428, doi:10.1029/2002JB001802.

Jones, J. H., Segnit, E. R., 1971. Genesis of cristobalite and trydemite at low temperatures. Journal of the Geological Society of Australia, 18, 419 – 422.

Jones, E. J. W., Bigg, G. R., Handoh, I. C., Spathopoulos, F., 2007. Distribution of deep-sea black shales of Cretaceous age in the eastern Equatorial Atlantic from seismic profiling. Palaeogeography, Palaeoclimatology, Palaeoecology, 248, 1-2, 233 – 246.

Kastner, M., Keene, J. B., Gieskes, J. M., 1977. Diagenesis of siliceous oozes-I. Chemical controls on the rate of opal-A to opal-CT transformation an experimental study. Geochimica et Cosmochimica Acta, 41, 1041 – 1059.

Kennett, J. P., 1977. Cenozoic evolution of Antarctic glaciation, the circum-Antarctic Ocean and their impact on global paleoceanography. Journal of Geophysical Research, 82, 3843 – 3860.

König, M. and Jokat, W., 2006. The Mesozoic breakup of the Weddell Sea. Journal of Geophysical Research, 111, B12102, doi:10.1029/2005JB004035, 2006.

Kuroda, J. and Ohkouchi N., 2006. Implication of spatiotemporal distribution of black shales deposited during the Cretaceous Oceanic Anoxic Event-2. Paleontological Research, 10, 4, 345 – 358.

Labrecque, J. L. and Hayes, D. E., 1979. Seafloor spreading history of the Agulhas Basin. Earth and Planetary Science Letters, 45, 2, 411 – 428.

Lee, G. H., Kwon, Y. I., Yoon, C. S., Kim, H. J., Yoo, H. S., 2006. Igneous complexes in the eastern Northern South Yellow Sea Basin and their implications for hydrocarbon systems. Marine and Petroleum Geology, 23, 631 – 645.

Martin, A. K. and Hartnady, C. J. H., 1986. Plate tectonic development of the southwest Indian Ocean: a revised reconstruction of east Antarctica and Africa. Journal of Geophysical Research, 91, 4767 – 4786.

McQuillin, R., Bacon, M., Barclay, W., 1984. An introduction to seismic interpretation. Reflection Seismics in Petroleum Exploration. ISBN 0860104559. pp. 287.

Meyers, P. A., Bernasconi, S. M. and Foster, A., 2006. Origins and accumulation of organic matter in expanded Albian to Santonian blck shale sequences on the Demara Rise, South American margin. Organic Geochemistry, 37, 1816 – 1830.

Meyers, P. A., 2006. Paleoceanographic and paleoclimatic similarities between Mediterranean sapropels and Cretaceous black shales. Palaeogeography, Palaeoclimatology, Palaeoecology, 235, 1-3, 305 – 320.

Meyers, S. R., Sageman, B. B., Hinnov, L. A., 2001. Integrated quantitative stratigraphy of Cenomanian-Turonian Bridge Creek Limestone Member using evolutive harmonic analysis and stratigraphic modelling. Journal of Sedimentary Research, 71, 628 – 644.

Niemi, T. M., Ben-Avraham, Z., Hartnady, C. J. H., Reznikov, M., 2000. Post-Eocene seismic stratigraphy of the deep ocean basin adjacent to the southeast African continental margin: a record of geostrophic bottom current systems. Marine Geology, 162, 2-4, 237 – 258.

Ogg, J., Agterberg, F. P. and Gradstein, F. M., 2004. The Cretaceous Period. In: Gradstein, F., Ogg, J., Smith, A. (Eds.), A Geologic Time Scale. Cambridge University Press, Cambridge, pp. 344 – 383.

Parsons, B., and McKenzie, D., 1978. Mantle convection and the thermal structure of plates. Journal of Geophysical Research, 83, 4485 – 4496.

Pecher, I. A., Minshull, T. A., Singh, S. C., von Huene, R., 1996. Velocity structure of a bottom simulating reflector offshore Peru. Earth and Planetary Science Letters, 139, 459 – 469.

Petersen, C. J., Papenberg, C., Klaeschen, D., 2007. Local seismic quantification of gas hydrates and BSR characterization from multi-frequency OBS data at northern Hydrate Ridge. Earth and Planetary Science Letters, 255, 3-4, 414 – 431.

Planke, S., Symonds, P. A., Alvestad, E., Skogseid, J., 2000. Seismic volcanostratigraphy of large-volume basaltic extrusive complexes on rifted margins. Journal of Geophysical Research, 105, 19335 – 19351.

Poole, I., Cantrill, D., Utescher, T., 2005. A multi-proxy approach to determine Antarctic terrestrial palaeoclimate during Late Cretaceous and early Tertiary. Palaeogeography, Palaeoclimatology, Palaeoecology, 222, 1-2, 95 – 121.

Riech, V., Von Rad, U., 1979. Silica diagenesis in the Atlantic Ocean: Diagenetic potential and transformations. In: M. Talwani et al. (Editor), Deep Drilling Results in the Atlantic Ocean: Continental Margins and Paleoenvironmets. (M. Ewing Ser., 3) American Geophysical Union, Washington, 315 – 340.

Sain, K., Minshull, T. A., Singh, S. C., Hobbs, R. W., 2000. Evidence for a thick free gas layer beneath the bottom simulating reflector in the Makran accretionary prism. Marine Geology, 164, 1-2, 3 – 12.

Schlüter, P. and Uenzelmann-Neben, G., 2007. Seismostratigraphic analysis of the Transkei Basin: A history of deep-sea current controlled sedimentation. Marine Geology, 240 (1-4), 99-111.

Schlüter, P. and Uenzelmann-Neben, G., 2007. Indications for bottom current activity since Eocene times: The climate and ocean gateway archive of the Transkei basin, South Africa. Global and Planetary Change, (in press), doi:10.1016/j.gloplacha.2007.07.002.

Sellwood, B. W., Valdes, P. J., 2006. Mesozoic climates: General circulation models and the rock record. Sedimentary Geology, 190, 1-4, 269 – 287.

Shipley, T. H., Huston, M. H., Buffer, R. T., Shaub, F. J., McMillen, K. J., Ladd, J. W., Worzel, J. L., 1979. Seismic evidence for widespread possible gas hydrate horizons on continental slopes and rises. American Association of Petroleum Geologists, Bulletin, 63, 2204 – 2213.

Sloan, E. D., 1998. Gas Hydrates: Review of Physical/Chemical Properties. Energy and Fuels, 12, 191 – 196.

Smith, W. H. F. and Sandwell, D. T., 1997. Global Sea Floor Topography from Satellite Altimetry and Ship Depth Soundings. Science, 277, 1956 – 1962.

Stein, R., Rullkötter, J., Welte, D. H., 1986. Accumulation of organic-carbon-rich sediments in the Late Jurassic and Cretaceous Atlantic Ocean – A Synthesis. Chemical Geology, 56, 1 – 32.

Tikku, A. A., Marks, K. M. and Kovacs, L. C., 2002. An Early Cretaceous extinct spreading center in the northern Natal Valley. Tectonophysics, 347, 87 – 108.

Tingdahl, K. M., Bril, A. H., de Groot, P. F., 2001. Improving seismic chimney detection using directional attributes. Journal of Petroleum Science and Engineering, 29, 3-4, 205 – 211.

Tribble, J. S., MacKenzie, F. T., Urmos, J., O`Brien, D. K., Manghnani, M H., 1992. Effects of biogenic silica on acoustic and physical properties of clay-rich marine sediments. American Association of Petroleum Geologists Bulletin, 76, 6, 792 – 804.

Trude, J., Cartwright, J., Davies, R. J., Smallwood, J., 2003. New technique for dating igneous sills. Geological Society of America, 31, 9, 813 – 816.

Tucholke , B. E., Embley, R. W., 1984. Cenozoic regional erosion of the abyssal sea floor off South Africa. Interregional Unconformities and Hydrocarbon Accumulation. AAPG Memoir, 36, 145 – 164.

Volpi, V., Camerlenghi, A., Hillenbrand, C.-D., Rebesco, M., Ivaldi, R., 2003. Effects of biogenic silica on sediment compaction and slope stability on the Pacific margin of the Antarctic Peninsula. Basin Research, 15, 3, 339 – 363.

Wagner, T., Sinninghe Damsté, J. S., Hofmann, P. and Beckmann, B., 2004. Euxinia and primary production in Late Cretaceous eastern equatorial Atlantic surface waters fostered orbitally driven formation of marine black shales. Paleoceanography 19. doi:10.1029/2003PA00089, PA3009.

7 Conclusions and Outlook

In the following, the conclusions of this thesis are described, according to each of the four major tasks.

1)   When and how did the large scale heat transfer, triggered by water mass exchange, between the Southeast Atlantic Ocean and the Southwest Indian Ocean begin?

To maintain heat transfer by water mass exchange within the world's oceans, there have to be cold and dense deep water masses, as well as warm and light surface related water masses. In deep sea basins, like the Transkei Basin, surface related currents do not influence the sedimentary infill, directly. Bottom currents do affect the basin's infill by depositing, eroding or simply shaping (e.g. Agulhas Drift) sediments.

Within the first period, from ~90 Ma to ~ 36 Ma, we observe that the sediments of the central Transkei Basin are deposited predominantly in the deeper and trough-like areas.

This excludes a stable and directed inflow of bottom currents over a long period of time (see Chapters 4.5; 5.5). Additionally, black shales, most likely deposited during an Oceanic Anoxic Event (OAE), can be observed within sediments from the Upper Cretaceous, which supports the hypothesis of reduced water mass inflow (see Chapters 6.6.4; 6.5). Though it is uncertain, whether bottom currents with changing attributes have been active in this region, in late Cretaceous and early Paleogene times. Certainly, these currents would not have been able to maintain a stable heat transfer between the Atlantic Ocean and the Indian Ocean, due to their instability.

The first indication for a strong and directed bottom current influence within the Transkei Basin is recognised at ~36 Ma (see Chapters 4.5; 5.5). This event can be correlated with the first opening of the Drake Passage and Tasman Gateway for deep water in late Eocene. These deep water pathways are fully established at ~34 Ma, where in the adjacent Natal Valley the beginning build up of the Oribi-Drift is observed (see Chapter 4.4.4). Thus, heat transfer between the Indian Ocean and the Atlantic Ocean, which was triggered by Thermohaline Circulations, has been established, at least, since ~34 Ma.

2)   Is it possible to reconstruct variations in flow paths and flow strengths of (proto-) NADW and (proto-) AABW in detail and how does it look like?

One of the main aims of this thesis was the reconstruction of deep and bottom currents south of South Africa. As a first step, the palaeo flow paths of proto-AABW since ~36 Ma were reconstructed by the shape and orientation of the Oribi-Drift, the M-Drift and the Agulhas Drift (see Chapters 4.4 - 4.6). Due to the Coriolis Force, on the Southern Hemisphere water masses (and their sedimentary content) are deflected to the left side of their flow direction (see Chapters 2.2; 2.3). In combination with the drift appearances, a palaeo flow path of proto-AABW for the region south of South Africa was reconstructed. The palaeo flow paths of (proto-) NADW were reconstructed with their onset at ~3 Ma (see Chapter 4.6).

The second step was a more detailed analysis, not only of the flow paths, but also of the flow strengths and sedimentation rates for the different periods and for each deep and bottom current. Therefore, depocentre locations and interface outlines, as well as

sedimentation rates for each period, were calculated and the results were merged into a depositional model for the Transkei Basin since the Late Eocene (see Chapters 5.5; 5.6).

The result is a detailed model of the (proto-) AABW and (proto-) NADW activity within the central Transkei Basin, which shows the precise pathways and depocentre locations for each of the five periods.

The result shows that the flow paths and flow strengths of (proto-) NADW and (proto-) AABW off South Africa recurrently changed significantly within the past ~36 Ma (see Chapter 5.5).

3)   What can a detailed deep and bottom current reconstruction reveal about transport and deposition of sediments within the Transkei Basin?

The reconstruction of bottom current activity was carried out by the analysis of depocentre locations, interface outlines and sedimentation rates (see Chapters 5.4 - 5.6)

The transport and sedimentation within the Transkei Basin were dependent on the bottom current attributes. These attributes are mainly triggered by the regional tectonic/morphology and by global events. The regional setting of the Transkei Basin and surrounding regions seemed to have been rather stable since ~90 Ma, except for its depth range (see Chapter 6.5). Certainly, the main influence on bottom currents are global events, such as the opening of the Drake Passage and Tasman Gateway for deep water at ~36 Ma, or a global cooling event in Middle Miocene. In fact, large scale events trigger the attributes of deep and bottom currents and, thus, influence their ability to transport and deposit sediments in the Transkei Basin.

The combination of flow paths and strengths of currents and the origin of the sedimentary infill of the central Transkei Basin would help to reconstruct their transport and deposition behaviour. Certainly, the origin of the sedimentary infill is unknown, due to the inaccessibility of any drill core data from this region. Consequentially, the transport behaviour of sediments within deep and bottom currents off South Africa could not be reconstructed in detail.

4)   Which climatic conditions can be reconstructed for the initial period of sedimentation within the Transkei Basin before the onset of deep and bottom current activity, in the late Cretaceous?

The period before the onset of pronounced bottom current activity within the Transkei Basin at ~36 Ma is characterised by slowly ongoing deep sea sedimentation. There are no accessible drill core information about the sedimentary content or texture of the basin's infill, what makes a climate reconstruction difficult. The period between ~90 Ma and ~36 Ma is characterised by homogeneous sedimentation nearly without any extraordinary feature, except for a reflector with recurrently appearing high amplitudes within the lowest parts of the basin's infill with an approximated age of ~80 Ma (see Chapter 6.5). These bright spots were identified as black shales, which were taken as an indication for an anoxic event (see Chapter 6.6.4). The reasons for these anoxic conditions can be manifold. The recalculation of the subsidence since ~80 Ma revealed that the Transkei Basin and adjacent regions may have been up to 3100 m higher than today (see Chapters 6.5; 6.6). This means, anoxic conditions could have been triggered by a reduced water inflow, due to a cut off of at least bottom current activity from the surrounding ocean (Tethys). Though, an Oceanic Anoxic Event (OAE 3) has been reported for this period,

which supports the thesis of greenhouse conditions with high temperatures and increased bio productivity, also south of South Africa.

Finally, there is no secure information about the climatic conditions before the onset of bottom currents in the Transkei Basin at ~36 Ma.

Due to the missing sedimentary samples and drill cores, the origin and the exact age of the Transkei Basin's sedimentary infill remains uncertain. Consequently, the origin of the black shales within the oldest sediments could not be fully reconstructed.

Further investigations of this region should contain drill core data from the Transkei Basin infill, which can be tied to the reflection seismic data. These information would help to determine more exact age estimations and to reconstruct the areas where the sedimentary freight of the deep and bottom currents originates.

Besides, a deeper drill core could reach the oldest sediments and would shed light on the origin of the black shales. This would improve the knowledge about climatic and hence palaeoceanographic conditions before the onset of proto-AABW at ~36 Ma.

9 Acknowledgements